

Tropical Lagrangians and Homological Mirror Symmetry

Jeff Hicks

March 2, 2022

Abstract

We produce for each tropical hypersurface $V(\phi) \subset Q = \mathbb{R}^n$ a Lagrangian $L(\phi) \subset (\mathbb{C}^*)^n$ whose moment map projection is a tropical amoeba of $V(\phi)$. When these Lagrangians are admissible in the Fukaya-Seidel category, we show that they are mirror to hypersurfaces in a toric mirror. These constructions are extended to tropical varieties given by locally planar intersections, and to symplectic 4-manifolds with almost toric fibrations. We also explore relations to wall-crossing, dimer models, and Lefschetz fibrations. An example is worked out for the mirror pair $(\mathbb{CP}^2 \setminus E, W), X_{9111}$.

Contents

1	Introduction	1
2	Some Background	7
3	Tropical Lagrangian Hypersurfaces in X	13
4	Mirror Symmetry, Tensor Products, and Intersections	40
5	Tropical Lagrangians in Almost Toric Fibrations	55
6	Dimers, del Pezzos and Wall-Crossing	66
7	The example of \mathbb{CP}^2.	77
A	A-model on $((\mathbb{C}^*)^n, W_\Sigma)$	95

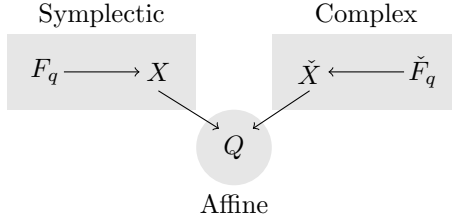
1 Introduction

1.1 SYZ Fibrations and Mirror Symmetry

Mirror symmetry was proposed by physicists as a duality for Calabi-Yau manifolds which interchanges the symplectic geometry on space X with the complex geometry on a mirror

space \check{X} [COGP91]. One version of this duality comes from the homological mirror symmetry conjecture, which advances that the categories $\text{Fuk}(X)$ and $D^b \text{Coh}(\check{X})$ are equivalent as triangulated A_∞ categories [Kon94]. Here, $\text{Fuk}(X)$ is the Fukaya category of X , whose objects are Lagrangian submanifolds L and whose morphisms are given by Floer cochain groups $CF^\bullet(L_0, L_1)$. On the mirror side, the complex space \check{X} has the derived category of coherent sheaves $D^b \text{Coh}(\check{X})$. Though the analytic and algebraic technicalities of working with Fukaya categories are substantial, this conjecture has been proven on a growing number of examples. A first example outside of Calabi-Yau manifolds are toric varieties \check{X}_Σ with fan Σ , which are mirror to Landau Ginzburg models $((\mathbb{C}^*)^n, W_\Sigma)$ [HV00]. [Abo09] proves that the $\text{Fuk}((\mathbb{C}^*)^n, W_\Sigma)$ is mirror to $D^b \text{Coh}(\check{X}_\Sigma)$.

Separately from homological mirror symmetry, an approach to constructing mirror pairs (X, \check{X}) was proposed by Strominger, Yau, and Zaslow, who posited that mirror spaces X and \check{X} carry dual torus fibrations [SYZ96]. In this framework, $X \rightarrow Q$ and $\check{X} \rightarrow Q$ are almost toric Lagrangian fibrations over a common base Q . The data of an affine structure on Q gives rise to a symplectic structure on X , and a complex structure on \check{X} . These fibrations provide a mechanism for mirror symmetry where the symplectic geometry of X and complex geometry of \check{X} are mutually compared to the tropical geometry of the base Q in the so-called large complex structure limit [GS03; GS13].



From this perspective, both the symplectic geometry of X and complex geometry on \check{X} may be compared to tropical geometry on Q , recovering mirror symmetry.

The correspondence between complex geometry on \check{X} and tropical geometry on Q can be understood by replacing the defining polynomials for an affine variety with the corresponding tropical polynomials [Mik05; KS01]. In particular, the image $\text{val}(D)$ of complex subvarieties of $D \subset \check{X}$ can be described in certain examples as a tropical “amoeba” of a tropical variety $V(\phi) \subset Q$.

On the A -model, the lack of rigidity of Lagrangian submanifolds means that there is no reason for $\text{val}(L) \subset Q$ to live near a tropical curve. To obtain a well defined correspondence between Lagrangian submanifolds and tropical geometry one can use perspective from family Floer homology [Abo14; Fuk02], which provides a bridge between SYZ fibrations and the Fukaya category. Starting with the observation that fibers of the SYZ fibration $F_q \subset X$ are candidate mirrors to skyscraper sheaves of points on the space \check{X} , family Floer theory associates to each Lagrangian submanifold $L \subset X$ a sheaf \mathcal{L} on a rigid analytic mirror space \check{X}^Λ . The valuation of this sheaf gives us a tropical subvariety related to the original Lagrangian L . When L is a section of $X \rightarrow Q$, the sheaf built is a line bundle. The tropical support becomes all of Q .

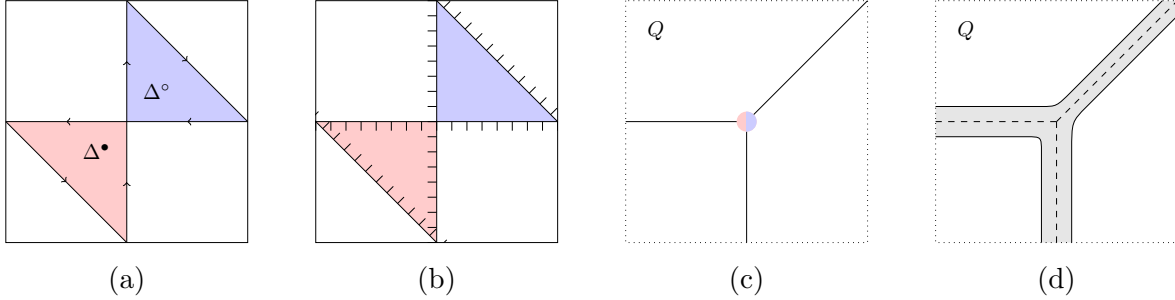


Figure 1: Building a tropical Lagrangian out of easy to understand blocks.

The primary goal of this paper is to provide an inverse to this construction; namely given a tropical subvariety $V(\phi) \subset Q$, we construct a *tropical Lagrangian* submanifold $L(\phi) \subset X$ whose image under $\text{val} : X \rightarrow Q$ is nearby the original tropical subvariety. Additionally, a homological mirror symmetry statement is proven for these tropical Lagrangians, thereby extending the intuition above to holomorphic sheaves supported on cycles of intermediate dimension.

1.2 Some Concrete Geometry in T^*T^2

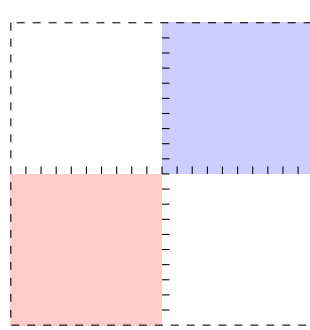
We begin with some concrete geometry to both motivate and orient our future constructions of tropical Lagrangians. We will fix our symplectic manifold to be the space $X = (\mathbb{C}^*)^2$. It will frequently be convenient to think of this instead as T^*T^2 . After fixing a point $0 \in T^2$, the valuation projection can be understood as projection to the fiber $Q := T_x^*\mathbb{R}^2$. Our first construction of tropical Lagrangians will be motivated by smoothing conical Lagrangians in T^*T^2 .

Consider the stratification of the torus drawn in fig. 1a. This stratification contains 3 cycles $C_{\langle -1,0 \rangle}, C_{\langle 0,1 \rangle}$ and $C_{\langle 1,-1 \rangle}$. We've also labeled two triangular faces, Δ° and Δ^\bullet which provide an oriented two-chain whose boundary is the sum of affine cycles C_α . Associated to this data is a conical Lagrangian cycle $L_{\text{pants}}^0 \subset X$, which is given by the disjoint union of the positively oriented conormal bundles $N_+^*C_\alpha$, and the union of the two triangular faces Δ° and Δ^\bullet (drawn using notation from the microlocal sheaf literature in fig. 1b.)

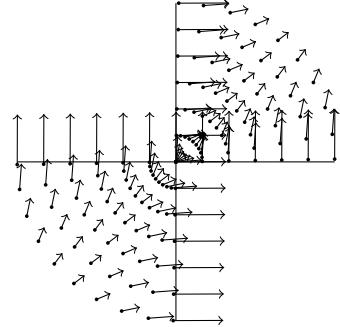
The conical Lagrangian is homotopic to a pair of pants, and its valuation projection to the base Q is the union of three rays travelling in the $\langle 0, -1 \rangle, \langle -1, 0 \rangle$ and $\langle 1, 1 \rangle$ directions— see fig. 1c. If we can build a smooth Lagrangian which is close to L_{pants}^0 , we will have succeeded in building a Lagrangian with valuation projection given by fig. 1d.

The portion of this construction which appears to be most problematic to smooth is where the corners of the polygon meet each other. We exhibit a small smooth Lagrangian which fits into this region by hand.

Lemma 1.2.1. *For $\epsilon > 0$, there exists an oriented smooth Lagrangian $L_\square^\epsilon \subset T^*D^2 \subset \mathbb{C}^2$,*



(a)



(b) The submanifold given by the image of f expressed as a covector field.

Figure 2

which is ϵ close in the Hausdorff metric to the conical Lagrangian variety:

$$\begin{aligned} L_{\blacksquare}^0 = & \{(x_1, y_1, x_2, y_2) \mid x_1, x_2 \geq 0, y_1 = y_2 = 0\} \\ & \cup \{(x_1, y_1, x_2, y_2) \mid x_1, x_2 \leq 0, y_1 = y_2 = 0\} \\ & \cup \{(x_1, y_1, x_2, y_2) \mid x_1, y_2 = 0, y_1 \geq 0\} \\ & \cup \{(x_1, y_1, x_2, y_2) \mid x_2, y_1 = 0, y_2 \geq 0\} \end{aligned}$$

For reference, the Lagrangian L_{\blacksquare}^0 is drawn in fig. 2a.

Proof. Consider the Lagrangian given by the explicit chart $f : \mathbb{R} \times (0, \pi/2) \rightarrow T^*D^2 \subset \mathbb{C}^2$.

$$\begin{aligned} f_\epsilon(r, \theta) \mapsto & (x_1 + iy_1, x_2 + iy_2) \\ = & (r \cos \theta + i \ln(\tan \theta + \sec(\theta)), r \sin \theta + i \ln(\cot(\theta) + \csc(\theta))) \end{aligned}$$

It is a computation to check that the image of this map is a Lagrangian submanifold. For ease of visualization, we've provided a graph of this Lagrangian as a set of covectors in fig. 2b. By studying the behavior of f as θ limits to 0 or $\pi/2$, we see that the image of f approaches the conical Lagrangians $N_+^* \mathbb{R}_x$ and $N_+^* \mathbb{R}_y$. It remains to show that we can bring this Lagrangian arbitrarily close to L_{\blacksquare} . This can be achieved by applying a (conformally symplectic) real scaling of \mathbb{C}^2 . While not a symplectomorphism, this scaling preserves Lagrangian submanifolds giving us Lagrangians $L_{\blacksquare}^\epsilon$ which can be brought as close as desired to L_{\blacksquare}^0 . \square

Having built a Lagrangian $L_{\blacksquare}^\epsilon$ which smoothly approximates L_{\blacksquare}^0 , we proceed to build a Lagrangian L_{pants}^ϵ which approximates L_{pants}^0 built out of the following local pieces:

1. Over the interior regions Δ° and Δ^\bullet , we model L_{pants}^ϵ on the zero section.

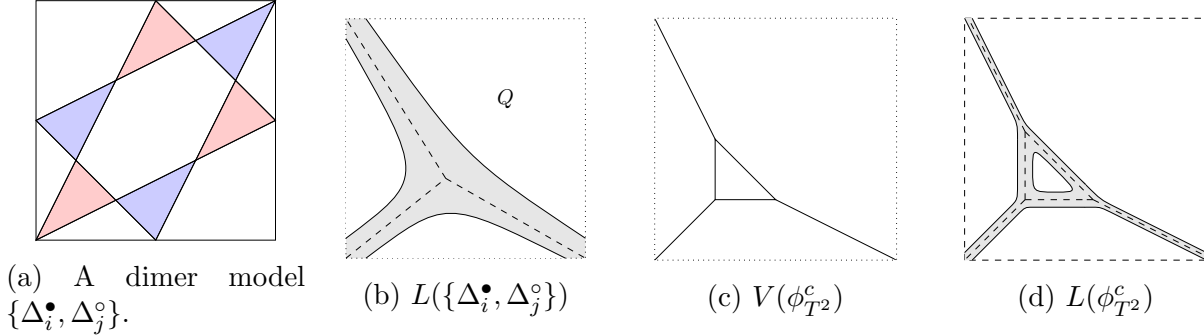


Figure 3: Building some more interesting tropical Lagrangians.

2. Near cycles (but away from the crossings), we model L_{pants}^ϵ on charts resembling

$$f_\epsilon(x_1, x_2) \mapsto (x_1 - i \ln x_1, x_2).$$

This approximates the smoothing $L_{\blacksquare}^\epsilon$ in the region where the x_1 coordinate approaches 0.

3. At each crossing, model L_{pants}^ϵ on $L_{\blacksquare}^\epsilon$.

This technique was also used in [STWZ15]. It must be shown that these three pieces can be glued together by making them agree on overlaps using cut-off functions. As we will later give a less ad-hoc construction of tropical Lagrangians we omit this discussion. This model of a tropical Lagrangian is still useful as a way to understand how to build these Lagrangians from concrete pieces.

We now introduce two examples which we will return to throughout this paper. The techniques discussed in the construction of L_{pants}^ϵ may be extended in two ways. The first way is to look at more intricate diagrams of the form fig. 1a. For example, one may take 6 triangles assembled in a hexagonal configuration fig. 3a. This assembles into the tropical Lagrangian with valuation projection fig. 3b. While the tropical curve described by the Lagrangian in fig. 3b is not a smooth tropical curve, the associated Lagrangian submanifold is embedded.

The second extension that we consider is to use the Lagrangians L_{pants}^ϵ as basic building blocks to assemble tropical Lagrangians associated to other tropical curves. For example, the tropical curve $V(\phi_{T^2}^c)$ drawn in fig. 3c is a smooth tropical curve with a decomposition into three pairs of pants. By gluing together tropical Lagrangians L_{pants}^ϵ together for each pair of pants, we build the tropical Lagrangian whose valuation is drawn in fig. 3d.

Both of these techniques were explored in the recent work of [Mat18; Mik18] as methods to produce Lagrangian submanifolds with tropical valuation.

Family Floer theory gives us the expectation that if a divisor $D \subset \check{X}_\Sigma$ has tropicalization $\text{val}(D)$, that the mirror Lagrangian to a sheaf supported on D should have a similar tropicalization. For this reason, the construction and study of tropical Lagrangians gives a particularly geometric understanding of the homological mirror symmetry correspondence. From that viewpoint, this paper has the following goals:

- Construct tropical Lagrangians using surgery techniques for Lagrangian submanifolds.
- Prove a homological mirror symmetry statement for tropical Lagrangians and hypersurfaces with tropical valuation.
- Relate different constructions of tropical Lagrangians (for example: figs. 3b and 3d) and geometric properties of these Lagrangians from the perspective of Lagrangian Floer theory.

1.3 Summary of Results

In section 2, we provide necessary background related to tropical geometry and Lagrangian cobordisms. The review of tropical geometry is mostly designed to fix notation, and introduce the difference between a smooth tropical hypersurface and a non-self-intersecting tropical hypersurface. The section on Lagrangian cobordisms may be safely skipped by experts who are familiar with the results of [BC14; FOO07]. Our notation for Lagrangian cobordism follows [Hau15b].

Section 3 associates to each tropical polynomial $\phi : Q = \mathbb{R}^n \rightarrow \mathbb{R}$ a Lagrangian submanifold $L(\phi) \subset X = (\mathbb{C}^*)^n$ whose projection under the valuation map $\text{val} : X \rightarrow Q$ lies near the tropical variety $V(\phi) \subset Q$. The section also proves that the constructed tropical Lagrangians are unobstructed admissible objects of the Fukaya category (see theorem 3.3.2.) In section 3.4 these tropical Lagrangians are compared to those already considered in the existing work of [Mat18; Mik18], and examples are given to provide grounding to the future discussion.

In section 4 we prove that the constructed Lagrangians $L(\phi)$ are mirror to structure sheaves of divisors in a mirror toric variety \check{X}_Σ (theorem 4.2.1.) The idea of proof is to use a Lagrangian cobordism to construct $L(\phi)$ and understand this construction in the Fukaya category via mapping cone. In addition, a generalization of these results to tropical subvarieties beyond hypersurfaces is discussed, as well as how to build mirrors to line bundles supported on complex hypersurfaces.

Between sections 3 and 4, the main results of this paper can be understood as follows:

Theorem. *Let \check{X}_Σ^Λ be a toric variety, and let $X = ((\mathbb{C}^*)^n, W_\Sigma)$ be its mirror Landau Ginzburg model. Let D be a base point-free divisor of \check{X}_Σ^Λ with tropicalization given by the tropical variety $V(\phi)$, for a tropical polynomial $\phi : Q \rightarrow \mathbb{R}$. Then there exists a tropical Lagrangian $L(\phi) \subset (\mathbb{C}^*)^n$ whose valuation projection is ϵ -close to $\text{val}(D)$. Furthermore, $L(\phi)$ is homologically mirror to a structure sheaf $\mathcal{O}_{D'}$, where D and D' are rationally equivalent.*

The remainder of the paper is a survey of tropical Lagrangians and connections to mirror symmetry.

In section 5.1, we generalize beyond tropical Lagrangians in $(\mathbb{C}^*)^n$ to tropical Lagrangians in almost toric fibrations. We introduce a Lagrangian torus $L_{T^2} \subset \mathbb{CP}^2$ which becomes a running example for the remainder of discussions. Additionally, we construct a large family of immersed Lagrangians in \mathbb{CP}^2 which may be of further interest.

Section 6 extends a discussion from section 3.4 regarding mutations of tropical Lagrangians. This section uses the combinatorial framework of dimers to encode the structure of a Lagrangian seed (see [PT17]) in our tropical Lagrangians. Furthermore, preliminary computations on the support of the tropical Lagrangian are made, similar to the computation of the Kasteleyn operator with the microlocal sheaf model in [TWZ18].

Finally, we wrap up our discussion of tropical Lagrangians in section 7, where we apply the previous sections to understand homological mirror symmetry for the Lagrangian $L_{T^2} \subset \mathbb{CP}^2 \setminus E$, which is shown to be mirror to a fiber of the superpotential on the Landau-Ginzburg mirror. This section also involves a comparison between the geometry of SYZ fibrations and Lefschetz fibrations.

The construction of a homological mirror symmetry statement for tropical Lagrangians requires a version of the Fukaya-Seidel category which admits bounding cochains. A summary of that construction is included in appendix A.

Acknowledgements

I would firstly like to thank my advisor Denis Auroux whose guidance and comments have helped me at every step of this project. I would also like to thank Andrew Hanlon for walking me through the construction of the monomial admissible Fukaya-Seidel category. This project has also benefited from useful conversations with Ailsa Keating, Diego Matessi, and Nick Sheridan. Additionally, I am especially grateful to Paul Biran and ETH Zürich for their hospitality while hosting me.

A portion of this work was completed at ETH Zürich. This work was partially supported by NSF grants DMS-1406274 and DMS-1344991 and by a Simons Foundation grant (#385573, Simons Collaboration on Homological Mirror Symmetry).

2 Some Background

2.1 Review of Tropical Geometry

The tropical semiring $(\mathbb{R}, \oplus, \odot)$ is the set $\mathbb{R} \cup \{+\infty\}$ equipped with the following two binary operations

$$\begin{aligned} x_1 \oplus x_2 &= \min(x_1, x_2) \\ x_1 \odot x_2 &= x_1 + x_2. \end{aligned}$$

These two operations are called *tropical plus* and *tropical times* respectively, and they obey the distributive law. Tropical polynomials of multiple variables describe piecewise linear concave functions $\phi : Q := \mathbb{R}^n \rightarrow \mathbb{R}$ of rational slope. It will frequently be useful for us to use the following characterization of tropical linear polynomials.

Claim 2.1.1. *The tropical polynomials are exactly the piecewise linear concave functions with $d\phi(x) \in T_{\mathbb{Z}}^*\mathbb{R}^n$ at all points where ϕ is differentiable.*

When $d\phi$ is piecewise linear and convex, but not integral, we will instead call ϕ a *tropical function*. One can approximate tropical polynomials with regular polynomials via logarithms and the estimates

$$-\log_{1/q}(q^{x_1} + q^{x_2}) \sim \min(x_1, x_2) = x_1 \oplus x_2 \quad (1)$$

$$-\log_{1/q}(q^{x_1}q^{x_2}) = x_1 + x_2 = x_1 \odot x_2. \quad (2)$$

We'll frequently describe tropical polynomials of two variables in terms of their tropical varieties by drawing a planar graph whose faces describe the domains of linearity of ϕ . This graph generalizes in higher dimensions to a stratification of Q which describes many of the combinatorial properties of a tropical polynomial.

Definition 2.1.2. *Let $\phi : Q \rightarrow \mathbb{R}$ be a tropical polynomial. Each monomial term in ϕ can be labelled by its exponent $v \in \mathbb{Z}^n$. The linearity stratification of Q is the stratification*

$$\emptyset \subset Q_0 \subset \cdots Q_n,$$

where $p \in Q_k$ if and only if there is no $k+1$ dimensional affine neighborhood $A \subset Q$, with $p \in A$ on which the restriction $\phi|_A$ is a $k+1$ -affine map. Each stratum will be denoted $U_{\{v_i\}}$, where $\{v_i\}$ is the collection of monomial terms which achieve their minimum along the strata. We define the tropical variety of Q to be $V(\phi) = Q_{n-1}$, which describes the locus of non-linearity of ϕ .¹

One interpretation to the approximation given in eq. (2) is that $V(\phi)$ provides a dominating term approximation of $\text{val}(f^{-1}(0))$. This intuition allows one to bridge classical algebraic geometry and tropical geometry.

Example 2.1.3. Consider the tropical polynomial

$$\phi(x_1, x_2) = 0 \oplus x_1 \oplus x_2.$$

On the first quadrant, we have that $0 \leq x_1$ and $0 \leq x_2$, so that the value of the tropical polynomial here is zero. On the remaining 3 quadrants, the value of ϕ is the smaller of x_1 or x_2 . The domain where this is nonlinear form a “tropical pair of pants,” which is supposed to correspond to the pair of pants $\{1 + z_1 + z_2 = 0\} \subset (\mathbb{C}^*)^2$. We've labelled each stratum with its appropriate monomial in fig. 4

There is an involution on smooth concave functions f with convex domains Δ given by the Legendre transform. An analogous involution exists in the setting of tropical polynomials.

Definition 2.1.4. *Let $\phi = \bigoplus_v a_v \odot x^v$. Let $\Delta_\phi^\mathbb{Z}$ be the set of integer points v so that a_v is nonzero. Define the Newton polytope $\Delta_\phi \subset T^*Q$ to be the convex hull of $\Delta_\phi^\mathbb{Z}$. We define the Legendre transform $\check{\phi}(v)$ to be the minimal-fit concave piecewise linear function to the data*

$$\check{\phi}(v) = a_v \text{ for all } v \in \Delta_\phi^\mathbb{Z}.$$

¹The V in $V(\phi)$ should either stand for valuation, or variety.

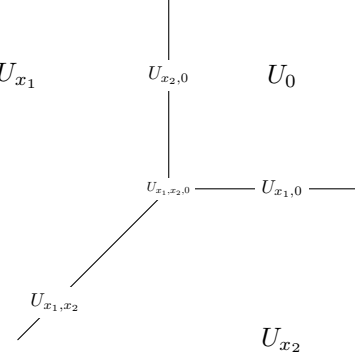


Figure 4: Stratification of Q given by the tropical line $\phi = 0 \oplus x_1 \oplus x_2$

We will denote the linearity stratification induced by $\check{\phi}$ on the Newton polytope as

$$\Delta_\phi^{\mathbb{Z}} = \Delta_\phi^n \subset \cdots \subset \Delta_\phi^0 = \Delta_\phi.$$

We will denote² the stratum with vertices v_i by $\underline{U}^{\{v_i\}}$.

The Newton polytope is a lattice polytope which is determined by the leading order behavior of the tropical polynomial ϕ . It will also be convenient for us to interpret this Newton polytope as the image of $d\phi$ under the projection $\pi_0 : T^*\mathbb{R}^n \rightarrow T_0^*\mathbb{R}^n$

$$\Delta_\phi = \text{Hull}(\{\pi_0 \circ d\phi(x) \mid \phi \text{ is differentiable at } x\}).$$

As the Legendre transform contains the data of the coefficients of ϕ , the polynomials ϕ and $\check{\phi}$ determine each other completely. This relation is also reflected in that the two stratifications $\underline{U}_{\{v_i\}}$ and $\underline{U}^{\{v_i\}}$ are dual to each other.

Definition 2.1.5. We say that a non-maximal stratum $\underline{U}_{\{v_i\}}$ is smooth if $\underline{U}^{\{v_i\}}$ is a standard simplex. The self-intersection number of a strata $\underline{U}_{\{v_i\}}$ is defined as the number of interior lattice points of $\underline{U}^{\{v_i\}}$.

When a tropical variety comes as the tropicalization of family of complex curves, the self-intersection number gives the genus of the family of curves which degenerate in the family. In our constructions of tropical Lagrangians, this self-intersection number will give the number of self-intersection points of our tropical Lagrangian.

Remark 2.1.6. The condition of being smooth is stronger than having no self-intersections. For example, the tropical variety $V(1 \oplus x_1 \oplus x_2 \oplus x_1 x_2)$ has no self-intersections, but is not tropically smooth.

²It's worth pointing out that this naming convention is very different than the one for the strata of Q , but will make notation a lot easier in the future.

Every maximal stratum has zero self-intersections, as the interior of a point is empty.

Claim 2.1.7. *We say that $V(\phi)$ has no self-intersections if it satisfies the following equivalent conditions*

1. *Every lattice point of Δ_ϕ belongs to a minimal (zero-dimensional) stratum $U^{\{v_i\}}$.*
2. *For every $v \in \Delta_\phi^\mathbb{Z}$, there exists an open subset U so that $x^v|_U = \phi(x)|_U$.*³

We say that ϕ has the stronger property of being smooth if it satisfies any of the following equivalent conditions.

1. *ϕ has no self-intersections and the linearity stratification of Δ_ϕ^n is a triangulation of the Newton polytope by standard simplexes.*
2. *Every non-maximal stratum $U_{\{v_i\}}$ is smooth.*
3. *The combinatorial type of the stratification is unchanged under small perturbations of the coefficients a_i for all $i \in \Delta_\phi \cap \mathbb{Z}^n$.*

This discussion and notation is probably easiest seen in the following running example which we'll use in our future constructions.

Example 2.1.8. *One of our favorite examples to work with will be the tropical polynomial*

$$\phi_{T^2}^0(x_1, x_2) = x_1 \oplus x_2 \oplus (x_1 x_2)^{-1}$$

This has 3 domains of linearity, where each of the monomial terms dominate. Notice that the dual stratum $U^{x_1, x_2, (x_1 x_2)^{-1}}$ contains an internal lattice point, and so this vertex is non-smooth (see fig. 5a.) If we modify the coefficients of the monomials in the tropical polynomial to

$$\phi_{T^2}^c(x_1, x_2) = x_1 \oplus x_2 \oplus (c \odot x_1^{-1} x_2^{-1}) \oplus 0$$

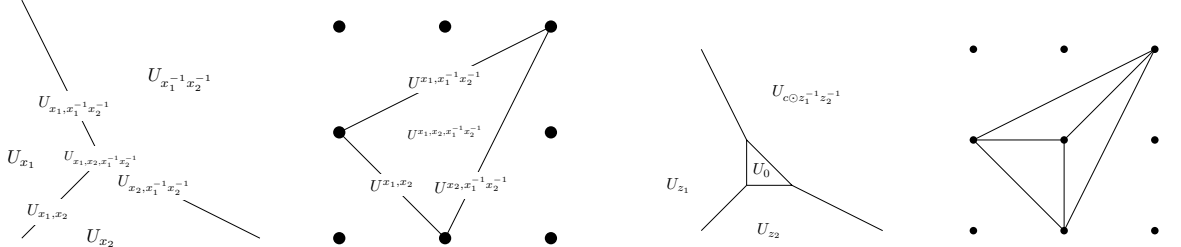
with $c > 0$, we get a smooth tropical curve instead (see fig. 5b.) The dual stratification is a triangulation.

2.2 Lagrangian Surgery and Cobordisms

The bulk of this paper will revolve around constructing new Lagrangian submanifolds. Our most-used tool for these constructions is Lagrangian surgery, which allows us to make local modifications to a Lagrangian submanifold to obtain new Lagrangians.

By the Weinstein neighborhood theorem, we can locally model the transverse intersection of

³This means that every monomial is maximal among all monomials on some open subset.



(a) The non-smooth punctured immersed sphere with 3 punctures

(b) The smooth tropical 3-punctured torus

two Lagrangians by the zero section and cotangent fiber of $T^*\mathbb{R}^n$. The model *Lagrangian neck* in $T^*\mathbb{R}^n$ is the Lagrangian parameterized by

$$\begin{aligned} I \times S^{n-1} &\hookrightarrow \mathbb{R}^n \times \mathbb{R}^n \\ (t, \hat{u}) &\mapsto (\epsilon \cdot e^t \hat{u}, \epsilon \cdot e^{-t} \hat{u}). \end{aligned}$$

Notice that this Lagrangian neck is asymptotic to the disjoint union of the zero section and $T_0^*\mathbb{R}^n$. The parameter ϵ is called the *neck radius* of the smoothing. Given a Lagrangian L with a transverse self-intersection, one can replace a neighborhood of the self-intersection with a Lagrangian neck. In summary:

Theorem 2.2.1 ([Pol91]). *Let L be a (not necessarily connected) Lagrangian submanifold with a transverse self-intersection point p . Then there exists a smooth Lagrangian L'_ϵ which agrees with L outside of the intersection point, and is modeled on the Lagrangian neck in a neighborhood of p .*

There are many non-Hamiltonian isotopic ways of doing this smoothing depending on the choice of neck inserted. As the neck radius approaches 0 the Lagrangian L'_ϵ approaches L in the Hausdorff metric. Given Lagrangians L_0 and L_1 intersecting transversely at a single point q , we denote by $L_0 \#_q L_1$ the Lagrangian connect sum, which is obtained by inserting a neck at a neighborhood of the intersection point.⁴ Lagrangian surgery also has an interpretation as an algebraic operation in the Fukaya category.

Theorem 2.2.2 ([FOOO07]). *Let L_0, L_1 be unobstructed Lagrangians intersecting at a unique point q . Then there is an exact triangle*

$$L_1 \xrightarrow{q} L_0 \rightarrow L_0 \#_q^\epsilon L_1$$

in the Fukaya category.

The proof of this theorem comes from a comparison of holomorphic triangles with corner at q , and holomorphic strips in $L_0 \#_q L_1$ which are obtained from rounding this corner. The notion of Lagrangian surgery has been extended to a notion of antisurgery along *isotropic surgery disks* [Hau15a].

⁴Here, the neck we choose is consistent with the orientations from [Aur14], and opposite of the orientation chosen in [BC13].

Theorem 2.2.3 ([Hau15a]). *Suppose that D^k is a isotropic disk with boundary contained in L and cleanly intersecting L along the boundary. Then there exists an immersed Lagrangian $\alpha_D(L) \subset X$ called the Lagrangian antisurgery of L along D , which satisfies the following properties*

- $\alpha_D(L)$ is topologically obtained by performing surgery along D^k ,
- $\alpha_D(L)$ agrees with L outside of a small neighborhood of D^k ,
- If L was embedded and disjoint from the interior of D^k , then $\alpha_D(L)$ has a single self-intersection point.

When we perform antisurgery of an embedded Lagrangian along a Lagrangian disk D^n the resulting Lagrangian has a single self-intersection.⁵ There exists a choice of surgery neck so that the resolution of the self-intersection of $\alpha_{D^n}(L)$ by Lagrangian surgery is L . However, if we choose a Lagrangian surgery neck in the opposite direction of the disk D^n to combine anti-surgery with surgery, we can obtain a new embedded Lagrangian.

Definition 2.2.4. *Let L be an embedded Lagrangian submanifold, and D^n a surgery disk. Let $\alpha_D(L)$ be obtained from D^n by antisurgery. The mutation of L along D^n is the Lagrangian $\mu_D(L)$ obtained from $\alpha_D(L)$ by resolving the resulting single self-intersection point with the opposite choice of neck.*

It is expected that Lagrangians submanifolds which are related by mutation give different charts on the moduli space of Lagrangian submanifolds in the Fukaya category, and that these charts are related by a wall crossing formula [PT17]. A typical example of Lagrangians related by mutation are the Chekanov and Clifford tori in \mathbb{C}^2 obtained by taking two different resolutions of the Whitney sphere.

The topological operation of surgery can be understood via cobordisms. In the symplectic world, there is an analogous notion of *Lagrangian cobordism* relating Lagrangian surgeries.

Definition 2.2.5 ([Arn80]). *Let $\{L_i^+\}_{i=0}^{k-1}, L^-$ be Lagrangian submanifolds of X . A Lagrangian cobordism between $\{L_i^+\}$ and L^- is a Lagrangian $K \subset X \times \mathbb{C}$ which satisfies the following conditions:*

- Fibered over ends: *There exists constants $\{c_i^+\}, c^- \in \mathbb{R}$ with $c_i^+ < c_{i+1}^+$, as well as constants $t^- < t^+ \in \mathbb{R}$ such that*

$$K \cap \{(x, z) \mid \text{Re}(z) \geq t^+\} = \bigsqcup_i L_i^+ \times \{(t + ic_i^+) \mid t \geq t^+\}$$

$$K \cap \{(x, z) \mid \text{Re}(z) \leq t^-\} = L^- \times \{(t + ic^-) \mid t \leq t^-\}$$

- Compactness: *The projection $Im_z : L_K \rightarrow i\mathbb{R} \subset \mathbb{C}$ is bounded.*

⁵The notation $\alpha_D(L)$ is chosen as the character α results from applying antisurgery on the character c .

We denote such a cobordism $K : (L_0^+, \dots, L_{k-1}^+) \rightsquigarrow L^-$.

Remark 2.2.6. We follow the cohomological grading of [Hau15b], where a cobordism between $(L_0^+, \dots, L_{k-1}^+) \rightsquigarrow L^-$ has input ends L_0^+, \dots, L_{k-1}^+ with positive real value, and end L^- with negative real value. This is opposite the convention from [BC14]. This can be slightly confusing when considering Lagrangian cobordisms, as the “from” side of the cobordism is on the right in its projection to \mathbb{C} .

Some simple examples of Lagrangian cobordisms include the trivial cobordism $L \times \mathbb{R}$, or the suspension of a Hamiltonian isotopy. Given Lagrangians L_0, L_1 intersecting transversely at a single point q , there exists a surgery trace Lagrangian cobordism $(L_0, L_1) \rightsquigarrow L_0 \#_q L_1$. Just as Lagrangian surgery gave us a way to understand $L_0 \#_q L_1$ as a mapping cone, there is a broad-reaching theorem which tells us how to relate cobordant Lagrangians as objects of the Fukaya category.

Theorem 2.2.7 ([BC13]). *Let $K : (L_i^+)_i \rightsquigarrow L^-$ be a monotone Lagrangian cobordism. Then there are k objects Z_0, \dots, Z_{k-1} in the Fukaya category, with $Z_0 = L_0^+$ and $Z_k \simeq L^-$ which fit into k exact triangles*

$$L_i^+ \rightarrow Z_{i-1} \rightarrow Z_i \rightarrow L_i^+[1]$$

In particular when $k = 2$, we have an exact triangle

$$L_1^+ \rightarrow L_0^+ \rightarrow L^-.$$

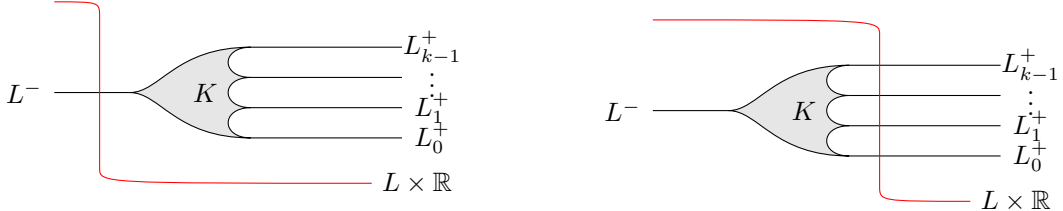
In the case where $k = 1$, we have an isomorphism

$$0 \rightarrow L^+ \rightarrow L^- \rightarrow 0.$$

This can be restated as a relation between the Lagrangian cobordism category of X , and a category which describes triangular decompositions of objects in the Fukaya category. The proof of this theorem computes for test objects $L \in \text{Fuk}(X)$ the Floer homology $CF^\bullet(L \times \mathbb{R}, K)$ in two different ways (See figs. 6a and 6b). We outline how to extend this result to the setting where the Lagrangian cobordism K can be unobstructed by bounding cochain in theorem A.4.1.

3 Tropical Lagrangian Hypersurfaces in X

The goal of this section is to expand the construction of section 1.2 to general tropical hypersurfaces. More precisely, we construct for each tropical polynomial $\phi : Q \rightarrow \mathbb{R}$ a Lagrangian $L(\phi)$ whose projection $\text{val}(L(\phi))$ is ϵ -close to $V(\phi)$ in the Hausdorff metric. Our construction will be rooted in the language of Lagrangian cobordisms, giving us a path to prove a homological mirror symmetry statement for $L(\phi)$. We additionally prove that the Lagrangian $L(\phi)$ is an unobstructed object of the Fukaya category.



(a) When the test object is brought to the left side, the intersection Lagrangian Floer complex between $L \times \mathbb{R}$ and K is $CF^\bullet(L, L^-)$.

(b) On the right side, intersection Lagrangian Floer complex between $L \times \mathbb{R}$ and K is generated by $\bigoplus_i CF^\bullet(L, L_i^+)$.

Figure 6: Biran and Cornea's Cobordism argument

3.1 Surgery Profiles

We will need an explicit surgery profile to build $L(\phi)$.

Proposition 3.1.1. *Let $f_0 : \mathbb{R}^n \rightarrow \mathbb{R}$ be the constant function $f_0 = 0$, and let $f_1 : \mathbb{R}^n \rightarrow \mathbb{R}$ be a smooth convex function. Let U be the region where $df_1 = 0$. Suppose that U is compact. Consider the Lagrangian sections $L_0 = df_0$, and $L_1 = df_1$ in $T^*\mathbb{R}^n$. Then there exists a Lagrangian $L_0 \#_U^\epsilon L_1$ in a small neighborhood of the symmetric difference*

$$L_0 \#_U^\epsilon L_1 \subset B_\epsilon((L_0 \sqcup L_1) \setminus (L_0 \cap L_1)).$$

Furthermore, there exists a Lagrangian cobordism K^ϵ with ends $(L_0, L_1) \rightsquigarrow L_0 \#_U^\epsilon L_1$. We call $L_0 \#_U^\epsilon L_1$ the Lagrangian surgery with neck given by U .

We may relax the condition that U be compact if the second derivative of f is bounded in a neighborhood of U . When the parameter ϵ is unimportant, we will drop it and simply write $L_0 \#_U L_1$.

Proof. We first give a description of a Lagrangian $L_0 \#_U L_1$ which satisfies the desired properties. Normalize f_1 by adding a constant so that $f_1 = 0$ on U . By convexity, $f_1 > 0$ on the complement of U . Let $r_\epsilon : \mathbb{R}_{>\epsilon} \rightarrow \mathbb{R}$ and $s_\epsilon : \mathbb{R}_{>\epsilon} \rightarrow \mathbb{R}$ be functions satisfying the following properties:

- $r(t) = t$ for $t \geq 2\epsilon$ and $s(t) = c$ for $t \geq 2\epsilon$.
- $r'(\epsilon) = s'(\epsilon) = \frac{1}{2}$
- $r(t)$ is concave, while $s(t)$ is convex.
- The concatenation of curves $(t, r'(t))$ and $(t, s'(t))$ is a smooth plane curve.

The profiles of these functions are drawn in figs. 7a and 7b. Consider the Lagrangian submanifolds given by the graphs

$$d(r_\epsilon \circ f_1) \quad d(s_\epsilon \circ f_1)$$

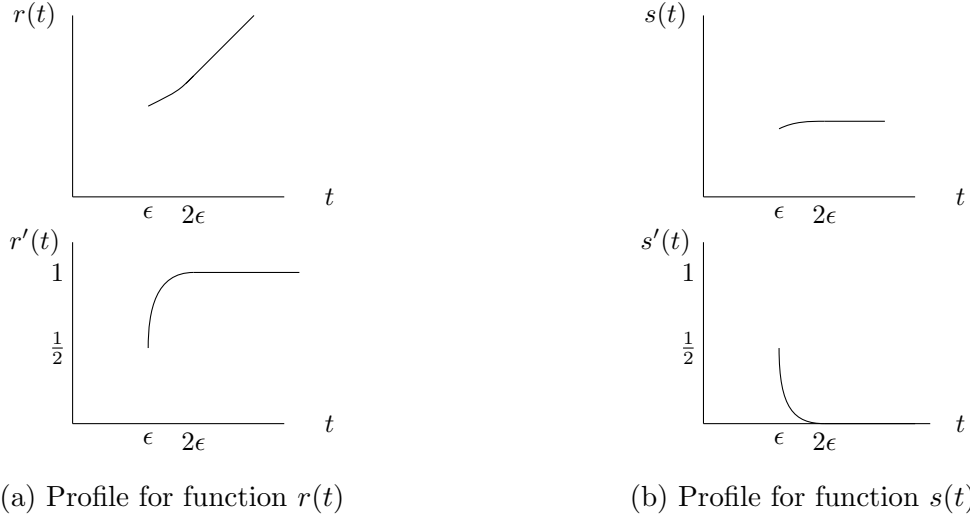


Figure 7: Some profiles for constructing $L_0 \#_U L_1$

defined as sections over the domain $f_1 \geq \epsilon$. The union of these two charts is a smooth Lagrangian submanifold, which is our definition of $L_1 \#_U^\epsilon L_0$.

The profile is only defined where $f \geq \epsilon$, so $L_0 \#_U^\epsilon L_1$ is disjoint from the set $L_0 = L_1$. As r_ϵ is the identity for $f > 2\epsilon$, we have that $d(r_\epsilon \circ f_1) = L_1$ on the region where $f(x) > 2\epsilon$. A similar statement can be made about s_ϵ , and these observations give us that $L_1 \#_U^\epsilon L_0$ is contained a small neighborhood of the symmetric difference.

It remains to show that L_0, L_1 and $L_0 \#_U^\epsilon L_1$ fit into a cobordism. This cobordism will be constructed as a Lagrangian surgery in one dimension higher. Consider the constant function $\tilde{f}_0 : \mathbb{R}^{n+1} \rightarrow \mathbb{R}$ and the function

$$\begin{aligned} \tilde{f}_1 : \mathbb{R}^n \times \mathbb{R} &\rightarrow \mathbb{R} \\ (x, t) &\mapsto f_1(x) + g(t) \end{aligned}$$

where the function $g(t)$ satisfies the following properties:

- $g(t)$ is convex
- $dg|_{t < -\epsilon} = 0$ and $dg|_{t > 0} = 1$.

We will now take the surgery of sections $\tilde{L}_0 = d\tilde{f}_0$ and $\tilde{L}_1 = d\tilde{f}_1$. Let U be the region where $df_1 = 0$. \tilde{L}_0 and \tilde{L}_1 agree on the region $\tilde{U} = U \times (-\infty, -\epsilon)$ (see fig. 8). As the intersection over this region is defined by the intersection of convex primitives, we may use our previous construction to define the surgery cobordism

$$K := \tilde{L}_0 \#_{\tilde{U}} \tilde{L}_1.$$

Since K agrees with \tilde{L}_0 and \tilde{L}_1 outside of U ,

$$K|_{t > 0} = ((L_0 \times \{0\}) \sqcup (L_1 \times \{dt\})) \times \mathbb{R}_{t > 0}$$

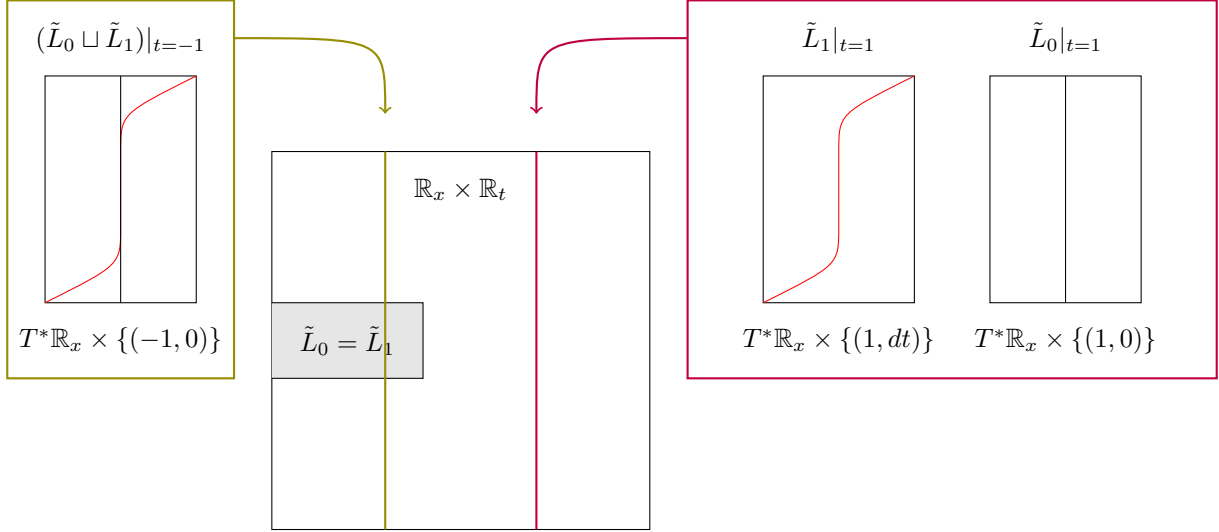


Figure 8: The Lagrangians \tilde{L}_0 and \tilde{L}_1 whose surgery give the Lagrangian cobordism K .

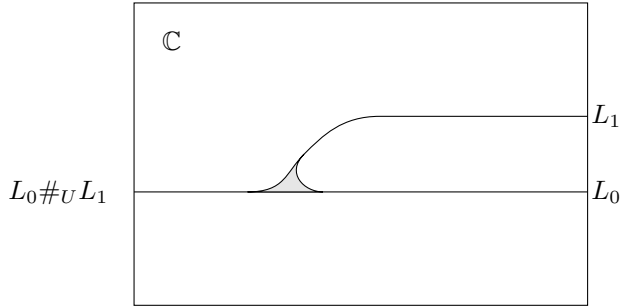


Figure 9: The projection of the surgery cobordism to the \mathbb{C} -parameter. The curve defining the upper boundary of this projection is parameterized by $z = t + i\frac{dg}{dt}$.

As the function $g(t)$ is constant on each t -fiber, we obtain that $K|_{t=-\epsilon} = L_0 \#_U L_1$ and conclude

$$K|_{t<-\epsilon} = (L_0 \#_U L_1) \times \{0\} \times \mathbb{R}_{t<-\epsilon}.$$

These are the conditions required for K to be a Lagrangian cobordism between L_0, L_1 and $L_1 \#_U^\epsilon L_0$. \square

Remark 3.1.2. *We could have chosen f_1 to be concave and still have had a surgery construction. However the existence of a surgery cobordism depends on the convexity of f . If instead we had started with a concave primitive f_1 , the function*

$$\begin{aligned} \tilde{f}_1 : \mathbb{R}^n \times \mathbb{R} &\rightarrow \mathbb{R} \\ (x, y) &\mapsto f_1(x) + g(t) \end{aligned}$$

is neither concave or convex, and we are unable to construct our cobordism using the surgery profile previously described. This manifests itself as an ordering on the ends of the cobordism. In particular, there is no Lagrangian cobordism with ends (L_1, L_0) and $(L_0 \#_U L_1)$.

In the setting where U is a compact region, this is nothing different than a special choice of neck on the standard Lagrangian connect sum cobordism. The construction above provides an alternative definition to the surgery trace cobordism considered in [BC13]. In the non-compact setting, we get an interpretation of what it means to take the connect sum of Lagrangians which agree on a non-compact set. By iterating proposition 3.1.1 at each intersection point we get the following statement about symmetric differences of Lagrangians.

Corollary 3.1.3. *Let L_0 and L_1 be two Lagrangian submanifolds of X . Suppose that for each connected component U_k of the intersection $U = L_0 \cap L_1$, there is a neighborhood $U_k \subset V_k \subset L_0$ which may be identified with a subset $V_k \subset \mathbb{R}^n$. Consider the Weinstein charts $B_\epsilon^* V_k \subset X$. Suppose that L_1 restricted to this chart $B_\epsilon^* V_k$ is the graph of an exact differential form $df_k : V_k \rightarrow B^* V_k$ which vanishes on U_k . Suppose additionally that the primitives f_k are all convex functions on V_k .*

Then there exists a Lagrangian $L_0 \#_U^\epsilon L_1$ in a small neighborhood of the symmetric difference

$$L_0 \#_U^\epsilon L_1 \subset B_\epsilon((L_0 \sqcup L_1) \setminus (L_0 \cap L_1)).$$

and a Lagrangian cobordism $K^\epsilon : (L_0, L_1) \rightsquigarrow L_0 \#_U^\epsilon L_1$.

Example 3.1.4. *We compare our Lagrangian surgery with fixed neck in the non-compact setting to ordinary Lagrangian surgery as drawn in fig. 10. Let $L_0, L_1 \subset T^* S^1$ be a cotangent fiber and its image under inverse Dehn twist around the zero section (see figs. 10a and 10b). An application of proposition 3.1.1 shows that $L_0 \sqcup L_1$ is cobordant to the zero section of $T^* S^1$ by applying surgery on the overlapping regions outside a neighborhood of the zero section (see fig. 10c)*

Let us compare this to the surgery obtained by first perturbing L_1 by the wrapping Hamiltonian θ and then taking the Lagrangian connect sum. Then L_0 and $\theta(L_1)$ intersect at two points, which we can resolve in the usual way. The resulting Lagrangian $L_0 \#(\theta(L_1))$ has three connected components, two of which are non-compact (see fig. 10d.) Despite this, $L_0 \#(\theta(L_1))$ and $L_0 \#_U^\epsilon L_1$ agree as objects of the Fukaya category, as an additional argument shows that the non-compact components of $L_0 \#(\theta(L_1))$ are trivial as objects of the Fukaya category.

In the setting of the cotangent bundle $T^* \mathbb{R}^n$, the connect sum has image under the projection to \mathbb{R}^n which lives in a neighborhood of the complement of the regions U_k . We now examine what the projection to the fiber of $T_0^* \mathbb{R}^n$ of this surgery looks like. Let $\arg : T^* \mathbb{R}^n \rightarrow T_0^* \mathbb{R}^n$ be projection to a cotangent fiber, and for any set U , let $\arg(U)$ be the image of this set under the projection.

Proposition 3.1.5. *Let L_0 and L_1 be sections of $T^* \mathbb{R}^n$ as in proposition 3.1.1. Then for ϵ sufficiently small,*

$$\arg(L_0 \#_U^\epsilon L_1) = \arg(L_1).$$

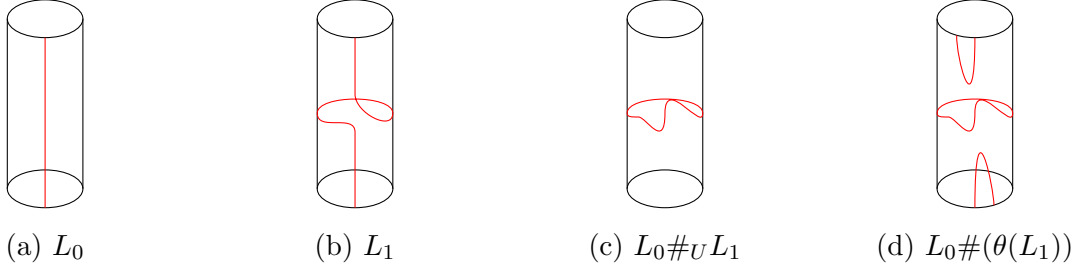


Figure 10: The difference between surgery with neck U and ordinary Lagrangian surgery.

Proof. The decomposition of $L_0 \#_U L_1$ into the r and s charts breaks $\arg(L_0 \#_U L_1)$ into two components,

$$\arg(\{d(r \circ f)(x) \mid \epsilon \leq f(x)\}) \cup \arg(\{d(s \circ f)(x) \mid \epsilon \leq f(x)\}).$$

Choose ϵ small enough that $\arg(\{df(x) \mid f(x) < 2\epsilon\})$ is an interior subset of $\arg(\{df(x) \mid x \in \mathbb{R}^n\})$. Consider the following three parameterized subsets of $T_0^* \mathbb{R}^n$:

$$\begin{aligned} B &: \{x \mid f(x) \leq 2\epsilon\} \xrightarrow{\arg(df)} T_0^* \mathbb{R}^n \\ C_r &: \{x \mid \epsilon \leq f(x) \leq 2\epsilon\} \xrightarrow{\arg(d(r \circ f))} T_0^* \mathbb{R}^n \\ C_s &: \{x \mid \epsilon \leq f(x) \leq 2\epsilon\} \xrightarrow{\arg(d(s \circ f))} T_0^* \mathbb{R}^n \end{aligned}$$

Since $r \circ f = f$ outside of $f(x) \leq 2\epsilon$, to prove the proposition it suffices to check that we have the following equality of subsets,

$$B = C_r \cup C_s.$$

From the chain rule on $r \circ f$ and $s \circ f$ we obtain the inclusion $(C_r \cup C_s) \subset B$. As topological chains, C_r and C_s have boundary components corresponding to where $f(x) = \epsilon$ and $f(x) = 2\epsilon$. The boundary components have the following identifications:

$$\begin{aligned} \partial_{2\epsilon} C_r &= \partial_{2\epsilon} B = \arg(df)|_{f(x)=2\epsilon} \\ \partial_\epsilon C_r &= \partial_\epsilon C_s = \frac{1}{2} \arg(df)|_{f(x)=\epsilon} \\ \partial_{2\epsilon} C_s &= 0 \end{aligned}$$

As the inner boundaries of C_r and C_s match, we may glue these two charts into a single chain C_{r+s} , with boundary $\partial(C_{r+s}) = \partial B + \{0\}$. The chain C_{r+s} provides a contraction of the boundary sphere of B . Since every point of B must be in the image of such a contraction, we obtain (as sets) that $B \subset C_{r+s}$, completing the proof. \square

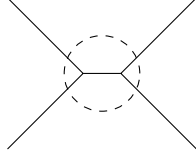


Figure 11: The kind of behavior we wish to rule out by making ϵ small.

3.2 Tropical Lagrangian Sections

There is a nice collection of admissible Lagrangians inside of $\text{Fuk}_\Delta(X, W)$ called the tropical Lagrangian sections of $X \rightarrow Q$ which we will use as building blocks in our construction. These were introduced in [Abo09]. For our model of the Fukaya Seidel category, we use the monomial admissible Fukaya Seidel category $\text{Fuk}_\Delta(X, W)$. This version of the FS category is due to [Han18], and an outline of its construction and extension to the non-monotone setting is in appendix A.

Let $\phi : Q \rightarrow \mathbb{R}$ be a tropical polynomial. Choose ϵ small enough so that for any point $q \in \underline{U}_{\{v_i\}}$ the convex hull of $d\phi(B_\epsilon(q))$ is either all of $\underline{U}^{\{v_i\}}$, or contains $\underline{U}^{\{v_i\}}$ as a boundary component. This means that ϵ is small enough that the induced stratification of $B_\epsilon(q)$ from the tropical variety has at most one vertex. See fig. 11 for a non-example.

Define $\tilde{\phi}^\epsilon$ to be the smoothing of ϕ by convolution with a symmetric bump function ρ_ϵ with support $B_\epsilon(0)$, a small ball around the origin. When we have fixed a size ϵ , we will simplify notation and refer to this as a smoothing $\tilde{\phi}$. The smoothing $\tilde{\phi}$ enjoys many of the same properties of ϕ .

Claim 3.2.1 (Properties of $\tilde{\phi}$). *The function $\tilde{\phi}$ satisfies the following properties.*

- (Nearly Tropical) The function $\tilde{\phi}$ and ϕ agree outside of an ϵ neighborhood of $V(\phi)$
- (Concavity) $\tilde{\phi}$ is a concave function
- (Newton Polytope) $\arg(d\tilde{\phi}(\mathbb{R}^n)) = \Delta_\phi \subset T^*\mathbb{R}^n$.

Proof. The first property comes from the preservation of linear functions under symmetric smoothing. The second property is a general statement about convolutions. The third property follows from the first two. \square

For each $\{v_i\} \subset \Delta_\phi$, let

$$U_{\{v_i\}} := \{q \mid d(\tilde{\phi})(q) \subset \text{Interior Hull of } \{v_i\}\}.$$

Each $U_{\{v_i\}}$ is ϵ -close to $\underline{U}_{\{v_i\}}$ discussed in our earlier treatment of tropical geometry. These sets $U_{\{v_i\}}$ can be characterized in terms of the smoothing ball B_ϵ and the combinatorics of ϕ .

Claim 3.2.2. *The set $U_{\{v_i\}}$ is the set of all points $q \in Q$ such that $d\phi|_{B_\epsilon(q)}$ belongs to $\underline{U}^{\{v_i\}}$, and is not contained in the boundary of $\underline{U}^{\{v_i\}}$.*

Proof. We show two inclusions. If $d\phi|_{B_\epsilon(q)}$ belongs to $\underline{U}^{\{v_i\}}$ then $d\tilde{\phi}(q) \in \underline{U}^{\{v_i\}}$ as the argument of the smoothing convolution is a weighted average over the arguments on the smoothing ball. The only concern may be that $d\tilde{\phi}(q)$ is not in the interior of $\underline{U}^{\{v_i\}}$, however the requirement that $d\phi|_{B_\epsilon(q)}$ is not contained in the boundary of $\underline{U}^{\{v_i\}}$ rules out this possibility. Therefore, $q \in U_{\{v_i\}}$.

Suppose now that $q \in U_{\{v_i\}}$. We would like to show that within an ϵ -radius of q , $d\phi(q)$ belongs to $\underline{U}^{\{v_i\}}$, and that at least one point is not contained in the boundary. We first show containment. Suppose for contradiction that $d\phi|_{B_\epsilon(q)} \not\subset \underline{U}^{\{v_i\}}$. Then take additional vertices w_k so that $d\phi|_{B_\epsilon(q)} \subset U^{\{v_i\} \cup \{w_k\}}$. We break into two cases.

- The set $\{w_k\}$ only contains one element. In this case, the weighted average over arguments defining $d\phi(q)$ cannot possibly lie in $\underline{U}^{\{v_i\}}$.
- The set $\{w_k\}$ contains at least 2 elements. This contradicts our assumption on the size of ϵ , as we now see top dimensional strata corresponding to two different boundaries of $\underline{U}_{\{v_i\}}$.

This proves that $d\phi|_{B_\epsilon(q)} \subset \underline{U}^{\{v_i\}}$. As the value of $d\tilde{\phi}(q)$ is an interior point of $\underline{U}^{\{v_i\}}$, it cannot be the case all of $d\phi|_{B_\epsilon(q)}$ is contained in the boundary of $\underline{U}^{\{v_i\}}$. \square

This claim gives us a clean description of the sets $U_{\{v_i\}}$, and additional information on the restriction of ϕ to each of these subsets.

Claim 3.2.3. *Let ϕ be a tropical polynomial, and $w \in \Delta$ be a (not necessarily lattice) point. Let $\tilde{\phi}$ be a smoothing of ϕ constructed as above. Let $\underline{U}^{\{v_i\}}_{i=0}^k$ be the stratum containing w . Then $d\tilde{\phi}^{-1}(w)$ is locally an $n - k$ dimensional affine subspace of Q , and the restriction of $\tilde{\phi}$ to $d\tilde{\phi}^{-1}(w)$ is linear.*

In the special case of a top dimensional strata, we have an inclusion $U_v \subset \underline{U}_v$, and $d(\tilde{\phi})|_{U_v} = v$.

The graph of $d\tilde{\phi}$ is a Lagrangian in T^*Q rather than in $X = (\mathbb{C}^*)^n$, but after periodizing the cotangent bundle, we get sections of the SYZ fibration.

Definition 3.2.4 ([Abo09]). *The tropical Lagrangian section $\sigma_\phi^\epsilon : Q \rightarrow X$ associated to ϕ is the composition*

$$\begin{array}{ccc} T^*Q & \xrightarrow{\wedge T_{\mathbb{Z}}^*Q} & X \\ \downarrow d\tilde{\phi}^\epsilon & & \\ Q & & \end{array}$$

When the smoothing radius ϵ is not important, we will drop it and simply write σ_ϕ . The key observation is that for each lattice point v ,

$$\sigma_\phi|_{U_v} = \sigma_0|_{U_v}. \tag{3}$$

Given a monomial admissibility condition $(W_\Sigma, \Delta_\Sigma)$, we say that ϕ is an admissible tropical polynomial if σ_ϕ is an admissible Lagrangian. From here on out, we will only work with admissible tropical polynomials.

After taking an admissible Hamiltonian perturbation of σ_0 , the intersections between $\sigma_{-\phi}$ and σ_0 become transverse and are in bijection to the lattice points of Δ_ϕ . This observation, along with a characterization of holomorphic strips on convex functions allows one to describe the Floer cohomology of the tropical Lagrangian sections combinatorially.

Theorem 3.2.5 ([Abo09; Han18]). *Let \check{X}_Σ be a toric variety, and let (X, W_Σ) be its mirror Landau-Ginzburg model. Let Δ_Σ be a monomial admissibility condition. Let ϕ_1, ϕ_2 be the support functions for line bundles on \check{X}_Σ . Then after appropriately localizing, there is a quasi-isomorphism*

$$CF^\bullet(\sigma_{\phi_1}, \sigma_{\phi_2}) = \hom(\mathcal{O}(\phi_1), \mathcal{O}(\phi_2)).$$

Furthermore, the A_∞ structure on the Fukaya category is quasi-isomorphic to the dg-structure on the derived category of coherent sheaves on \check{X}_Σ .

Assuming \check{X}_Σ is smooth and projective, line bundles generate the derived category of coherent sheaves on \check{X}_Σ . This proves that the subcategory of $\text{Fuk}_\Delta(X, W_\Sigma)$ generated by tropical Lagrangian sections is equivalent to $D^b \text{Coh}(\check{X}_\Sigma)$.

3.3 Tropical Lagrangian Hypersurfaces

For this section, we fix $(W_\Sigma, \Delta_\Sigma)$ some monomial division and work in the setting where theorem 3.2.5 holds.

It is usually desirable for Lagrangians to be in a transverse intersection. However, the highly non-transverse configuration of unperturbed tropical Lagrangian sections will work in our favor as locally the intersection of σ_0 and $\sigma_{-\phi}$ is given by the graphs of one-forms with convex primitives. This allows us to apply our surgery profile from proposition 3.1.1.

Definition 3.3.1. *Let ϕ be a tropical polynomial on \mathbb{R}^n . Let $\{U_v \mid \dim U_v = n\}$ be the collection of intersections between σ_0 and $\sigma_{-\phi}$ corresponding to monomials of ϕ , i.e. the top-dimensional linearity strata $Q_n \setminus Q_{n-1}$ of ϕ . We define the tropical Lagrangian associated to ϕ and necks U_v by the surgery*

$$L(\phi) := (\sigma_0) \#_{\{U_v\}}^\epsilon (\sigma_{-\phi})$$

In the definition of a tropical Lagrangian submanifold, we've taken the connect sum along each strata of U_v corresponding to the non-self-intersection strata of the tropical polynomial ϕ . As a result, a tropical variety with self-intersections only lifts to an immersed Lagrangian. These intersections may be transverse, but they need not be — an example is $\phi = x_1 \oplus x_2 \oplus \frac{1}{x_1 x_2}$ as a tropical function on $Q = \mathbb{R}^3$, where the self-intersection is a clean intersection $\mathbb{R} \subset L(\phi)$.

The distinction in terminology between the smoothness and self-intersections of tropical curves becomes important at this juncture. Let us compare the complex and Lagrangian lifts of the tropical curve $V(\phi) = 1 \oplus x_1 \oplus x_2 \oplus x_1 x_2$. This is not a smooth tropical curve, but has no self-intersections. The complex variety $1 + z_1 + z_2 + z_1 z_2 = 0$ has a single self-intersection along $z_1 = z_2 = -1$. However, the tropical Lagrangian $L(\phi)$ does not have such a self-intersection.

We now summarize some properties of these tropical Lagrangians.

Theorem 3.3.2. *Let ϕ be a tropical polynomial. The tropical Lagrangian hypersurface $L^\epsilon(\phi)$ and corresponding cobordism $K^\epsilon(\phi)$ satisfy the following geometric properties:*

- **Independence from Choices:** Different choices of parameters in the construction of these Lagrangians produce Hamiltonian isotopic tropical Lagrangians.
- **Valuation Projection:** As ϵ approaches zero, the valuation of our tropical Lagrangian $\text{val}(L^\epsilon(\phi))$ approximates the tropical hypersurface $V(\phi)$.
- **Argument Projection:** The argument projection $\arg(L(\phi))$ is the Newton polytope Δ_ϕ associated to the line bundle $\mathcal{O}(-D)$.
- **Topology:** The self-intersections of $L(\phi)$ are in bijection with the lattice points $v \in \Delta_\phi$ where the tropical polynomial never achieves the value of a monomial with exponent v . In particular, when $V(\phi)$ is a smooth tropical variety, $L(\phi)$ is embedded.

Additionally, they satisfy these technical requirements giving them well defined Floer cohomology.

- **Unobstructedness:** There exists an unobstructing bounding cochain on the Lagrangian cobordism $K(\phi) : (\sigma_0, \sigma_{-\phi}) \rightsquigarrow L(\phi)$
- **Admissibility:** Let $(W_\Sigma, \Delta_\Sigma)$ be a monomial admissibility condition as defined in [Han18]. Then whenever $\sigma_{-\phi}$ is monomially admissible, so are $L(\phi)$ and $K(\phi)$.

Proof. The proof of the geometric properties are propositions 3.1.1, 3.3.3 and 3.1.5 and definition 3.3.1, and the proofs of the Floer cohomology properties are propositions 3.3.4 and 3.3.8. \square

3.3.1 Independence from Choices

In our definition of $L(\phi)$, we've made two choices: a size of neck for the Lagrangian surgery, and a choice of radius for the smoothing function ρ_ϵ . Fortunately, neither of these choices affect the Hamiltonian isotopy class of $L(\phi)$.

Proposition 3.3.3. *Assume that ϕ has no self-intersections. For parameters $\alpha_1, \alpha_2, \beta_1, \beta_2$ sufficiently small, the Lagrangians*

$$\sigma_0 \#_{\{U_v\}}^{\beta_1} (\sigma_{-\phi}^{\alpha_1}) \quad \sigma_0 \#_{\{U_v\}}^{\beta_2} (\sigma_{-\phi}^{\alpha_2})$$

are Hamiltonian isotopic.

Proof. These two Lagrangians are Lagrangian isotopic, as we can smoothly vary the parameters α and β in our construction. Let L_t be a Lagrangian isotopy between the choices of data. Since $(\mathbb{C}^*)^n$ is exact, we can prove the proposition by showing that the integral of the Liouville form $d\eta = \omega$ on cycles of L_t is independent of the choices that we've made. For this computation, we will choose a convenient basis for $H_1(L(\phi))$.

We now assume that $L(\phi)$ is connected, and the 0 is a lattice point of Δ_ϕ . To compute $H_1(L(\phi))$, decompose $L(\phi) = L_r \cup L_s$, where L_r and L_s are the charts corresponding to the profiles $r(t), s(t)$ in figs. 7a and 7b. These charts are homotopic to the tropical amoeba $\mathbb{R}^n \setminus \{U_v\}$, so $H_1(L_s) = H_1(L_r) = H_1(V(\phi))$. The Meyer-Vietoris sequence allows us to decompose the homology of $L(\phi)$ as

$$H_1(L(\phi)) = H_1(V(\phi)) \oplus H_0(L_r \cap L_s, \mathbb{Z})/\mathbb{Z}$$

The connected components of $L_r \cap L_s$ are in bijection with the smooth lattice points of Δ_ϕ , giving $\{e_v\}_{v \in \mathbb{Z}^n \cap \Delta_\phi \setminus 0}$ as an explicit basis for $H_0(L_r \cap L_s, \mathbb{Z})/\mathbb{Z}$. For each top strata $\underline{U}_{\{v_i, v_j\}}$ of our tropical hypersurface, define the cycle

$$c_{\{v_i, v_j\}} = e_{v_i} - e_{v_j}.$$

The cycles $c_{\{v_i, v_j\}}$ along with the inclusion of $H_1(V(\phi))$ generate $H_1(L(\phi))$. Geometrically the $c_{\{v_i, v_j\}}$ arise as the conormal fiber to the $\underline{U}_{\{v_i, v_j\}}$ strata of our tropical Lagrangian. We now compute the integral of η on generators for $H_1(L(\phi))$ coming from this decomposition.

To compute the integral of the Liouville form on a cycle c included via $i : H_1(V(\phi)) \hookrightarrow H_1(L(\phi))$, we may always select a representative for c which lies completely inside of the chart L_r . Since L_r is exact, the Liouville form vanishes, $\eta(c) = 0$ and we may conclude $\eta(i(H_1(V(\phi)))) = 0$. Therefore, the integral of the Liouville form on this portion of homology is independent of the choices α_i, β_i .

To compute the integral of the Liouville form on cycles which are of the form $c_{\{v_i, v_j\}}$, we give a local description of $L(\phi)$ containing the cycle $c_{\{v_i, v_j\}}$. We now need to make an assumption on the size of ϵ , so that at each facet $\underline{U}_{\{v_i, v_j\}}$ there exists a point $p \in U_{\{v_i, v_j\}}$ with a sufficiently small neighborhood

$$B_{2\epsilon}(p) \subset \left(\underline{U}_{\{v_i, v_j\}} \cup \underline{U}_{\{v_i\}} \cup \underline{U}_{\{v_j\}} \right).$$

We assume that α_i, β_i are smaller than this ϵ .

When restricted to $B_\epsilon(p)$, the tropical Lagrangian ϕ has only 2 domains of linearity, and so the restriction may be written as $\phi|_{B_\epsilon} = a_{v_i}x^{v_i} \oplus a_{v_j}x^{v_j}$. Because of the extra ϵ of room from the larger neighborhood $B_{2\epsilon}(p)$, the smoothing $\tilde{\phi}|_{B_\epsilon}$ is only dependent on the local combinatorics of our strata. The function $\tilde{\phi}|_{B_\epsilon}$ is invariant with respect to translations in the $(v_i - v_j)^\perp$ hyperplane. This means that the function $\tilde{\phi}|_{B_\epsilon}$ factors as $\tilde{\psi}(x^{v_i - v_j})$ where $\tilde{\psi}$ is the smoothing of a tropical function $a_0 \oplus a_1t$. This function has the symmetry

$$d\tilde{\psi}(t) = -d\tilde{\psi}(-t) + 1 \tag{4}$$

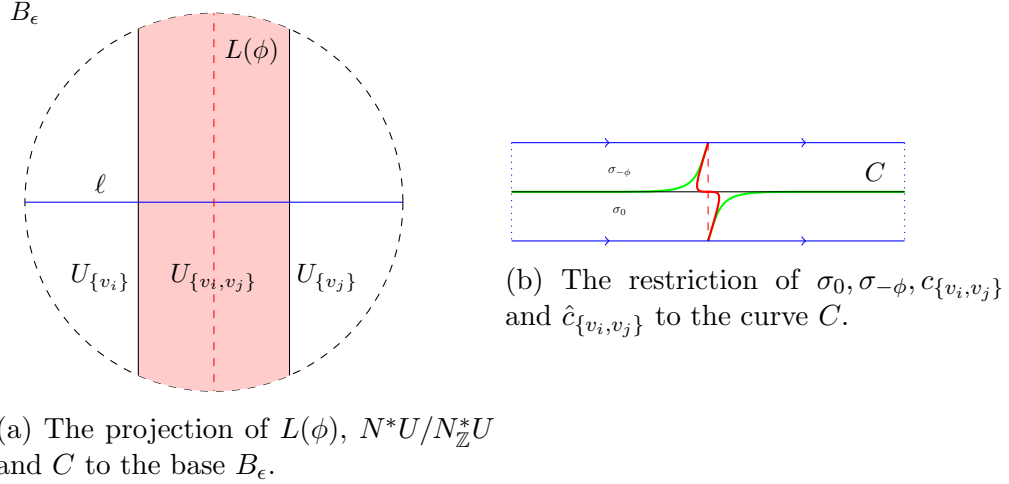


Figure 12

We now will construct a cycle representing the homology class $[c_{\{v_i, v_j\}}]$. Consider the holomorphic cylinder C which is the lift of the line

$$\ell = t(v_i - v_j) + p \subset B_\epsilon$$

to a complex curve $C = T^*\ell/T_{\mathbb{Z}}^*\ell \subset \text{val}^{-1} B_\epsilon$. The intersection of C with $L(\phi)|_{B_\epsilon}$ is a representative for the class $c_{\{v_i, v_j\}}$. Consider now the cycle $\hat{c}_{\{v_i, v_j\}} \subset C$ which is given by the intersection $C \cap N_{U_{\{v_i, v_j\}}}^*$. If we can show that $\eta(c_{\{v_i, v_j\}}) = \eta(\hat{c}_{\{v_i, v_j\}})$, we will be finished as we will have shown that $\eta(c_{\{v_i, v_j\}})$ is independent of choices of α_i, β_i . The difference between these two quantities $\int_{c_{\{v_i, v_j\}} - \hat{c}_{\{v_i, v_j\}}} \eta$ is now equated with the symplectic area between these two cycles on the holomorphic cylinder C . We now recenter our coordinates so that p is at the origin. In these coordinates, the symmetry from eq. (4) translates into the odd symmetry of the tropical section

$$\sigma_\phi(t \cdot (v_i - v_j)) = -\sigma_\phi(-t(v_i - v_j)).$$

The cycle $c_{\{v_i, v_j\}} \subset C$ also inherits this symmetry. We may use this symmetry to decompose the integral

$$\int_{c_{\{v_i, v_j\}} - \hat{c}_{\{v_i, v_j\}}} \eta$$

into two equal cancelling components, and conclude that $\eta(c_{\{v_i, v_j\}}) = \eta(\hat{c}_{\{v_i, v_j\}})$. \square

Proposition 3.3.3 shows we can take a Hamiltonian isotopy to bring $\text{val}(L(\phi))$ arbitrarily close to $V(\phi)$ if desired. The Lagrangian $L(\phi)$ does project to a tropical amoeba of $\text{val}(L(\phi))$ as the tentacles of the Lagrangian do not winnow off to zero radius as we increase valuation.

3.3.2 Floer Theory: Admissibility and Unobstructedness

In order for us to study this object in the Fukaya category, we will have to show that it satisfies the admissibility conditions of $\text{Fuk}_\Delta(X, W)$, and show that this Lagrangian is unobstructed.

Proposition 3.3.4. *Suppose that the section $\sigma_{-\phi}$ is Δ_Σ admissible. Then $L(\phi)$ is Δ_Σ admissible.*

Proof. In order to show that $L(\phi)$ is admissible, we need show that over each region C_α from definition A.0.1, the argument of $c_\alpha z^\alpha$ is zero outside of a compact set. If we associate the exponent α to a vector $\alpha \in \mathbb{Z}^n$, the admissibility condition can be restated as the argument of L lying inside the $T_{\alpha^\perp}^{n-1}$ subtorus of the fibers F_q of $(\mathbb{C}^*)^n$ over the regions of C_α . Both $\sigma_{-\phi}$ and σ_0 are constrained within this subtorus as $\arg(\sigma_{-\phi}), \arg(\sigma_0) \subset T_{\alpha^\perp}^{n-1}$ on the region C_α . Proposition 3.1.5 allows us to conclude that $\arg(\sigma_0 \#_U \sigma_{-\phi}) = \arg(L(\phi))$ is similarly contained within the region C_α . \square

The Lagrangian $L(\phi)$ is not necessarily monotone. However, as a corollary of proposition 3.3.3, the only disks which may appear on our tropical Lagrangian have Maslov index 0.

Corollary 3.3.5. *The Maslov class of $L(\phi)$ is trivial in $H^1(L, \mathbb{Z})$.*

Proof. The cycles in homology which arise from $H_1(V(\phi))$ will all live in the zero section, and near these cycles $L(\phi)$ agrees with the zero section and therefore has Maslov class zero. For the other generators of homology, take a Hamiltonian isotopy of our tropical Lagrangian so that in a neighborhood of a cycle $c_{\{v_i, v_j\}}$ the Lagrangian $L(\phi)$ agrees with $N^*U_{\{v_i, v_j\}}/N_{\mathbb{Z}}^*U_{\{v_i, v_j\}}$ (see the proof of proposition 3.3.3). This is a special Lagrangian, and so the Maslov class of $c_{\{v_i, v_j\}}$ is zero as well. \square

Hence, every disk with boundary on $L(\phi)$ has Maslov index zero. As a result, in low dimensions disks will show up in negative dimensional families, and therefore do not appear for regular J .

Corollary 3.3.6. *For $n = 1, 2$, the Lagrangians $L(\phi) \subset (\mathbb{C}^*)^n$ bound no holomorphic disks for regular J .*

In the general case, we cannot hope for this kind of unobstructedness result. Later we will explore a mutation structure on these Lagrangian submanifolds, and we'll show that there exists almost complex structures so that $L(\phi)$ bounds disks of Maslov index 0 (See corollary 3.4.5.) Despite this, our expectation is that the tropical Lagrangians $L(\phi)$ do not bound holomorphic disks for the standard J .

Conjecture 3.3.7. *With the standard complex structure the Lagrangian cobordism $K(\phi)$ bounds no holomorphic disks.*

See [SS18, Remark 1.4] for a similar discussion on the presence of holomorphic disks on tropical Lagrangians.

Instead, we show that the pearly A_∞ algebra of this Lagrangian cobordism is unobstructed by bounding cochain. The model that we use for the pearly A_∞ algebra is the “treed-disk” model as described in [Fuk93; CL06; CW15; LW14]. In this model, we pick a Morse function $h : L \rightarrow \mathbb{R}$ for our Lagrangian, and the Floer group $CF^\bullet(L, h)$ is an A_∞ algebra arising as a deformation of the Morse complex by inserting holomorphic disks at the vertices of Morse flow trees. When the Morse function is unimportant, we will simply write $CF^\bullet(L)$. An outline of the pearly model and bounding cochains is included in appendix A.

Proposition 3.3.8. *The Lagrangian $L(\phi)$ is unobstructed by bounding cochain.*

The proof is in three steps. We first describe a geometric relation between $L(\phi)$ and $L^{tr}(\phi)$, the transverse intersection between two sections. We then show that $CF^\bullet(L(\phi))$ may be expressed as a quotient of the Floer theory of $CF^\bullet(L^{tr}(\phi))$. Finally, we show that $CF^\bullet(L^{tr}(\phi))$ is unobstructed by bounding cochain.

3.3.3 Unobstructedness: Some tools

Before proving proposition 3.3.8, we look at three tools largely independent from the discussion of tropical Lagrangians. The first is a comparison between our tropical Lagrangians and the geometry of symplectic fibrations. The second is a statement about bottlenecked Lagrangians and their bounding cochains. The third is an existence result for bounding cochains on sequences of Lagrangians converging to tautologically unobstructed Lagrangians.

Tropical Symplectic Fibrations. We now summarize a discussion in [Han18] relating the monomial admissibility condition to an admissibility condition by [Abo09] called the tropically localized superpotential.

Definition 3.3.9. *Let $W : (\mathbb{C}^*)^n \rightarrow \mathbb{C}$ be a symplectic fibration, and let $M = W^{-1}(1)$. A W -admissible Lagrangian with boundary on M is a compact Lagrangian L with boundary on M . We additionally require that $W(L) \subset \mathbb{R}_{\leq 1}$ in $D \subset \mathbb{C}$, a neighborhood of $1 \in \mathbb{C}$.*

Starting with an ample divisor $\sum v_\alpha D_\alpha$ on X with polytope P , Abouzaid constructs a family of superpotentials $W_{t,1} : (\mathbb{C}^*)^n \rightarrow \mathbb{C}$ deforming W_Σ . The fiber $M_{t,1} := W_{t,1}^{-1}(1)$ has valuation projection $\text{val}(M_{t,1})$ which lives close to a tropical variety. Additionally, $Q \setminus \text{val}(M_{t,1})$ has a distinguished connected component $\mathcal{P}_{t,1}$ which can be rescaled to lie close to P . Near the boundary of P , the tropically localized superpotential can be explicitly written as

$$W_{t,1} = \sum_{\alpha} t^{-v_\alpha} (1 - \rho_\alpha(z)) z^\alpha$$

where the ρ_α are smooth functions. The functions $\rho_\alpha(z)$ only depend on $\text{val}(z)$, and are constructed so that

- Whenever $\text{val}(z)$ is outside a small neighborhood of the dual facet of α , $\phi(z) = 1$.

- Whenever $\text{val}(z)$ is nearby the dual face of α , $\phi(z) = 0$.

The upshot of working with the tropically localized superpotential is the following. With the usual superpotential, the fiber $W_\Sigma^{-1}(1)$ should roughly have a decomposition into regions where the subsets of monomials of W_Σ codominate the other terms. On each of these regions, W_Σ is approximately equal to the dominating monomials. With the tropically localized superpotential the surface $M_{t,1}$ similarly admits a decomposition, however $W_{t,1}$ honestly matches the dominating monomials on each region of domination.

The monomial admissibility condition for $W = \sum c_\alpha z^\alpha$ only requires that each monomial term z_α dominates in the region C_α after possibly being raised to some power k_α . We may assume that the k_α are rational, and therefore find an integer N and rescalings c_α^N of c_α defining a new Laurent polynomial

$$\tilde{W}_N := \sum_\alpha c_\alpha^N z^{\alpha \cdot k_\alpha \cdot N}.$$

Associated to this W_N we have a divisor D_N and polytope $P_N \subset Q$. As we increase N , the polytopes P_N scale to cover all of Q . Therefore, we may additionally assume that N is chosen large enough so that a given monomially admissible Lagrangian L satisfies the monomial admissibility condition in a neighborhood of the boundary of P_N .

As $W_{t,1}$ only involves the monomials z^α for which $\text{val}(z) \in C_\alpha$, and $z^\alpha(L) \in \mathbb{R}_+$ over these regions, we may conclude:

Lemma 3.3.10 ([Han18]). *Suppose that L is a monomial admissible Lagrangian submanifold. Then $L \cap \text{val}^{-1}(P)$ is a $W_{t,1}$ admissible Lagrangian submanifold with boundary on $M_{t,1}$.*

See, for instance, fig. 13a.

Bottlenecked Lagrangians and Bounding Cochains.

Definition 3.3.11. *Let $W : X \rightarrow \mathbb{C}$ be a symplectic fibration. We say that L is bottlenecked by $z_{bn} + i\mathbb{R} \in \mathbb{C}$ if in a neighborhood B of $W^{-1}(z_{bn} + i\mathbb{R})$, we have that*

$$W(L \cap B) = \{z_{bn} + t, t \in (-\epsilon, \epsilon)\}.$$

The condition of being bottlenecked means that our Lagrangian L looks like the concatenation of two Lagrangian cobordisms in a neighborhood of z_{bn} . Let $L \setminus W^{-1}(z_{bn}) = L^- \cup \bar{L}^+$, where

$$\begin{aligned} L^- &= L \cap \{z \mid \text{Re}(z) < \text{Re}(z_{bn})\} \\ \bar{L}^+ &= L \cap \{z \mid \text{Re}(z) \geq \text{Re}(z_{bn})\}. \end{aligned}$$

Recall that if L^+ is a manifold with boundary, the Morse cohomology relative boundary is computed by taking a Morse function whose flow is transverse and points inwards from the boundary ∂L^+ . If L is bottlenecked, there exists a Morse function $h : L \rightarrow \mathbb{R}$ so that the Morse complex of L splits as a vector space

$$CM^\bullet(L; h) = CM^\bullet(L^-; h|_{L^-}) \oplus CM^\bullet(L^+, \partial L^+; h|_{L^+})$$

In this setup, the flow of h is transverse to the fiber $W^{-1}(z_{bn})$, and points in the positive direction.

The values z_{bn} are called bottlenecks as flow lines only travel from the left side of $z_{bn} + i\mathbb{R}$ to the right side. As a result, $CM^\bullet(L^+, \partial L^+)$ is an ideal of $CM^\bullet(L)$, and

$$CM^\bullet(L^-; h|_{L^-}) = CM^\bullet(L, h) / CM^\bullet(L^+, \partial L^+; h|_{L^+}).$$

This decomposition extends to the Floer cohomology.

Claim 3.3.12. *Suppose that L is a bottlenecked Lagrangian. If assumption A.3.2 holds and our regularization method of treed disks is compatible with the open mapping principle, then for the Morse function h described above,*

$$CF^\bullet(L; h) = CF^\bullet(L^-; h|_{L^-}) \oplus CF^\bullet(L^+, \partial L^+; h|_{L^+})$$

Furthermore, $CF^\bullet(L^+, \partial L^+; h|_{L^+})$ is an ideal of $CF^\bullet(L; h)$.

Proof. The only portion which needs to be checked is that $CF^\bullet(L^+, \partial L^+)$ is an ideal. Let $u : \mathcal{T} \rightarrow X$ be any treed disk with boundary on L . Every disk component $u_v : (D, \partial D) \rightarrow (X, L)$ whose image under the valuation map intersects the bottleneck $W(u_v) \cap \{z_{bn} + t, t \in (-\epsilon, \epsilon)\}$ must be constant under composition with W by the open mapping principle. Therefore, for such disks u_v , we may write $W(u_v) = z_{bn} + t_v$ for some $t_v \in (-\epsilon, \epsilon)$. Therefore, the disk-portions of treed disks cannot have image intersecting both

$$\begin{aligned} W^{-1}(\{z_{bn} + t, t \in (0, \epsilon)\}) \cap L \\ W^{-1}(\{z_{bn} + t, t \in (-\epsilon, 0)\}) \cap L. \end{aligned}$$

Additionally, the gradient flow of h near t necessarily flows right and therefore away from z_{bn} . Therefore there are no treed disks connecting critical points on the positive end of the bottleneck to an output on the negative side of the bottleneck. \square

Note that there is nothing which prevents treed disks from having input in $CF^\bullet(L^-)$ and output in $CF^\bullet(L^+, \partial L^+)$. Since $CF^\bullet(L^+, \partial L^+)$ is an ideal of $CF^\bullet(L)$, we have a projection map $\pi : CF^\bullet(L) \rightarrow CF^\bullet(L^-)$. It immediately follows that

Corollary 3.3.13. *Suppose that L is bottlenecked, and $CF^\bullet(L)$ admits a bounding cochain. Then $CF^\bullet(L^-)$ admits a bounding cochain.*

Eventually Unobstructed Lagrangians and Bounding Cochains.

Definition 3.3.14. Let $\{L_\alpha\}_{\alpha \in \mathbb{N}}$ be a sequence of Hamiltonian isotopic Lagrangian submanifolds. We say that this sequence is eventually unobstructed if for every energy level λ , there exists α_λ so that $\beta \geq \alpha_\lambda$ implies that L_β bounds no holomorphic disks of energy less than λ belonging to treed disks contributing to $CF^\bullet(L_\beta)$.

Lemma 3.3.15. Let $\{L_\alpha\}_{\alpha \in \mathbb{N}}$ be a sequence of Hamiltonian isotopic Lagrangian submanifolds, and let $\{K_{\alpha, \alpha+1}\}_{\alpha \in \mathbb{N}}$ be the sequence of suspension cobordisms corresponding to choices of Hamiltonian isotopies between L_α and $L_{\alpha+1}$. Suppose both $\{L_\alpha\}_{\alpha \in \mathbb{N}}$ and $\{K_{\alpha, \alpha+1}\}_{\alpha \in \mathbb{N}}$ are eventually unobstructed sequences of Lagrangian submanifolds. Then L_0 is unobstructed by bounding cochain.

Proof. For Lagrangian L_α , we let m_α^k be the product structure on $CF^\bullet(L_\alpha)$. For a deforming chain $d \in CF^\bullet(L_\alpha)$, we let $(m_\alpha^k)_d$ be the deformed curved A_∞ structure. By our assumption, for each λ there is a α_λ so that $\beta \geq \alpha_\lambda$ implies that $\text{val}(m_\beta^0)$ will be greater than λ .

The suspension cobordism $K_{\alpha, \beta}$ given by the concatenation of our Lagrangian cobordisms induces a Λ -filtered curved A_∞ homomorphism

$$f_{\alpha, \beta} : CF^\bullet(L_\alpha) \rightarrow CF^\bullet(L_\beta)$$

as defined in proposition A.3.9. As these continuation maps are constructed by concatenation of cobordisms,

$$f_{\beta, \gamma} \circ f_{\alpha, \beta} = f_{\alpha, \gamma}.$$

Given a deformation $b_\alpha \in CF^\bullet(L_\alpha)$ and a (unital) curved A_∞ homomorphism $f_{\alpha, \beta} : CF^\bullet(L_\alpha) \rightarrow CF^\bullet(L_\beta)$, we get a pushforward map on deformations

$$b_\beta = (f_{\alpha, \beta})_*(b_\alpha) := \sum_{k \geq 0} f_{\alpha, \beta}^k(b_\alpha^{\otimes k}).$$

If b_α is a (weak) bounding cochain for $CF^\bullet(L_\alpha)$, then this pushforward is again a (weak) bounding cochain. The same is true for deformations which are bounding cochains up to a low valuation.

Claim 3.3.16. Suppose that $(m_\alpha^0)_{b_\alpha}$, the b_α deformed curvature term of $CF(L_\alpha)$, has valuation greater than λ . Let $b_\beta = (f_{\alpha, \beta})_*(b_\alpha)$. Then $(m_\beta^0)_{b_\beta}$ has valuation greater than λ .

In the simplest example, we define $b_\alpha = (f_{\alpha, 0})_*(0) \in CF^\bullet(L_0)$ be the pushforward of the trivial deformation of L_α . This deformation may be rewritten using the quadratic A_∞ relations as

$$(m_0)_{b_\alpha}^0 = \sum_k m_0^k(((f_{\alpha, 0})_*(0))^{\otimes k}) = \sum_k m_0^k((f_{\alpha, 0}^0)^{\otimes k}) = f_{\alpha, 0}^1 m_\alpha^0.$$

The condition that our Lagrangians successively only bound disks of increasing energy means that the m_α^0 have increasing valuation, so the sequence of cochains $(m_0)_{b_\alpha}^0 = (f_{\alpha, 0})_*(0)$

unobstruct $CF(L_0)$ to higher and higher valuations. We now show that this sequence $\{f_{\alpha,0}^0\}$ of deforming cochains converge to an actual bounding cochain.

From the quadratic relation for composition of A_∞ homomorphisms $f_{\alpha+1,0} = f_{\alpha,0} \circ f_{\alpha+1,\alpha}$ we obtain

$$f_{\alpha+1,0}^0 = \sum_{k \geq 0} f_{\alpha,0}^k((f_{\alpha+1,\alpha}^0)^{\otimes k}) = f_{\alpha,0}^0 + \sum_{k \geq 1} f_{\alpha,0}^k((f_{\alpha+1,\alpha}^0)^{\otimes k}).$$

To prove the convergence, it suffices to show that the differences

$$f_{\alpha+1,0}^0 - f_{\alpha,0}^0 = \sum_{k \geq 1} f_{\alpha,0}^k((f_{\alpha+1,\alpha}^0)^{\otimes k})$$

converge to zero (as we are proving convergence in an ultrametric space.) This can be done by providing a lower bound for the valuation of $f_{\alpha+1,\alpha}^0$. The valuation of $f_{\alpha+1,\alpha}^0$ can be bounded below by the energy of the smallest holomorphic disk which occurs in the Hamiltonian suspension cobordism $K_{\alpha,\alpha+1}$ between L_α and $L_{\alpha+1}$. By assumption, the minimal energy of a holomorphic disk can be bounded below by picking sufficiently large α . This shows that the valuation of the $f_{\alpha,\alpha+1}$ goes off to infinity, proving that the sequence of cochains $(f_{\alpha,0}^0)_*(0)$ converge in $CF^\bullet(L_0)$. \square

3.3.4 Unobstructedness: Returning to the Proof

We now compare the surgery profile defined in proposition 3.1.1, and the standard transversal surgery.

Claim 3.3.17. *Suppose that $U = L_0 \cap L_1$ is a compact convex region, satisfying the conditions for taking the generalized Lagrangian surgery as in proposition 3.1.1. Then there exists another Lagrangian L_1^1 which intersects L_0 transversely at a unique point q . Furthermore, $L_0 \#_q L_1^1$ is Lagrangian isotopic to $L_0 \#_U L_1$.*

Proof. We first describe a family of Lagrangians L_1^α . Let $U_1 \supset U_0 \supset U$ be small collared neighborhoods of U , and let $h^\alpha : [0, 1]_\alpha \times U_1 \rightarrow \mathbb{R}$ be a family of smooth functions satisfying the following:

- As a section, $dh^0 = L_1$ on all of U_1 .
- As a section, $dh^\alpha = L_1$ on $U_1 \setminus U_0$ for all α .
- $dh^1(x) = (\text{dist}_q(x))^2$ in a small neighborhood of q .
- h^α is convex for every α .

Let L_1^α be the Lagrangian obtained by removing the portion of L_1 which lives above U_0 , and gluing in dh^α instead. Clearly L_1^1 and L_1 are Lagrangian isotopic. By construction L_1^1 and L_0 intersect transversely. For each α , the Lagrangians L_0 and L_1^α have convex intersection region U_α . We may construct the surgeries $L_0 \#_{U^\alpha} L_1^\alpha$ in a smooth family. Since (with

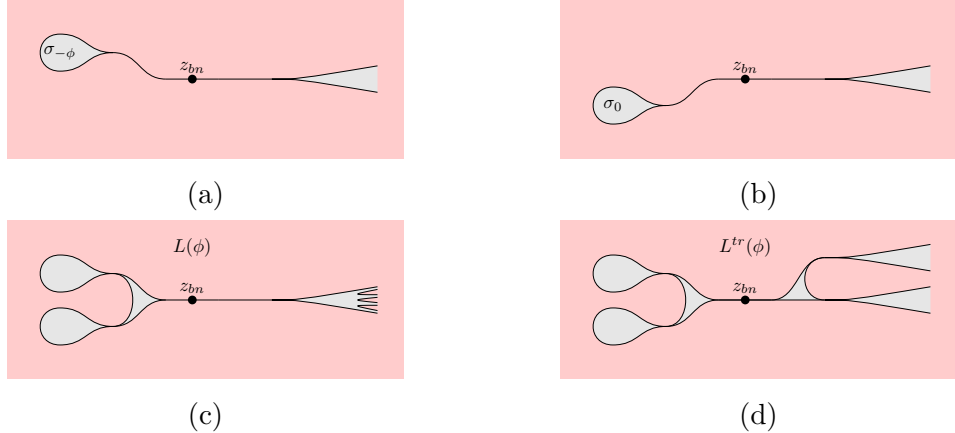


Figure 13: A comparison between $L^{tr}(\phi)$ and $L(\phi)$ under the projection of $W_{t,1}$

appropriate choices of surgery neck) $L_0 \#_{U^1} L_1^1 = L_0 \#_q L_1^1$, we may conclude that there is Lagrangian isotopy between our generalized Lagrangian surgery and the standard transverse surgery. \square

We will use this comparison for our tropical Lagrangians. We define the set

$$C_1 := W_{t,1}^{-1}(\{z \text{ such that } |z| \leq 1\}).$$

Claim 3.3.18. *Suppose that ϕ is a smooth tropical polynomial. Let $W_{t,1}$ be a tropically localized superpotential so that $L(\phi)|_{P_N}$ is $W_{t,1}$ admissible. There exists a monomial admissible Hamiltonian wrapping isotopy (see definition A.3.16) θ so that σ_0 and $\theta(\sigma_{-\phi})$ have transverse intersections q_v for each $v \in \Delta_\phi^\mathbb{Z}$. Furthermore there exists a Lagrangian $L^{tr}(\phi)$ satisfying the following properties:*

- $L^{tr}(\phi)$ is admissibly Lagrangian isotopic to $\sigma_0 \#_{\{q_v\}}(\theta(\sigma_{-\phi}))$.
- $L^{tr}(\phi)$ agrees with $L(\phi)$ on the set C_1 .

The Lagrangians $L^{tr}(\phi)$ and $L(\phi)$ are compared in fig. 13.

Note that $L(\phi)$ is bottlenecked by the symplectic fibration $W_{t,1}$. Similarly, the Lagrangian $L^{tr}(\phi)$ is bottlenecked by this symplectic fibration at the point $z_{bn} = 1$. Let $L^{tr,-}(\phi)$ and $L^{tr,+}(\phi)$ be the negative and positive ends of the bottleneck. By design, $L^{tr,-}(\phi)$ matches $L^-(\phi)$.

Claim 3.3.19. *$CF^\bullet(L(\phi))$ and $CF^\bullet(L^-(\phi))$ are isomorphic as curved A_∞ algebras.*

This follows from observing that the gradient flow of a monomially admissible Morse function at the boundary $\partial L^-(\phi)$ points outward, and that one can pick Morse function for $L(\phi)$ which only has critical points in the overlapping region with $L^-(\phi)$. By additionally picking matching Morse functions for $L^{tr,-}(\phi)$ and $L^-(\phi)$, we may conclude:

Lemma 3.3.20. *If $CF^\bullet(L^{tr}(\phi))$ is unobstructed by bounding cochain, then so is $CF^\bullet(L(\phi))$.*

This is virtue of the curved A_∞ homomorphisms

$$CF^\bullet(L^{tr}(\phi)) \xrightarrow{\pi^-} CF^\bullet(L^{tr,-}(\phi)) \xrightarrow{\sim} CF^\bullet(L(\phi)).$$

It remains to prove that $L^{tr}(\phi)$ is unobstructed by bounding cochain. We do this by constructing an eventually unobstructed sequence starting at $L^{tr}(\phi)$. We now describe a sequence of Hamiltonian isotopic Lagrangian submanifolds $\{L_\alpha^{tr}\}_{\alpha \in \mathbb{N}}$, with $L_0^{tr} = L^{tr}(\phi)$.

For notation, we denote the union of two tropical sections which have been made transverse by an infinitesimal wrapping Hamiltonian as $L_\infty^{tr} := \sigma_0 \cup (\theta'(\sigma_{-\phi}))$. For each $v \in \Delta$, let $q_v \in L_\infty^{tr}$ be the corresponding self-intersection point. Around each q_v there is a standard symplectic neighborhood $B_\epsilon(q_v)$, which we identify with a neighborhood of the origin in \mathbb{C}^n . We take a Hamiltonian isotopy of L_∞^{tr} so that its restriction to each $B_\epsilon(q_v)$ matches $\mathbb{R}^n \cup i\mathbb{R}^n$. The sequence of Hamiltonian isotopic Lagrangian submanifolds L_α^{tr} are constructed by replacing

$$L_\infty^{tr} \cap \left(\bigcup_{v \in \Delta_\phi^\mathbb{Z}} B_\epsilon(q_v) \right)$$

with a standard surgery neck of radius r_α . The constants r_α are chosen so that $\lim_{\alpha \rightarrow \infty} r_\alpha = 0$. In order to make this a sequence of Hamiltonian isotopic Lagrangian submanifolds, we cancel out the small amount of Lagrangian flux swept out by the surgery necks with an equal amount of Lagrangian isotopy on $L_\infty^{tr} \setminus \left(\bigcup_{v \in \Delta_\phi^\mathbb{Z}} B_\epsilon(q_v) \right)$. These Hamiltonian isotopies are chosen so that $L_\alpha^{tr} \setminus \left(\bigcup_{v \in \Delta_\phi^\mathbb{Z}} B_\epsilon(q_v) \right)$ converges smoothly.

By claim 3.3.17, the first member of this sequence L_0^{tr} can be constructed in such a way that it is Hamiltonian isotopic to $L^{tr}(\phi)$. [FOOO07] gives us a relation between disks on the $L^{tr}(\phi)$ and the disks on $\sigma_0 \cup (\theta'(\sigma_{-\phi}))$.

Claim 3.3.21. *If there exists a sequence of holomorphic disks*

$$u_\alpha : (D, \partial D) \rightarrow (X, L_\alpha^{tr})$$

contributing to the product on $CF^\bullet(L_\alpha^{tr})$, then there exists a holomorphic polygon or disk

$$u_\infty : (D, \partial D) \rightarrow (X, L_\infty^{tr}).$$

Proof. Let $\{u_\alpha\}$ be a sequence of holomorphic disks of bounded energy and boundary on L_α^{tr} contributing to $CF^\bullet(L_\alpha^{tr})$. Then the images of the $\{u_\alpha\}$ are mutually contained within a compact set of X . We would like to apply a Gromov-compactness argument on the sequence of u_α but cannot as the family L_α^{tr} does not converge to L_∞^{tr} in a strong enough sense. However, it is the case that $L_\alpha \setminus B_\epsilon(q_v)$ does converge to $L_\infty \setminus B_\epsilon(q_v)$ uniformly.

In [FOOO07, Section 62] it is shown that for such a sequence of disks $u_\alpha : (D^2, \partial D) \rightarrow (X, L_\alpha^{tr})$, one may construct a family of approximate solutions $u_{\alpha,app} : (D^2, \partial D) \rightarrow (X, L_\infty^{tr})$ by replacing the regions of the curve u_α which intersect $B_\epsilon(q_v)$ with holomorphic corners based on a standard model from [FOOO07, Section 59].

The following neck stretching argument is used to show that these approximate solutions approach an honest solution. As $\alpha \rightarrow \infty$, the restriction $L_\alpha \cap (B_\epsilon(q_v) \setminus \{q_v\})$ approaches the cylindrical Lagrangian $L_\infty^{tr} \cap (B_\epsilon(q_v) \setminus \{q_v\})$. As a result, the holomorphic maps $\{u_\alpha\}$ converge to cylindrical maps in the neck region $B_\epsilon(q_v) \setminus \{q_v\}$ [FOOO07, Section 62.4]. This provides an error bound on the failure of $u_{\alpha,app}$ to being a holomorphic polygon. As the $\{u_\alpha\}$ converge to cylindrical maps this error approaches zero.

Since the $\{u_\alpha\}$ have images confined a compact set of X , the maps $\{u_{\alpha,app}\}$ are similarly constrained. We can apply Arzela-Ascoli to take a subsequence of $\{u_{\alpha,app}\}$ which converge to a holomorphic map u_∞ with boundary on L_∞^{tr} . \square

In this case, we can rule out the existence of holomorphic polygons with boundary on L_∞^{tr} .

Claim 3.3.22. *If we are working in complex dimension greater than 1, there are no holomorphic polygons with boundary on $L_\infty^{tr} = \sigma_0 \cup (\theta'(\sigma_{-\phi}))$.*

Proof. This follows from an index computation. A holomorphic polygon with boundary contained in $\sigma_0 \cup (\theta'(\sigma_{-\phi}))$ has $2k - 1$ inputs and 1 output. The inputs must alternate between being an element of $CF^\bullet(\sigma_0, \theta'(\sigma_{-\phi}))$ and $CF^\bullet(\theta'(\sigma_{-\phi}), \sigma_0)$. We will look at the case where output p lies in $p \in CF^\bullet(\sigma_0, \theta'(\sigma_{-\phi}))$ and the inputs x_i, y_j are in

$$\begin{aligned} y_j &\in CF^\bullet(\theta'(\sigma_{-\phi}), \sigma_0) & 1 \leq i \leq k-1 \\ x_i &\in CF^\bullet(\sigma_0, \theta'(\sigma_{-\phi})) & 1 \leq i \leq k. \end{aligned}$$

The dimension of moduli space of regular polygons with these boundary conditions can be explicitly computed based on the index of the points x_i and y_j . The degree of the input intersections of the form x_i is n , and the degree of each intersection of the form y_j is 0. The output intersection p has degree n . The dimension of this space of disks is

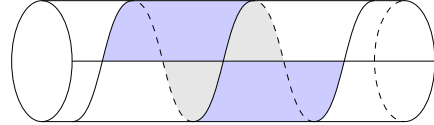
$$\begin{aligned} (2k-1) - 2 + \deg(p) - \left(\sum_{i=1}^k \deg(x_i) + \sum_{i=1}^{k-1} \deg(y_i) \right) \\ = (2-n)k - 3 + n \end{aligned}$$

which is negative whenever $n \geq 2$.

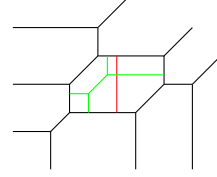
The argument for when the output marked point p is in $CF^\bullet(\theta'(\sigma_{-\phi}), \sigma_0)$ is the same. \square

By claims 3.3.21 and 3.3.22 the sequence of Lagrangians submanifolds L_α^{tr} is eventually unobstructed.

We additionally need to prove that the Lagrangians $K_{\alpha, \alpha+1}^{tr} \subset X \times \mathbb{C}$ given by the suspension of the Hamiltonian isotopy between L_α^{tr} and $L_{\alpha+1}^{tr}$ are an eventually unobstructed sequence. This follows from the same argument. A sequence of holomorphic disks with boundary on $K_{\alpha, \alpha+1}^{tr}$ produces a holomorphic disk with boundary on $K_\infty = L_\infty^{tr} \times \mathbb{R}$. Since $L_\infty^{tr} \times \mathbb{R}$ is a trivial cobordism and the complex structure was chosen to be the standard



(a) An example of a disk with boundary on σ_0 and σ_{x^2} in \mathbb{C}^* , corresponding to a holomorphic annulus after applying surgery at 3 points.



(b) Two examples of higher genus open curves with boundary on $L(\phi_{ell})$.

Figure 14

product structure, every holomorphic disk with boundary on $L_\infty^{tr} \times \mathbb{R}$ gives us a holomorphic disk with boundary on L_∞^{tr} . By claim 3.3.22, there are no such disks. Therefore, the Lagrangian cobordisms $K_{\alpha,\alpha+1}$ are eventually unobstructed.

As both $\{L_\alpha^{tr}\}_{\alpha \in \mathbb{N}}$ and $\{K_{\alpha,\alpha+1}^{tr}\}_{\alpha \in \mathbb{N}}$ are eventually unobstructed sequences of Lagrangians, it follows from lemma 3.3.15 that $L_0^{tr} = L^{tr}(\phi)$ is unobstructed, completing the proof of proposition 3.3.8.

Remark 3.3.23. Note that in dimension 1, the Lagrangian sections $\theta'(\sigma_{-\phi}) \cup \sigma_0$ may still bound interesting holomorphic disks. In dimension 1, see fig. 14a for an example of a disk which has boundary on tropical sections. We now provide some evidence that these disks correspond to higher genus open Gromov-Witten invariants of the tropical Lagrangian. In the 1 dimensional example, the disk in fig. 14a becomes a holomorphic annulus with boundary on $L(x_1^2)$.

We can replicate this phenomenon in higher dimensions. Let $\phi_E(x_1, x_2)$ be the tropical polynomial describing the tropical elliptic curve $V(\phi_E)$. Then the Lagrangian $L(\phi)$ bounds holomorphic annuli which are modelled on the previous example in one dimension higher. See fig. 14b for this example (in red) and an example of a 4-punctured holomorphic sphere with boundary on $L(\phi_E)$. At this point, it is unclear what the presence of these higher genus open Gromov-Witten invariants entail.

3.4 Two examples, and comparison to existing work

In this section, we work out two examples, highlighting how the valuation and argument projections relate to each other, and how we may visualize manipulations of these tropical Lagrangians via these projections. This will allow us to compare the tropical Lagrangians that we construct to the ones presented in the work of [Mat18; Mik18]. We will also introduce Lagrangian antisurgery disks into the picture.



Figure 15: Argument and valuation projections of the chart $L_r(\phi_{pants})$, with coloration indicating which regions correspond to each other in the projections.

3.4.1 Pants, Decompositions and modifying arguments.

The first example that we will work out is the tropical pair of pants. This Lagrangian lives in $(\mathbb{C}^*)^2$ and is admissible for the Landau-Ginzburg model superpotential given by

$$W_\Sigma = z_1 + z_2 + \frac{1}{z_2 z_2}.$$

The tropical polynomial describing the pair of pants is

$$\phi_{pants} = 0 \oplus x_1 \oplus x_2.$$

This divides Q into three regions, (see fig. 4.) Between the regions \underline{U}_0 and \underline{U}_{x_1} , the Lagrangian section $\sigma_{-\phi_{pants}}$ takes a twist in the argument direction of x_1 . The regions \underline{U}_0 , \underline{U}_{x_1} , and \underline{U}_{x_2} are all slightly interior to the \underline{U}_0 , \underline{U}_{x_1} and \underline{U}_{x_2} . The surgery $(\sigma_0) \#_U (\sigma_{-\phi_{pants}})$ glues the sections σ_0 and $\sigma_{-\phi_{pants}}$ together, while removing the three regions \underline{U}_0 , \underline{U}_{x_1} , \underline{U}_{x_2} . The three tentacles of the tropical pair of pants are Hamiltonian isotopic to the periodized conormal bundles to the three legs of the tropical variety.

After truncating the pair of pants along the tentacles, the argument projection of the three boundary circles are the affine subtori $\arg(z_1) = 0$, $\arg(z_2) = 0$ and $\arg(z_1) = -\arg(z_2)$. If we were to look at some other presentation of the pair of pants, there would be a different triple of affine subtori giving the boundaries of the pair of the pants.

Consider the decomposition of our Lagrangian into charts $L_r(\phi_{pants})$ and $L_s(\phi_{pants})$ coming from the construction of proposition 3.1.1. Each chart projects to a neighborhood of $V(\phi_{pants})$ and a portion of the polytope $\Delta_{\phi_{pants}}$ under the argument. See fig. 15 for a picture how the boundary components of the chart $L_r(\phi_{pants})$ correspond to each other in the valuation and argument projections. The $L_s(\phi_{pants})$ chart lives mostly near the zero section, so its projection to the argument is quite small.

We can modify the charts $L_r(\phi_{pants})$ and $L_s(\phi_{pants})$ to change the configuration of the three affine cycles which are the boundary of $L(\phi_{pants})$ in the argument projection. These three affine tori are characterized by their class in homology and the property that they contain the origin in T^2 (as determined by the section σ_0 .) While we cannot modify the class of the affine boundary subtori, we can modify their phase in the argument so that they no longer pass through the origin. A visualization for this modification can be phrased in

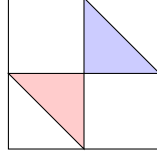


Figure 16: The argument projection of $\theta_{\psi_{\text{pants}}} L(\phi_{\text{pants}})$. The Lagrangian chart $\theta_{\psi_{\text{pants}}} L_s(\phi_{\text{pants}})$ is in red, while $\theta_{\psi_{\text{pants}}} L_r(\phi_{\text{pants}})$ has been shrunk to the blue area.

terms of the primitives for the sections L_r and L_s . The graph of $r_\epsilon \circ \tilde{\phi}_{\text{pants}}$ resembles a towel hanging from towel-rack determined by the restriction of ϕ_{pants} to $V(\phi_{\text{pants}})$. The conormal direction to the amoeba determines the homology class of the subtori, and the slope of this towel-rack determines the phase of the affine subtori in the argument projection. By increasing or decreasing the slopes of the primitive function $r_\epsilon \circ \tilde{\phi}_{\text{pants}}$ along the directions of the tropical amoeba, we modify the class of affine boundary subtori.

We can explicitly write this out in terms of the twisting Hamiltonians considered in [Han18]. Let $\psi : Q \rightarrow \mathbb{R}$ be a piecewise linear function, and let θ_ψ be the time 1 Hamiltonian flow associated to the pullback of the smoothing, $\tilde{\psi} \circ \text{val} : X \rightarrow \mathbb{R}$. This Hamiltonian sends sections which are the graphs of piecewise linear functions to other sections by

$$\theta_\psi(\sigma_\phi) = \sigma_{\phi+\psi}.$$

This Hamiltonian also modifies tropical Lagrangians by changing the arguments of the legs in the tropical Lagrangian.⁶

The construction of $L(\phi)$ required the polynomial ϕ to be concave so that σ_0 and $\sigma_{-\phi}$ satisfied the convexity condition needed to apply proposition 3.1.1. However, the twisting Hamiltonian ψ need only be a piecewise linear function (not necessarily a tropical polynomial!) Consider in the pair of pants example,

$$\psi_{\text{pants}}(z_1, z_2) = \frac{1}{2} \cdot \phi_{\text{pants}}(z_1, z_2)$$

where the product here is the honest product, not the tropical one. The Lagrangian $\theta_{\psi_{\text{pants}}}(L(\phi_{\text{pants}}))$ will have an argument projection composed of two triangles (See fig. 16). One triangle corresponds to the chart $\theta_{\psi_{\text{pants}}} L_r(\phi_{\text{pants}})$, which has been decreased in area under the argument projection. The other chart, $L_s(\phi_{\text{pants}})$ which previously occupied a small region of the argument projection, is enlarged under the Hamiltonian isotopy $\theta_{\psi_{\text{pants}}} L_s(\phi_{\text{pants}})$ to a triangle of equal area.

This Lagrangian matches the tropical Lagrangians as defined in [Mat18], and can also be expressed as the Lagrangian connect sum between two piecewise linear sections of the SYZ fibration by applying the wrapping Hamiltonian ϕ_{pants} before surgery. We can generalize this construction to Lagrangian hypersurfaces.

⁶From the perspective of the primitives $r \circ \phi$ which look like towels hanging off of towel racks, this modification changes the slope of the rack by adding on the slope of the function ψ .

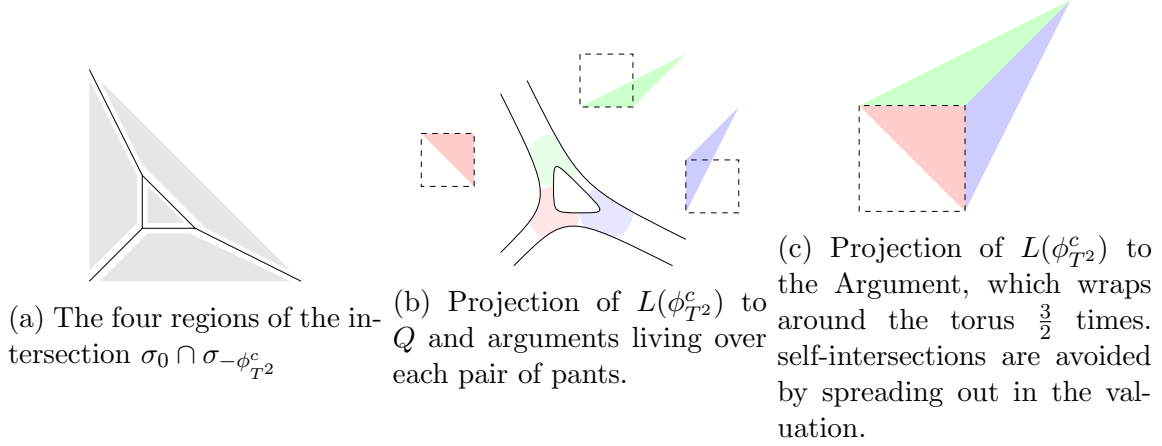


Figure 17: The smooth tropical Lagrangian elliptic, given by Lagrangian connect sum of $\sigma_{-\phi_{T^2}^c}$ and σ_0 for $c > 0$.

Definition 3.4.1. *Let ϕ be a smooth tropical polynomial. The balanced Lagrangian tropical hypersurface is the connect sum*

$$L^{1/2}(\phi) := \theta_{\frac{1}{2} \cdot \phi}(\sigma_0) \#_{U_v} \theta_{\frac{1}{2} \cdot \phi}(\sigma_{-\phi}).$$

This Lagrangian seems more natural to work with than the ones that we've constructed, as the argument projection of the Lagrangian pair of pants now matches the *coamoeba* of the complex pair of pants. However, these tropical Lagrangians are not admissible objects of the Fukaya category with admissibility condition determined by $W = z_1 + z_2 + \frac{1}{z_1 z_2}$. This is because the arguments of the tentacles have been modified in a non-admissible way. One can change the admissibility condition on the category to make this an admissible Lagrangian, although it is unclear if there are other geometric reasons why a modified admissibility condition would be more natural to consider from the perspective of mirror symmetry.

A second observation about these balanced tropical Lagrangians is that they closely match the ones constructed in section 1.2. We'll explore the relation between different constructions of these tropical Lagrangians later when we generalize this discussion to construct tropical Lagrangians related to dimer models in section 6.

3.4.2 Tropical Torus, Pair of Pants Decompositions, and self-intersections

In this section, we look at the tropical polynomial

$$\phi_{T^2}^c := \psi(x_1, x_2) = x_1 \oplus x_2 \oplus (c \odot x_1^{-1} x_2^{-1}) \oplus 0$$

which for values of $c > 0$ is a smooth tropical polynomial. See fig. 17.

The tropical Lagrangian $L(\phi_{T^2}^c)$ has argument projection $\Delta_{\phi_{T^2}^c}/\mathbb{Z}^2$. $\Delta_{\phi_{T^2}^c}$ comes with a stratification from the dual function $\check{\phi}_{T^2}^c$. This stratification gives a decomposition of $L(\phi_{T^2}^c)$.

Since our surgery profile is built locally, for small enough ϵ the pieces of this decomposition can be studied independently.

Claim 3.4.2. *Let $\dim X = n$ and $\phi : Q \rightarrow \mathbb{R}$ be a smooth tropical polynomial. Then the subsets*

$$\text{val}^{-1}(U_{\{v_i\}}) \cap L(\phi)$$

for $|\{v_i\}| \geq 2$ give a decomposition of $L(\phi)$ so that each component has valuation projection corresponding to strata $\underline{U}^{\{v_i\}}$. Furthermore, each component is modelled on $P_k \times \mathbb{R}^{n-k}$ where

$$\begin{aligned} k &= |\{v_i\}| - 1 \\ P_k &:= L(\phi_{\text{pants}}(x_1, \dots, x_k)) \\ \phi_{\text{pants}}(x_1, \dots, x_k) &:= x_1 \oplus \dots \oplus x_k \oplus 0 \end{aligned}$$

is the real k -dimensional Lagrangian pair of pants.

One could run this claim in reverse, building tropical Lagrangians using a pair of pants decomposition of $V(\phi)$, which is the approach taken by [Mik18; Mat18]. While each individual pair of pants has an easy-to-understand argument projection, the argument projection of the entire Lagrangian $L(\phi_{T^2}^c)$ multiply covers the fiber F_q and is easiest understood as the Newton polytope of $\phi_{T^2}^c$ (see fig. 17b versus fig. 17c.) The preimage of $0 \subset \Delta_{\phi_{T^2}^c}$ is a cycle in $L(\phi_{T^2}^c)$, corresponding to the boundary cycle the region U_0 in the valuation. More generally, we have

Claim 3.4.3. *Let $\phi : Q \rightarrow \mathbb{R}$ be a smooth tropical polynomial. The preimage $\text{val}^{-1}(0) \cap L(\phi)$ has a decomposition into connected components $\{c_v\}_{v \in \Delta_{\phi}^{\mathbb{Z}}}$.*

If one was to look at argument of the $L_r(\phi_{T^2}^c)$ chart, we would see a cycle which lived above the origin. As we let c shrink to zero, the size of this cycle decreases until we arrive at $L(\phi_{T^2}^0)$, which has a self-intersection. This can be a bit difficult to visualize in the argument projection, as the origin becomes quite busy once we periodize the fiber. The topology of $L(\phi_{T^2}^0)$ is that of a sphere with 3 punctures and a single self-intersection. Antisurgery provides a formalization of this intuition. Consider the disk D_0 which is a section of the valuation map above the U_0 region of the tropical Lagrangian, with boundary along the curve c_0 contained within the tropical Lagrangian. We see that $L(\phi_{T^2}^0)$ is obtained by antisurgery from $L(\phi_{T^2}^c)$ along D_0 :

$$L(\phi_{T^2}^0) = \alpha_{D_0} L(\phi_{T^2}^c).$$

By applying the opposite surgery at this double point, we obtain the Lagrangian mutation $\mu_{D_0}(L(\phi_{T^2}^c))$. This Lagrangian has valuation $\text{val}(\mu_{D_0}(L(\phi_{T^2}^c))) = \text{val}(L(\phi_{T^2}^0))$. This is an embedded Lagrangian submanifold whose valuation is a non-smooth tropical curve. Notably, $\mu_0(L(\phi_{T^2}^c))$ is *not* cobordant to $\sigma_{-\phi} \sqcup \sigma_0$ via surgery cobordism. Figure 18 draws out these two mutants for $L(\phi_{T^2}^c)$.

It is easier to visualize this mutation in the balanced Lagrangian, $L^{1/2}(\phi_{T^2}^c)$, which is Hamiltonian isotopic to our original Lagrangian. In this configuration, the two charts which

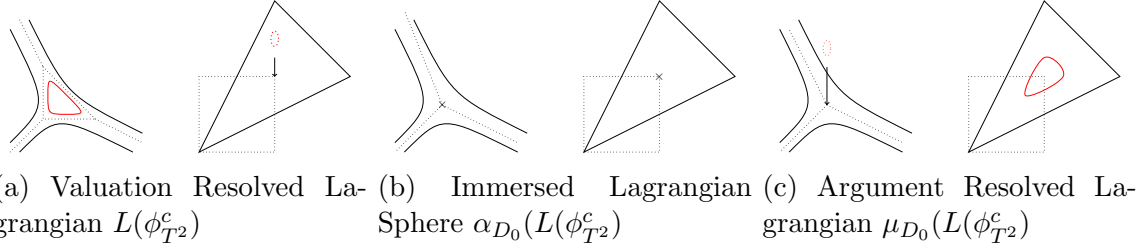


Figure 18

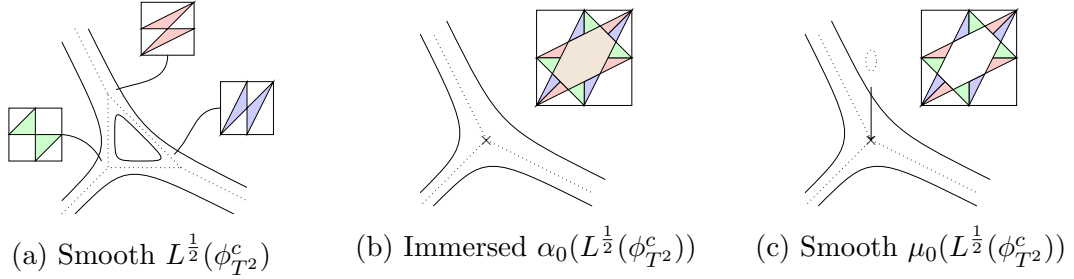


Figure 19: The balanced Lagrangian has a particularly nice argument projection revealing the mutation structure. Notice the 3 white hexagons on the right hand side giving different antisurgery disks. The self-intersection in the middle picture is marked with a \times in both the argument and valuation projections.

assemble to give our Lagrangian torus are opposite isosceles triangles. Their overlap is exactly where we must take a surgery when $c \geq 0$. However, when drawn in the balanced configuration, it becomes clear that we may have reversed the roles of argument and valuation when taking the surgery, and instead treated both $L_r^{1/2}(\phi_{T^2}^c)$ and $L_s^{1/2}(\phi_{T^2}^c)$ as two sections over triangles in the argument projection. The symmetric difference of these two Lagrangian taken in this configuration has a hexagonal puncture in the area where $L_r^{1/2}(\phi_{T^2}^c)$ and $L_s^{1/2}(\phi_{T^2}^c)$ previously intersected. The Lagrangian $\mu_0(L^{1/2}(\phi_{T^2}^c))$ was also described in [Mat18, Section 5.2], and it has an especially nice argument projection consisting of 6 triangles (see fig. 19c). There are in fact three antisurgery disks of this Lagrangian, which can be clearly seen in the argument projection as the three unshaded hexagons (compare figs. 19b and 19c).

The presence of these two different surgeries exposes an underlying mutation structure on the moduli space of these tropical Lagrangians.

Claim 3.4.4. *Let $\phi : Q \rightarrow \mathbb{R}$ be a tropical polynomial. For each smooth internal vertex $v \in \Delta_\phi$, there exists a Lagrangian antisurgery disk D_v which is a section $X \rightarrow Q$ over a neighborhood of the subset $U_v \subset Q$. The boundary of this disk is the cycle c^v from claim 3.4.3. We write $\mu_v(L(\phi))$ for the mutation at this disk.*

The two Lagrangians $L(\phi)$ and $\mu_v(L(\phi))$ belong to different charts of the moduli space of tropical Lagrangians. From the perspective of symplectic geometry, these two Lagrangians

should be treated on equal footing, and there should be some wall-crossing transformation relating families of these two Lagrangians. We'll explore this later in section 7 when discussing mirror symmetry on the projective plane.

The presence of these Lagrangian mutations gives us two new corollaries about our tropical Lagrangians.

Corollary 3.4.5. *There exists a complex structure J so that the tropical Lagrangian $L(\phi_{T^2}^c)$ bounds a (non-regular) Maslov index 0 holomorphic disk. More generally, there are choices of complex structure in dimension greater than two so that the tropical Lagrangians bound (regular) Maslov index 0 holomorphic disks.*

The existence of the mutation structure gives us a relation between tropical Lagrangians constructed from smooth and non-smooth tropical polynomials.

Corollary 3.4.6. *The Lagrangians $L^{1/2}(\phi_{T^2}^c)$ and $\mu_0(L^{1/2}(\phi_{T^2}^c))$ are Lagrangian isotopic.*

We reserve a further discussion on the existence of mutation structure until section 6 once we have developed notation to talk about these Lagrangians.

4 Mirror Symmetry, Tensor Products, and Intersections

4.1 Background: Mirror Symmetry for Toric Varieties

Let \check{X}_Σ be a toric variety given by the fan $\Sigma \subset \mathbb{R}^n = Q$. We review some notation and concepts from [CLS11] related to line bundles, divisors and tropical geometry. Each lattice generator v of a ray of Σ gives a torus equivariant divisor D_v of \check{X}_Σ . In the setting where \check{X}_Σ is smooth we may express any linear equivalence class of divisor as a sum $\sum_{v \in \Sigma} a_v D_v$. An *integral support function* for Σ is a function $\phi : Q \rightarrow \mathbb{R}$ which is linear on each cone of Σ , and is integral on the fan in the sense that $\phi(\Sigma \cap \mathbb{Z}^n) \subset \mathbb{Z}$. To each divisor class $[D]$, we may associate an integral support function $\phi_{[D]}$ which is determined by the values

$$\phi_{[D]}(v) = a_v.$$

Properties of the line bundle $\mathcal{O}(D)$ can be read from the support function: the line bundle is *base point-free* whenever $\phi_{[D]}$ is concave, and *ample* if and only if $\phi_{[D]}$ is strictly concave. The function $\phi_{[D]}$ is piecewise linear, so when D is base point free the function $\phi_{[D]}$ is a maximally degenerate tropical polynomial (in the sense that every stratum of the tropical variety contains the origin.) The tropical variety of the support function of a base point free line bundle can be related to the valuation projection of the corresponding divisor of the line bundle. Let D be a base point free divisor transverse to the toric anticanonical divisor, and let $\Delta_{\phi_{[D]}}$ be the Newton polytope of $\phi_{[D]}$. Then over the open torus of \check{X}_Σ , each choice of

constants c_v defines a polynomial

$$f_D : (\mathbb{C}^*)^n \rightarrow \mathbb{C}$$

$$f_D := \sum_{v \in \Delta_{\phi_D}} c_v z^v$$

which gives a section of the line bundle over the compactification $\mathcal{O}_D \rightarrow \check{X}_\Sigma \supset (\mathbb{C}^*)^n$. There exists a choice of constants so that $f^{-1}(0) = D$.

Example 4.1.1. *In the case of a hyperplane H in \mathbb{CP}^2 , the support function is $\phi_H = 1 \oplus x_1 \oplus x_2$ and $f = 1 + z_1 + z_2$. The valuation projection of H to the moment polytope is the amoeba of the tropical pair of pants.*

We now consider Laurent polynomials $f_D = \sum_{v \in \Delta_{\phi_D}} c_v z^v$, where the constants c_v are elements of the Novikov field. The valuation projection of the variety $f_D = 0$ is a tropical hypersurface defined by a tropical polynomial ϕ_D , which we call the tropicalization of f_D . ϕ_D is a deformation of $\phi_{[D]}$. In the complex setting the tropical variety $V(\phi_D) \subset \Delta_\Sigma$ approximates the image of D under the moment map projection $\text{val} : \check{X}_\sigma \rightarrow \Delta_\Sigma$. The observation that the strata of the tropical variety $V(\phi)$ meet the toric boundary of the moment polytope of X_Σ transversely is compatible with the existence of a compactification for the variety $f^{-1}(0) \subset (\mathbb{C}^*)^n$ inside of \check{X}_Σ .

Mirror symmetry for toric varieties is based on an understanding of how compactifications modify the mirror construction. It is an expectation in mirror symmetry that compactification on \check{X} corresponds to the incorporation of a superpotential $W : X \rightarrow \mathbb{C}$ in the mirror and vice versa. One proposed method for constructing mirror spaces for toric varieties is to consider \check{X}_Σ as a compactification of $\check{X}_\Sigma \setminus D_\Sigma = (\mathbb{C}^*)^n$, where D_Σ is the toric anticanonical divisor. A choice of symplectic form for \check{X}_Σ picks out the coefficients of a Laurent polynomial,

$$W_\Sigma = \sum_{v \in \Sigma} c_v z^v : (\mathbb{C}^*)^n \rightarrow \mathbb{C}$$

the *Hori-Vafa* superpotential for \check{X}_Σ .

Notation 4.1.2. *For the remainder of this section, $X = \check{X} = (\mathbb{C}^*)^n$, $Q = \mathbb{R}^n$, \check{X}_Σ is a toric variety determined by fan Σ , and $W_\Sigma : X \rightarrow \mathbb{C}$ is the mirror Hori-Vafa superpotential.*

This Hori-Vafa superpotential provides the taming conditions for our Lagrangians through the monomial admissibility condition associated to W_Σ .

Theorem 4.1.3 ([Han18]). *Let \check{X} be a smooth complete toric variety with Hori-Vafa superpotential W_Σ . Let $\text{Tw}^\pi \mathcal{P}_\Delta(X, W_\Sigma)$ be the category of twisted complexes generated by tropical sections. The A and B-models*

$$\text{Tw}^\pi \mathcal{P}_\Delta(X, W_\Sigma) \simeq D^b \text{Coh}(\check{X})$$

are quasi-equivalent A_∞ categories.

The equivalence is proven using theorem 3.2.5. For an outline of the construction of the monomial admissible Fukaya category of [Han18], and an extension of this category to include Lagrangians which are unobstructed by bounding cochain, we refer the reader to appendix A.

Notation 4.1.4. *In this section, our Lagrangian submanifolds will have the additional structure of a Lagrangian brane, meaning that they are equipped with a choice of Morse function, spin structure, and bounding cochain. To simplify notation, we will often refer to data of a Lagrangian brane by the Lagrangian submanifold L .*

Since the Lagrangians $L(\phi)$ that we study are not exact we are required to work with the Fukaya category defined over Novikov coefficients. The mirror to the Landau-Ginzburg model (X, W_Σ) is the rigid analytic space \check{X}_Σ^Λ . The intuition for our constructions should be understood independently of the requirements of Novikov coefficients.

The Novikov toric variety \check{X}_Σ^Λ comes with a valuation map $\text{val} : X_\Sigma^\Lambda \rightarrow Q$ using the valuation on the Novikov ring. A difference between complex geometry and geometry over the Novikov ring is that in the non-Archimedean setting the valuation of a divisor is described exactly by its tropicalization, as opposed to living in the amoeba of the tropicalization.

4.2 Mirror Symmetry for tropical Lagrangian hypersurfaces

Theorem 4.2.1. *Let $D_{\check{f}} \subset \check{X}_\Sigma^\Lambda$ be a divisor transverse to the toric divisors, defined by the equation $\check{f} = 0$. Let ϕ be the tropicalization of \check{f} . The tropical Lagrangian brane $L(\phi)$ is mirror to $\mathcal{O}_{D'}$, with D' rationally equivalent to D .*

We first give a family Floer argument motivating this mirror statement. From SYZ mirror symmetry we know that the mirror to a point in the complement of the anticanonical divisor $z \in \check{X}_\Sigma^\Lambda \setminus D$ is a fiber of the SYZ fibration equipped with local system. One method to compute the mirror sheaf to $L(\phi)$ is to compute $CF^\bullet(L(\phi), F_q)$ and assemble this data into a sheaf over X using techniques from family Floer theory. This line of proof is rooted in a long-known geometric intuition for mirror symmetry via tropical degeneration (see fig. 20.) However, the precise computation of the support is difficult due to the need to count holomorphic strips contributing to the Floer differential. We outline how we expect this computation to work in section 4.3, see also section 6.3.

Proof of theorem 4.2.1. We use Lagrangian cobordisms to prove this theorem. The function \check{f} associated to the effective divisor $D \subset \check{X}$ defines a section of the line bundle $\mathcal{O}_{\check{X}_\Sigma}$, giving us an exact triangle

$$\mathcal{O}_{\check{X}_\Sigma}(-D) \xrightarrow{\check{f}} \mathcal{O}_{\check{X}_\Sigma} \rightarrow \mathcal{O}_{D_{\check{f}}}. \quad (5)$$

This gives us a description of $\mathcal{O}_{D_{\check{f}}}$ in terms of line bundles on \check{X}_Σ . By theorem 4.1.3, we have an identification of $\text{Fuk}((\mathbb{C}^*)^n, W_\Sigma)$ with $D^b \text{Coh}(\check{X}_\Sigma^\Lambda)$ giving us the following mirror correspondences between sheaves and Lagrangian submanifolds:

$$\mathcal{O}_{\check{X}_\Sigma^\Lambda} \leftrightarrow \sigma_0 \quad \mathcal{O}_{\check{X}_\Sigma^\Lambda}(-D) \leftrightarrow \sigma_{-\phi_{[D]}}.$$

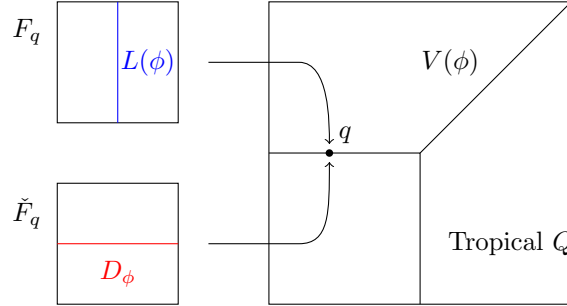


Figure 20: SYZ mirror symmetry predicts that Lagrangians are swapped with complex subvarieties by fiberwise duality over a tropical curve in the base.

where ϕ_D is the support function of the divisor D . The Lagrangians $\sigma_{-\phi}$ and $\sigma_{-\phi_{[D]}}$ are Hamiltonian isotopic. Using theorems 2.2.7 and A.4.1 we obtain an exact triangle

$$\sigma_{-\phi} \xrightarrow{g} \sigma_0 \rightarrow L(\phi) \quad (6)$$

for some map g . $L(\phi)$ is therefore identified under the mirror functor to a sheaf $\mathcal{O}_{D_{\check{g}}}$ supported on $D_{\check{g}}$, an effective divisor for the bundle $\mathcal{O}(D)$. The divisors $D_{\check{g}}$ and $D_{\check{f}}$ are rationally equivalent. \square

If we wish to prove that $D_{\check{g}}$ and $D_{\check{f}}$ match up exactly, we need to better understand the map \check{g} in eq. (6). Though we cannot determine this map without making a computation of holomorphic strips with boundary on the cobordism K , we conjecture

Conjecture 4.2.2. *Let ϕ be the tropicalization of \check{f} . There exists a choice of bounding cochain making the Lagrangian brane $L(\phi)$ mirror to $\mathcal{O}_{D_{\check{f}}}$.*

One way to determine the mirror sheaf to $L(\phi)$ is to return to family Floer theory and compute the support of the Lagrangian. We will now look at pairs (F_q, ∇) , where ∇ is a Λ -unitary local system on F_q , and compute Floer homology with coefficients determined by this local system.⁷ We let $HF^\bullet(L, (F_q, \nabla))$ be the Floer homology computed with this local system.

Definition 4.2.3. *Let L be a Lagrangian brane, and $X \rightarrow Q$ be a SYZ fibration. The valuation support of L is the set*

$$\text{Supp}(L) := \{q \in Q \mid \exists \nabla \text{ such that } HF^\bullet(L, (F_q, \nabla)) \neq 0\}.$$

Notice that whenever $q \notin \text{val}(\phi)$, there exists a Hamiltonian isotopy of $L(\phi)$ so that $F_q \cap L(\phi) = \emptyset$ and therefore $q \notin \text{Supp}(L(\phi))$. Since $\text{val}(L(\phi))$ can be made arbitrarily close to $V(\phi)$, there is an inclusion

$$\text{Supp}(L(\phi)) \subset V(\phi)$$

⁷This does not require any additional setup beyond incorporating bounding cochains into our story. The higher order corrections to the holonomy of the local system considered here are equivalent to bounding cochains of positive valuation. The data of the local system can therefore be replaced with a bounding cochain – although the valuation of this bounding cochain may be zero.

It is not the case that $q \in \text{Supp}(L(\phi))$ implies that $CF^\bullet(L(\phi), F_q)$ is non-nullhomotopic, as we usually need to equip F_q with a nontrivial local system to detect some nontrivial homology.

We will say that the homology $CF^\bullet(L(\phi), (F_q, \nabla))$ is wide when it is quasi-isomorphic to $C^\bullet(S^1)$.

Claim 4.2.4. *Let $q \in Q_{n-1}(\phi)$ be a point in a maximal stratum of the tropical variety $V(\phi)$. Then there exists a local system on the torus so that $CF^\bullet(L(\phi), (F_q, \nabla))$ is wide.*

Proof. Let q be a point in $V(\phi)$ which lies in Q_{n-1} . There exists a neighborhood $U \subset Q$ of q so that $\text{val}^{-1}(U)$ can be identified with $(\mathbb{C}^*)^n$, and $V(\phi)$ can be identified after a change of coordinates with the tropical variety $V(0 \oplus x_1)$. The local neighborhood we use is very similar to that described in fig. 12. When we write $CF^\bullet(L(\phi)|_U, (F_q|_U, \nabla))$, we will mean the Floer theory of $L(\phi)$ and F_q in the neighborhood U .⁸ Since all of the intersections between $L(\phi)$ and F_q are contained in the neighborhood U , there is an isomorphism of graded vector spaces

$$CF^\bullet(L(\phi)|_U, (F_q, \nabla)) = CF^\bullet(L(\phi), (F_q, \nabla)) = \Lambda\langle e \rangle \oplus \Lambda\langle x \rangle$$

where e and x are generators in degrees 0 and 1 respectively. However the differentials

$$\begin{aligned} m_U^1 : CF^\bullet(L(\phi)|_U, (F_q|_U, \nabla)) &\rightarrow CF^\bullet(L(\phi)|_U, (F_q|_U, \nabla)) \\ m^1 : CF^\bullet(L(\phi), (F_q, \nabla)) &\rightarrow CF^\bullet(L(\phi), (F_q, \nabla)) \end{aligned}$$

will not necessarily agree, as the second differential counts holomorphic strips which may leave the neighborhood U . As a result, $CF^\bullet(L(\phi), (F_q, \nabla))$ is a deformation of $CF^\bullet(L(\phi)|_U, (F_q, \nabla))$ with non-zero valuation, and we may write $m^1(e) = m_U^1(e) + b \cdot x$ where b is some deforming chain with positive valuation.

We can compute $CF^\bullet(L(\phi)|_I, (F_q, \nabla))$ explicitly. The complex $CF^\bullet(L(\phi)|_U, (F_q, \nabla))$ is quasi-isomorphic to $C^\bullet(S^1, \nabla_{S^1})$, where ∇_{S^1} is the local system restricted to a cycle of F_q which is identified with the normal direction of $L(\phi)|_U$. There exists a Hamiltonian deformation of $L(\phi)$ making the strips of $CF^\bullet(L(\phi)|_U, (F_q, \nabla))$ have valuation less than ϵ . After applying such a Hamiltonian deformation, every deformation of this complex of valuation greater than ϵ can be realized by changing the local system on F_q . In this particular setting, we change the holonomy on F_q by a factor of $(1 + T^{-a}b)$, where a is the area of the small strips contributing to the differential m_U^1 . For this local system ∇ we have nontrivial support, $HF^\bullet(L(\phi), (F_q, \nabla)) \neq 0$. \square

The geometric intuition behind this claim is easiest seen through a worked out example, which we include in section 4.3. One interpretation of this claim is that once we ignore corrections at high valuation, $HF^\bullet(L(\phi), F_q)$ is wide if and only if $q \in V(\phi)$.

The valuation of the correction to the differential will be bounded below by the size of the neighborhood U , so points q which are far away from Q_{n-2} need smaller corrections to pair with $L(\phi)$ nontrivially. In dimension 2, this can be summarized as the following:

⁸Somewhere in the background of all of this, we are viewing the Lagrangian intersection Floer theory as a cosheaf on $(\mathbb{C}^*)^n$ and we are restricting to a small Weinstein chart around the torus F_q , and computing there.

Claim 4.2.5. *Let $Q = \mathbb{R}^2$. Let ∇_0 be the zero-valuation portion of ∇ . For any $E > 0$ there exists a compact set $K \subset Q$ so that for all $q \in Q \setminus K$ making $CF^\bullet(L(\phi), (F_q, \nabla))$ wide, the valuation of the correcting local system is large in the sense that*

$$\text{val}(\nabla - \nabla_0) > E.$$

This claim means we can determine the points where the support of $L(\phi)$ intersects the toric anticanonical divisor. This data can sometimes be enough to determine the mirror sheaf \mathcal{O}_D completely.

Corollary 4.2.6. *Let $Q = \mathbb{R}^2$. Let $D \subset \check{X}_\Sigma^\Lambda$ be a divisor transverse to the toric divisors defined by the equation $f = 0$ over the $(\mathbb{C}^*)^2$ open torus. Let ϕ be the tropicalization of f and suppose that $V(\phi)$ has genus zero. The tropical Lagrangian brane $L(\phi)$ is then mirror \mathcal{O}_{D_f} .*

As an example, consider the Lagrangian drawn in fig. 21. As we take the fiber F_q southwest towards infinity, the amount that the blue strip contributes to the differential goes to zero.

An example where we cannot identify D by its intersection with the anticanonical divisor is the elliptic curve, as through the 9 points of intersection between the anticanonical divisor and D there is a whole pencil of elliptic curves. In some circumstances it is possible to identify these tori, for example see section 7.

4.3 A sample computation of support

In this subsection, we show how the ideas of claim 4.2.4 work in an example. In a discussion with Diego Matessi, the following example of a large holomorphic strip contributing to $CF^\bullet(L(\phi), F_q)$ was found. Consider the Lagrangian pair of pants $L^{\frac{1}{2}}(\phi_{\text{pants}})$, the Lagrangian fiber F_q and the holomorphic cylinder $z_1 = z_2$ as drawn in fig. 21. The Lagrangians $L^{\frac{1}{2}}(\phi_{\text{pants}})$ and F_q intersect at two points $e, x \in F_q \cap L^{\frac{1}{2}}(\phi_{\text{pants}})$.

From the symmetry of our setup, the Lagrangian $L^{\frac{1}{2}}(\phi_{\text{pants}})$ intersects the complex plane $z_1 = z_2$ cleanly along a curve. Furthermore, the holomorphic cylinder $z_1 = z_2$ intersects F_q along a circle; therefore the portion of $z_1 = z_2$ bounded by $L^{\frac{1}{2}}(\phi_{\text{pants}})$ and F_q gives an example of a holomorphic strip with boundary on $L^{\frac{1}{2}}(\phi_{\text{pants}})$ and F_q . The ends of this holomorphic strip limit toward e and x . The valuation projection of this strip is a line segment connecting the point q with the vertex of the tropical pair of pants. For this reason, we will call this holomorphic strip u_{qv} . We expect that this strip is regular and that the area of this strip is roughly given by the length of the line segment corresponding to $\text{val}(u_{qv})$.

In addition to this large holomorphic strip, there are the two smaller strips which are contained in the neighborhood $U \ni q$. We call these strips u_1 and u_2 . These two smaller strips have equal area, and (after choosing an appropriate Hamiltonian perturbation of F_q) can be chosen so that $\omega(u_1) = \omega(u_2) < \omega(u_{qv})$. We now assume that the strips u_{qv}, u_1 , and u_2 are the only holomorphic strips with boundary on $L^{\frac{1}{2}}(\phi_{\text{pants}})$ and F_q for the standard

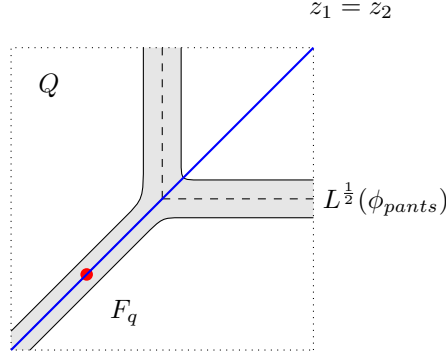


Figure 21: The intersection of the blue holomorphic cylinder and the tropical Lagrangian pair of pants is clean, and gives a holomorphic strip with boundary on $L^{\frac{1}{2}}(\phi_{pants})$ and F_q .

complex structure. This assumption is only for ease of exposition, as the symmetry $z_1 \leftrightarrow z_2$ can be used to show that any other holomorphic strips which have boundary on $L^{\frac{1}{2}}(\phi_{pants})$ and F_q will not contribute to the computation of the support of $L^{\frac{1}{2}}(\phi_{pants})$ in a meaningful fashion.

The strip u_{qv} is an example of a “large strip” which must be considered when computing exactly which local systems on F_q make $CF^\bullet(L^{\frac{1}{2}}(\phi_{pants}), (F_q, \nabla))$ wide. If no local systems are used, the differential on this Floer complex is given by the area of this strip:

$$m^1(e) = T^{\omega(u_{qv})} \cdot x.$$

By claim 4.2.4, the local system ∇_q with holonomy $1 + T^{-\omega(u_1) + \omega(u_{qv})}$ along the cycle of F_q corresponding to the conormal subtorus of $L^{\frac{1}{2}}(\phi_{pants})$ at the point q will correct the differential so that the Floer cohomology becomes wide.

The remainder of this example serves only to provide intuition, and is not a rigorous computation of the support of the Lagrangian $L^{\frac{1}{2}}(\phi_{pants})$. The goal is to show how one can recover the expected complex pair of pants as the complex support of the Lagrangian pair of pants.

We now assume the vertex of the tropical pair of pants is at $(0, 0)$, and give coordinates to Q so that $q = (-\log(r_1), -\log(r_2))$. We additionally will make a naïve assumption about the convergence of counts of holomorphic strips, and work over complex coefficients, and pick a value $E \in \mathbb{R}_+$ at which we evaluate the Novikov parameter. The local system ∇_q becomes non-unitary when one uses complex coefficients. We characterize the local system ∇_q in terms of its holonomy along the $\arg(z_1)$ and $\arg(z_2)$ loops of F_q , giving us quantities $(E^{a_1}, E^{a_2}) \in (\mathbb{C}^*)^2$. Following [Aur08, Section 4] we operate under the assumption that one may trade geometric deformations of F_q sweeping out Lagrangian flux for deformations of Floer theory through the use of non-unitary local systems on these tori. Barring the (very possible) issues of non-convergence in Floer differential when working with complex coefficients, one expects an identification of $(F_q, \nabla_q) \simeq (F_{q'}, \nabla_{q'})$ as objects in the Fukaya category whenever

$$(z_1, z_2) = (r_1 E^{a_1}, r_2 E^{a_2}) = (r'_1 E^{a'_1}, r'_2 E^{a'_2}).$$

The values (z_1, z_2) represent the coordinates of the point in $(\mathbb{C}^*)^2$ mirror to the Lagrangian brane (F_q, ∇_q) .

The points q which are on the “southwest” leg of the tropical pair of pants are those where $r = r_1 = r_2$. For ease of exposition, we take approximations for how local systems and area weight the counts of the strips u_1, u_2 and u_{qv} in the Floer differential.

$$\begin{aligned}\omega(u_1) &= 0 & \omega(u_2) &= 0 & \omega(u_{qv}) &= \log |r| \\ \text{hol}_{\nabla_q}(u_1) &= E^{\frac{1}{2}(a_1-a_2)} & \text{hol}_{\nabla_q}(u_1) &= E^{\frac{1}{2}(a_2-a_1)} & \text{hol}_{\nabla_q}(u_1) &= E^{\frac{1}{2}(a_1+a_2)}.\end{aligned}$$

Note that these values for the area of holomorphic strips cannot actually occur if $L^{\frac{1}{2}}(\phi_{\text{pants}})$ and F_q intersect transversely, however the relative areas and holonomy of the strips for any transverse intersection will match those chosen above. From these approximations, we may compute the differential explicitly in terms of the parameters a_i and r_i .

$$\begin{aligned}\langle m_{\nabla_q}^1(e), x \rangle &= \overbrace{(\text{hol}_{\nabla}(u_1) \cdot T^{\omega_{u_1}} - \text{hol}_{\nabla}(u_2) \cdot T^{\omega_{u_2}})}^{\text{Small Strips near } q} + \overbrace{\text{hol}_{\nabla}(u_{qv}) \cdot T^{\omega_{u_{qv}}}}^{\text{Large Strips}} \\ &= (E^{\frac{1}{2}(a_1-a_2)} - E^{\frac{1}{2}(a_2-a_1)}) + E^{\frac{1}{2}(a_1+a_2)} \cdot r \\ &= \left(\frac{z_1}{z_2}\right)^{\frac{1}{2}} - \left(\frac{z_2}{z_1}\right)^{\frac{1}{2}} + (z_1 z_2)^{\frac{-1}{2}} \\ &= (z_1 z_2)^{\frac{-1}{2}} (z_1 + z_2 + 1)\end{aligned}$$

This vanishes when $(1 - z_1 + z_2 = 0)$, which matches the support of the complex mirror pair of pants.

4.4 Fiberwise Sums and Subvarieties

Given a SYZ fibration $X \rightarrow Q$, there is a natural operation on pairs of Lagrangian submanifolds of X , called the *fiberwise sum* of Lagrangians [Sub10].

Definition 4.4.1. Let L_0 and L_1 be two Lagrangians in $X = (\mathbb{C}^*)^n = F_q \times Q$. Give this space coordinates (p, q) . Suppose that the projection maps $\text{val}|_{L_0} : L_0 \rightarrow Q$ and $\text{val}|_{L_1} : L_1 \rightarrow Q$ are transverse. Define the fiberwise sum to be the submanifold

$$L_0 + L_1 := \{(p_0 + p_1, q) \mid (p_0, q) \in L_1, (p_1, q) \in L_2\}.$$

If σ_ϕ and σ_ψ are two Lagrangian tropical sections, then the operation $\sigma_\phi + \sigma_\psi$ is always well defined and is equal to $\sigma_{\phi \odot \psi}$.

Claim 4.4.2 ([Sub10]). $L_1 + L_2$ is a Lagrangian submanifold.

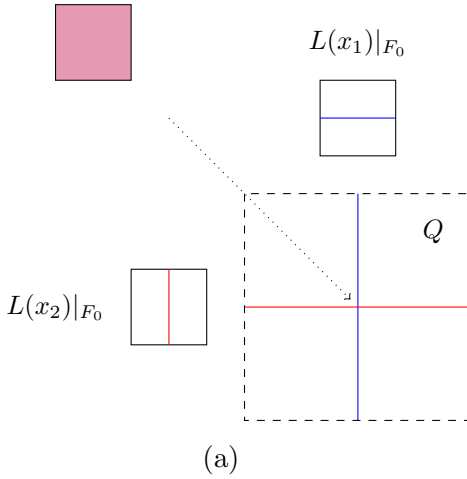
One immediate and useful property of this operation is that

$$\text{val}(L_0 + L_1) = \text{val}(L_0) \cap \text{val}(L_1).$$

Given $\phi, \psi : Q \rightarrow \mathbb{R}$ two tropical polynomials, $\text{val}(L(\phi) + L(\psi))$ is close to the tropical variety $V((\phi) + (\psi))$. Notice here the use of the standard plus sign in the left hand side, instead of the tropical plus sign. ⁹ As Lagrangian fiberwise sum is associative and commutative, we

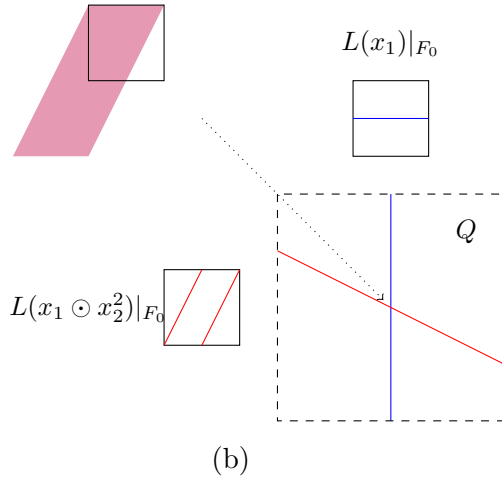
⁹The notation here is inspired by variety associated to the sum of ideals.

$$L(x_1) + L(x_2) = F_0$$



(a)

$$L(x_1) + L(x_1 \odot x_2^2) = 2 \cdot F_0$$



(b)

Figure 22: Fiberwise sum of tropical curves gives multiple copies of the SYZ fiber.

can define multiple intersections of tropical Lagrangians.

Definition 4.4.3. *Let ϕ_0, \dots, ϕ_k be tropical polynomials, and suppose that $L(\phi_i)$ have mutually transverse argument projections. Define the Lagrangian tropical variety generated by ϕ_i to be the submanifold*

$$L((\phi_0) + \dots + (\phi_k)) = L(\phi_0) + \dots + L(\phi_k).$$

There is no guarantee that this will produce an embedded submanifold.

Example 4.4.4. *Consider the tropical Lagrangian submanifolds $L(x_1)$ and $L(x_2)$ drawn in fig. 22a. Then $L(x_1) + L(x_2)$ is an SYZ fiber above the point of the intersection.*

However, if we take intersections of tropical Lagrangians where the intersection points have higher multiplicity, the fiberwise sum will not be immersed. The simplest such example, drawn in fig. 22b is $L(x_1)$ and $L(x_1 \odot x_2^2)$, whose fiberwise sum is a double cover of the fiber above the point of intersection.

There are two examples where we can guarantee that the fiberwise sum gives us an embedded Lagrangian: Locally planar intersections, and twisting by line bundles.

4.4.1 Locally planar intersections of Tropical Lagrangians

We now reduce to a setting where we can have an especially good characterization of the intersection between tropical subvarieties.

Definition 4.4.5. *Let $V(\phi)$ and $V(\psi)$ be two tropical hypersurfaces. We say that these tropical surfaces have locally planar intersection if for every point $p \in V(\phi) \cap V(\psi)$, there is a neighborhood $U \ni p$ and an integral special affine transform $u : U \rightarrow \mathbb{R}^n$ so that we can locally model the intersection on either*

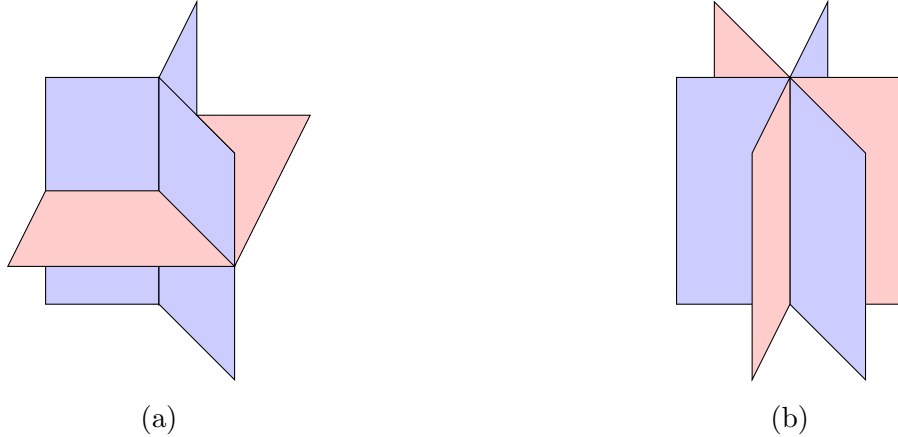


Figure 23: Example and non-example of a locally planar intersection of tropical hypersurfaces.

- $\phi \circ u^{-1} = x_1$ and $\psi \circ u^{-1} = \hat{\psi}(x_2, \dots, x_n)$.
- $\psi \circ u^{-1} = x_1$ and $\phi \circ u^{-1} = \check{\phi}(x_2, \dots, x_n)$.

Notice that this condition prohibits the intersection of the codimension 1 strata of $V(\phi)$ and $V(\psi)$. The condition generically occurs in dimensions 2 and 3. See figs. 23a and 23b for examples and non-examples. More generally, we say that $V(\phi_1), \dots, V(\phi_k)$ have mutually locally planar intersection if at every point in the intersection, there exist local coordinates so that these tropical polynomials can be rewritten as $x_1, x_2, \dots, x_{k-1}, \psi(x_k, \dots, x_n)$.

Claim 4.4.6. *Let $\{L(\phi_i)\}_{i=1}^{k+1}$ be a set of tropical embedded hypersurfaces with mutually locally planar intersection. At each point $p \in L((\phi_1) + \dots + (\phi_{k+1}))$, there is a neighborhood $U \subset Q$, a tropical polynomial $\psi : \mathbb{R}^{n-k} \rightarrow \mathbb{R}$, and a preferred decomposition $U = (\mathbb{C}^*)^{n-k} \times (\mathbb{C}^*)^k$ so we can model $L((\phi_1) + \dots + (\phi_{k+1}))$ on the smooth Lagrangian*

$$T^k \times L_{\mathbb{C}^{n-k}}(\psi) \subset (\mathbb{C}^*)^k \times (\mathbb{C}^*)^{n-k}.$$

Here, $T^k \subset (\mathbb{C}^*)^k$ is the standard product torus.

Proof. Let p be point in the intersection of the $V(\phi_i)$, and let U be a small neighborhood. By the planar intersection condition, we may take coordinates in which each tropical polynomial is rewritten as

$$\begin{aligned} \phi_i &= x_i \quad \text{For } 1 \leq i \leq k \\ \psi_{k+1} &= \psi(x_{k+1}, \dots, x_n) \end{aligned}$$

In these coordinates at the small neighborhood U the tropical Lagrangians take the form

$$\begin{aligned} L((\phi_1) + \dots + (\phi_k)) &= T^k \times \mathbb{R}^{n-k} \\ L(\psi) &= \mathbb{R}^k \times L_{\mathbb{C}^{n-k}}(\psi) \end{aligned}$$

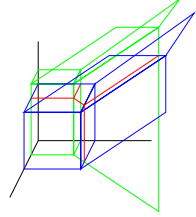


Figure 24: Two tropical hyperplanes with locally planar intersection drawn in red.

Since the operation of fiberwise sum is associative,

$$L((\phi_1) + \cdots + (\phi_{k+1})) = L((\phi_1) + \cdots + (\phi_k)) + L(\psi).$$

The claim now follows from the submanifold \mathbb{R}^{n-k} acting as the identity for Lagrangian fiber sum in the last $n - k$ components, and T^k acting as restriction to the fiber on the first k components. \square

Claim 4.4.6 shows that our Lagrangian associated to a tropical variety built from locally planar intersection matches the description from gluing together local pieces in [Mik18].

Example 4.4.7. *A first example that we look at in higher dimensions is the intersection of two generic hyperplanes $V(\phi_0), V(\phi_1)$ in \mathbb{R}^3 , which gives us a tropical curve in \mathbb{R}^3 (see fig. 24.) The intersection can be constructed from local pieces by taking two pairs of pants and gluing them together. Each pair of pants is modeled on $S^1 \times L(\phi_{\text{pants}}) \subset (\mathbb{C}^*)^{v_0^\perp} \times (\mathbb{C}^*)^{v_1} \subset (\mathbb{C}^*)^3$, where v_0 is the orthogonal direction to the plane of linearity of $V(\phi_1)$ where it intersects the codimension 1 stratum of $V(\phi_0)$ (and vice-versa for v_1). The two pants are connected by a cylinder modelled on $T^2 \times \mathbb{R}$. There is no common S^1 factor over the entire intersection.*

4.5 Twisting by Line Bundles

Let L be any Lagrangian submanifold, and $\psi : Q \rightarrow \mathbb{R}$ be a tropical polynomial. Recall that the wrapping Hamiltonian from section 3 can be compared to fiberwise sum with the section σ_ψ

$$\theta_\psi(L) = L + \sigma_\psi.$$

While wrapping is not an admissible Hamiltonian isotopy, it still sends admissible Lagrangian branes to admissible Lagrangian branes, giving an automorphism of the Fukaya category.

Theorem 4.5.1 ([Han18]). *Let $\psi : Q \rightarrow \mathbb{R}$ be the support function for a line bundle \mathcal{L}_ψ . The functor on the Fukaya category $L \mapsto L + \sigma_\psi$ is mirror to the functor $\mathcal{F}_L \mapsto \mathcal{F}_L \otimes \mathcal{L}_\psi$.*

A general expectation of mirror symmetry is that this theorem extends to Lagrangian submanifolds beyond line bundles. We give evidence towards this expectation in the setting of tropical Lagrangians in section 4.6.

Provided that $V(\phi)$ and $V(\psi)$ have a pair of pants decompositions and have locally planar intersection, the Lagrangian $L(\phi) + \sigma_\psi$ can be given an explicit description in terms of the pair of pants decomposition. We outline this construction in complex dimension 2, but the higher dimensional constructions are completely analogous. When $V(\phi)$ and $V(\psi)$ have locally planar intersection, the support of $V(\psi)$ is contained in the cylindrical region between each of the pants in the decomposition of $V(\phi)$. This means that if the smoothing and construction parameters for the tropical Lagrangians are chosen small enough, the strata

$$\begin{aligned} U_{\{v_i, v_j\}}^\psi \cap U_{\{w_i, w_j, w_k\}}^\phi &= \emptyset \\ U_{\{v_i, v_j\}}^\phi \cap U_{\{w_i, w_j, w_k\}}^\psi &= \emptyset \end{aligned}$$

are disjoint from one another. Therefore, the Lagrangian $L(\phi)$ matches $L(\phi) + \sigma_\psi$ over the charts near the vertices of the tropical curve, $U_{\{v_i, v_j, v_k\}}^\phi$.

To construct $L(\phi) + \sigma_\psi$ from this pair of pants decomposition, it suffices to modify the cylinders living over regions $U_{\{v_i, v_j\}}^\phi$. We construct this modification in a local model where $\phi = 0 \oplus x_1$ and $\psi = 0 \oplus x_2$. Topologically $L(\phi) + \sigma_\psi|_{U_{\{v_i, v_j\}}^\phi}$ is a cylinder, with an additional twist in the argument direction perpendicular to $V(\psi)$ at the point of intersection between the two tropical varieties, as drawn in fig. 25a, which shows $L(\phi_{\text{ell}}) + \sigma_{\phi_{\text{pants}}}$. This kind of modification to our tropical Lagrangian was remarked upon in [Mat18, Remark 5.2] as a more general way to construct tropical Lagrangians. This discussion shows that if $L(\phi)$ is mirror to \mathcal{O}_D , then the twisted Lagrangian $L(\phi) + \sigma_\psi$ is mirror to $\mathcal{O}_D \otimes \mathcal{L}_\psi$. This can also be understood as the mirror to the pushforward of a degree 3 line bundle on the curve D .

From the pair of pants description, it is clear that we can “twist” our Lagrangian in the argument along edges in ways that do not arise from adding on a section σ_ψ —see for instance, fig. 25b. These too should be mirror to pushforwards of line bundles on D , however these line bundles are not the pullbacks of line bundles on X . For comparison, we look at the corresponding construction on the B -model mirror.

Let $i : E \hookrightarrow \mathbb{CP}^2$ an elliptic curve, and let $\mathcal{O}(n)$ be a line bundle on \mathbb{CP}^2 . We can re-express twisting the sheaf $\mathcal{O}_E(E)$ by line bundles on \mathbb{CP}^2 by instead twisting on the elliptic curve instead,

$$i_*(\mathcal{O}_E) \otimes \mathcal{O}(n) = i_*(\mathcal{O}(n)|_E).$$

The line bundle $\mathcal{O}(n)|_E$ has degree $3n$. We have the same phenomenon on the A -model on $((\mathbb{C}^*)^2, z_1 + z_2 + (z_1 z_2)^{-1})$. In fig. 25a, we take the Lagrangian $L(\phi)$ which is mirror to an elliptic curve E , and the section $\sigma_{1 \oplus x \oplus y}$ which is mirror to $\mathcal{O}_{\mathbb{CP}^2}(1)$. The critical locus of $\sigma_{1 \oplus x \oplus y}$ meets $L(\phi)$ at 3 points. As a result, $L(\phi) + \sigma_{1 \oplus x_1 \oplus x_2}$ will be twisted at three points, corresponding to the fact that the degree of $\mathcal{O}|_E$ is three.

Returning to the B -model, it is not the case that every line bundle on E arises as the restriction of a line bundle on \mathbb{CP}^2 —only those line bundles whose degree are a multiple of three and whose divisors are in a balanced configuration. Let U be a small neighborhood of E . Then for any line bundle \mathcal{L}_E on E , there is a line bundle \mathcal{L}_U on U so that $i_*(\mathcal{L}_E) = \mathcal{O}_E \otimes \mathcal{L}_U$. However, \mathcal{L}_U will not necessarily extend to a line bundle on all of \mathbb{CP}^2 , while $i_*(\mathcal{L}_E)$ is always a well defined line bundle.

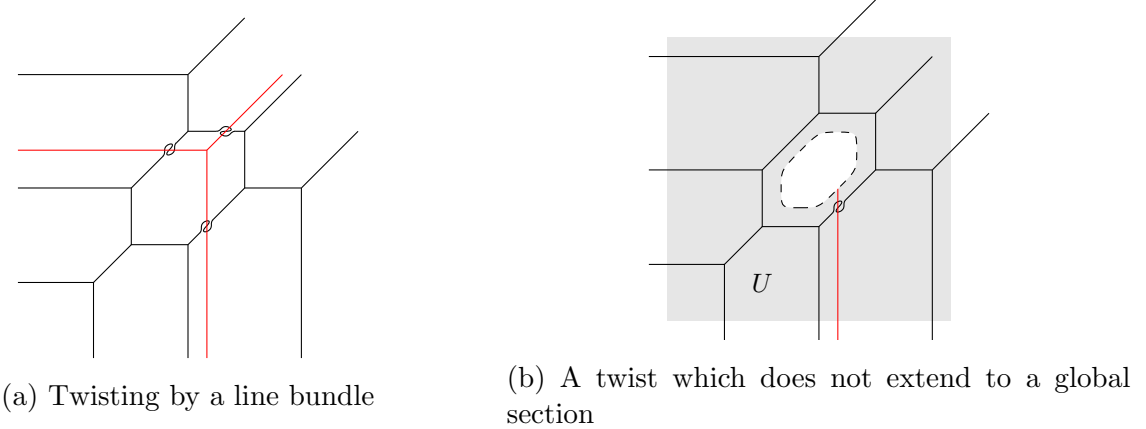


Figure 25: Inserting twists into tropical Lagrangians

In the A -model, we mimic this local twisting by working with the sheaf of affine differentials. On $U \subset \mathbb{R}^n$ these are the sections $\sigma : U \rightarrow \text{val}^{-1}(U)$ which are locally described as the differential of tropical polynomials. However, such a section need not be defined globally as the differential of a tropical polynomial. We denote set of such sections $\text{dTrop}(U)$ and defer the full definition until definition 5.1.2 when we explore the more general setting of tropical manifolds.

Definition 4.5.2. *Let L be a Lagrangian, with $\text{val}(L) \subset U$. Let $\sigma \in \text{dTrop}(U)$ be a tropical section defined over the subset U . Define the tropical Lagrangian twisted by σ to be the Lagrangian submanifold*

$$L(\phi; \sigma) := L(\phi) + \sigma.$$

As an example, in the mirror to \mathbb{CP}^2 we consider the open set U as drawn in fig. 25b. There exists a tropical differential which has critical locus intersecting the tropical curve defining E at a single point. The Lagrangian given by twisting along this tropical differential is expected to be mirror to the direct image of a degree 1 line bundle on E . We expect that we can understand these twistings by employing tropical geometry on the affine structure of $\text{val}(\phi)$ itself. This tropical differential does not extend to a section over the entire base.

Conjecture 4.5.3. *The twisted tropical Lagrangians $L(\phi; \sigma)$ are mirror to the direct image of line bundles on the mirror divisor D .*

4.6 Mirror Symmetry for locally planar intersections

Let D and E be two effective divisors. The scheme theoretic intersection of these divisors is given by

$$\mathcal{O}_{D \cap E} = \mathcal{O}_D \otimes \mathcal{O}_E.$$

This gives us the intuition for the extension of theorem 4.2.1.

Theorem 4.6.1. *For $0 \leq i \leq k$, let $L(\phi_i)$ be tropical Lagrangians mirror to \mathcal{O}_{D_i} . Suppose that the varieties $V(\phi_i)$ have locally planar intersections. There exists a Lagrangian cobordism with ends*

$$(L(\phi_1 + \cdots + \phi_k), L(\phi_1 + \cdots + \phi_k) - \sigma_{\phi_0}) \rightsquigarrow L(\phi_0 + \cdots + \phi_k).$$

Assuming that this cobordism is unobstructed, the Lagrangian $L((\phi_1) + \cdots + (\phi_k))$ is mirror to an object Chow-equivalent to $\bigotimes_{i=1}^k \mathcal{O}_{D_i}$.

Proof. We again use the tools of Lagrangian surgery. We will restrict to the case where we have two tropical Lagrangian submanifolds, $L(\phi_1)$ and $L(\phi_2)$, as the proof for additional intersections is analogous.

We first construct a cobordism with ends $(L(\phi_1), (L(\phi_1) + \sigma_{-\phi_2})) \rightsquigarrow L(\phi_1 + \phi_2)$. As the varieties $V(\phi_1)$ and $V(\phi_2)$ have locally planar intersections, we can use the neighborhoods described in claim 4.4.6 to locally model our Lagrangian intersection. We also use a strengthening of proposition 3.1.1, which works in the setting where the region U need not be a contractible subset convex subset of \mathbb{R}^n .

Proposition 4.6.2. *Let L_0 and L_1 be two Lagrangians with boundary. Let U be an open neighborhood of $L_0 \cap L_1$. Suppose there exists a choice of collar neighborhood for the boundary of U*

$$B_\epsilon(\partial U) \subset U = \partial U \times (0, r_0)_r$$

and a function $f : U \rightarrow \mathbb{R}$ with the following properties:

- *The function f is decreasing and convex in the r -variable*
- *The function vanishes on the complement of $B_\epsilon(\partial U)$.*
- *In a sufficiently small Weinstein neighborhood B_c^*U , the Lagrangian $L_1|_{B_c^*U}$ is the graph of the section df .*

Then there exists a Lagrangian $L_0 \#_U^\epsilon L_1$ satisfying the following properties:

- $L_0 \#_U^\epsilon L_1 \subset B_\epsilon((L_0 \cup L_1) \setminus (L_0 \cap L_1))$.
- *There exists a Lagrangian cobordism $K : (L_0, L_1) \rightsquigarrow L_0 \#_U^\epsilon L_1$*

The proof the lemma is completely analogous to proposition 3.1.1.

In each of these local charts, we may use proposition 4.6.2 to remove the intersections between $L(\phi_1)$ and $L(\phi_1) - \sigma_{\phi_2}$, giving us a cobordism $K(\phi_1 + \phi_2)$. A local analysis at the level of a pair of pants decomposition of $L(\phi_1) \# (L(\phi_1) + \sigma_{-\phi_2})$ shows that our constructed Lagrangian is Hamiltonian isotopic to the local charts constructed for $L(\phi_1 + \phi_2)$ in claim 4.4.6. This gives us the required Lagrangian up to small isotopy, and Lagrangian cobordism $K(\phi_1 + \phi_2)$.

Now suppose that the Lagrangians $L(\phi_1)$ and $L(\phi_2)$ are mirror to \mathcal{O}_{D_1} and \mathcal{O}_{D_2} . Consider the exact triangle

$$\mathcal{O}_{D_1} \otimes \mathcal{O}(-D_2) \rightarrow \mathcal{O}_{D_1} \rightarrow \mathcal{O}_{D_1} \otimes \mathcal{O}_{D_2}.$$

Provided that the Lagrangian $K(\phi_1 + \phi_2)$ is unobstructed, we have a mirror exact triangle

$$(L(\phi_1) - \sigma(\phi_2)) \rightarrow L(\phi_1) \rightarrow L(\phi_1 + \phi_2),$$

proving the theorem. \square

Remark 4.6.3. *A different approach to building tropical subvarieties comes from using a pair-of-pants decomposition; and with this approach one can build tropical Lagrangian submanifolds associated to any tropical subvarieties built in Q . However, not every tropical subvariety of Q arises as the tropicalization of some complex subvarieties of \check{X} . In a discussion with Abouzaid, it was pointed out to the author that superabundant tropical curves do not arise from complex subvarieties, and therefore by general Family Floer principles the tropical Lagrangians associated to such curves cannot represent unobstructed objects of the Fukaya category. However, as the construction for Lagrangian cobordisms associated to tropical subvarieties only holds in the setting that a tropical Lagrangian subvariety can be built from locally planar intersections, we expect that the tropical Lagrangians subvarieties which are constructed by taking intersections of hypersurfaces are unobstructed.*

We now return to conjecture 4.5.3. The cobordisms we've just constructed give us enough information to understand this conjecture in complex dimension 2.

Claim 4.6.4. *Provided that the cobordism constructed in theorem 4.6.1 is unobstructed, Conjecture 4.5.3 is true when $X = (\mathbb{C}^*)^2$.*

Proof. Pick $U \supset V(\phi)$ a neighborhood of the tropical curve, and a twisting section $\sigma = d\text{Trop}(U)$ whose critical locus is transverse to $V(\phi)$. Then we have an exact triangle

$$L(\phi) \rightarrow L(\phi; \sigma) \rightarrow \bigsqcup_{q \in V(\phi) \cap V(\psi)} F_q$$

which determines the mirror of $L(\phi; \sigma)$ up to rational equivalence. \square

A natural extension would be to look at intersections between transversely intersecting Lagrangian submanifolds whose intersection have multiplicity one. We expect that the Lagrangian surgery between $\theta_\psi(L_\phi)$ and $L(\phi)$ to be well defined whenever $V(\psi)$ and $V(\phi)$ are transverse and intersect with multiplicity one. However, the local model for $L(\phi) + L(\psi)$ is not as clear in this setting, making a comparison between the cobordism definition of the intersection and the fiberwise sum definition of the intersection more difficult.

5 Tropical Lagrangians in Almost Toric Fibrations

5.1 Almost Toric Fibrations

We have so far considered tropical Lagrangian hypersurfaces in $X = (\mathbb{C}^*)^n$, corresponding to tropical geometry on $Q = \mathbb{R}^n$. In general, it is expected that the base of an SYZ fibration should be a tropical manifold with singularities and boundary, giving us more spaces that we can study. We summarize a description of these tropical manifolds from [Gro11].

Definition 5.1.1. *An integral tropical affine manifold with singularities is a manifold with boundary Q containing an open subset Q_0 such that*

- Q_0 is an integral affine manifold admitting an atlas with transition functions in $SL(\mathbb{Z}^n) \ltimes \mathbb{R}^n$.
- $\Delta := Q \setminus Q_0$, the discriminant locus, is codimension 2
- $\partial Q \subset Q$ can be locally modelled after a $SL(\mathbb{Z}^n) \ltimes \mathbb{R}^n$ coordinate change on $\mathbb{R}^{n-k} \times \mathbb{R}_{\geq 0}^k$.

We will be interested in tropical manifolds where the discriminant locus additionally comes with some affine structure. A tropical manifold is a pair (Q, \mathcal{P}) , where \mathcal{P} is a polyhedral decomposition of Q . For a full definition of the data of a tropical manifold (Q, \mathcal{P}) , we refer the reader to [Gro11, Definition 1.27], and provide a short summary here. The vertices of this polyhedral decomposition are decorated with fan structures which are required to satisfy a compatibility condition so that the polyhedra may be glued with affine transitions across their faces. The compatibility need not extend to affine transitions in neighborhoods of the codimension 2 facets of the polyhedra, giving rise to the discriminant locus, a union of a subset of the codimension 2 faces. This determines the affine structure on Q_0 completely. We call such a manifold an integral tropical manifold if all of the polyhedra are lattice polyhedra. For most of the examples that we consider, Q will be real 2-dimensional, and the notions of tropical manifold and tropical affine manifold agree with each other.

In the setting where $Q = \mathbb{R}^n$, a tropical hypersurface is defined via the critical locus of a tropical function $\phi : Q \rightarrow \mathbb{R}$. However, in the general setting of tropical manifolds there are sets which are locally described by the critical locus of tropical functions but cannot be globally described by a tropical function due to monodromy around the singular fibers. Since the construction of tropical Lagrangians only requires the differential of the tropical function, this is not problematic.

Definition 5.1.2. *Let Q be a tropical manifold. The sheaf of tropical differentials on Q_0 is the sheaf Ω_{aff}^1 on the space Q_0 . It is given by the sheafification of the quotient:*

$$\Omega_{aff}^1(U) = \{\phi : U \rightarrow \mathbb{R}\}/\mathbb{R}$$

where $\phi : U \rightarrow \mathbb{R}$ is a piecewise linear polynomial satisfying the following conditions:

- $d\phi \in T_{\mathbb{Z}}^*U$ whenever $d\phi$ is defined,

- For every point $q \in U$ there exists an integral affine neighborhood $B_\epsilon(q)$ so that the restriction $\phi|_{B_\epsilon(q)}$ is concave.

The sheaf \mathbb{R} here is the sheaf of constant functions. The sheaf of integral tropical differentials is the subsheaf of constant sections of $T_{\mathbb{Z}}^*(Q_0)$.

Let $i : Q_0 \hookrightarrow Q$ be the inclusion. We define the sheaf of tropical sections¹⁰ to be the quotient sheaf

$$d\text{Trop} := i_*(\Omega_{aff}^1) / i_*(T_{\mathbb{Z}}^*Q_0).$$

We will call the sections of this sheaf the tropical sections, and denote them $\phi \in d\text{Trop}(U)$.¹¹ Given a tropical section ϕ , we denote the locus of non-linearity as $V(\phi) \subset Q$. Should ϕ have a representation in each chart by a smooth tropical polynomial, we say that ϕ is smooth.

Remark 5.1.3. *A point of subtlety: the quotient defining the sheaf of tropical sections is performed over Q , not Q_0 . Importantly, while the presheaves $i_*(\Omega_{aff}^1) / \text{pre}i_*(T_{\mathbb{Z}}^*(Q \setminus \Delta))$ and $i_*(\Omega_{aff}^1 / \text{pre}T_{\mathbb{Z}}^*(Q \setminus \Delta))$ agree, their sheafifications do not. In particular, the sheaf of tropical differentials remember that in the neighborhood of the discriminant locus, the tropical section must actually arise from a representative tropical differential.*

When $Q = \mathbb{R}^n$, there is no difference between the global sections of $d\text{Trop}$ and the differentials of global tropical polynomials.

Given a triple (Q, \mathcal{P}, ϕ) , one can construct a dual triple $(\check{Q}, \check{\mathcal{P}}, \check{\phi})$ using a process called the discrete Legendre transform. Away from the boundary the base manifolds Q and \check{Q} agree as topological spaces, however their affine structures differ at the singular points. At the boundary these spaces are modified so that the non-compact facets of Q are compactified in \check{Q} and vice-versa. The simplest example of this phenomenon is when $\check{Q} = \Delta_\Sigma \subset \mathbb{R}^2$ is a compact polytope. The Legendre dual to \check{Q} is the plane $Q = \mathbb{R}^2$, equipped with a fan decomposition whose non-compact regions correspond to the boundary vertices of \check{P} .

Given a tropical manifold Q , we can produce a torus bundle $X_0 = T^*Q_0 / T_{\mathbb{Z}}^*Q_0$ over Q_0 . This space X_0 comes with canonical symplectic and almost complex structure arising from the affine structure on Q_0 . In good cases this compactifies to an almost toric fibration X over Q . Similarly, we may produce a associated manifold \check{X} over \check{Q} . The pair of spaces X and \check{X} are candidate mirror spaces. When Q is non-compact we expect that Q is equipped with additional data in the form of a monomial admissibility condition or stops in order to obtain a meaningful mirror symmetry statement. This admissibility condition should be constructed by considering the open Gromov Witten invariants of \check{F}_p . The computation of these invariants is beyond the scope of our exposition, and we'll be content with constructing our admissibility conditions in an ad-hoc manner.

¹⁰In [Gro11], these are called piecewise linear affine multi-valued functions

¹¹This is an abuse of notation, as there may not be a globally defined function whose differential describes this section. However, this will make the remainder of our discussion consistent with the notation used to construct tropical Lagrangians.

The majority of our focus will be in $\dim(Q) = 2$, where there is a graphical notation for describing the affine geometry on Q and correspondingly the symplectic geometry of the 4-dimensional symplectic manifold X [Sym02].

To describe the affine structure on Q , we describe the monodromy around the singular fibers. This can be done diagrammatically with the following additional data.

Definition 5.1.4. *Let (Q, \mathcal{P}) be a 2-dimensional tropical manifold. Let Q^0 be the set of singular points. At each point $q_i \in Q^0$ we define the eigenray $R_i \subset Q$ to be the ray in the base starting at q_i pointing in the eigendirection of the monodromy around q_i . A base diagram is a map from $Q \setminus \bigcup_i R_i$ to \mathbb{R}^2 with the standard affine structure, with eigenrays marked with a dashed line at each singularity. We decorate the points q_i with the marker \times_k , where the monodromy around q_i is a k -Dehn twist.*

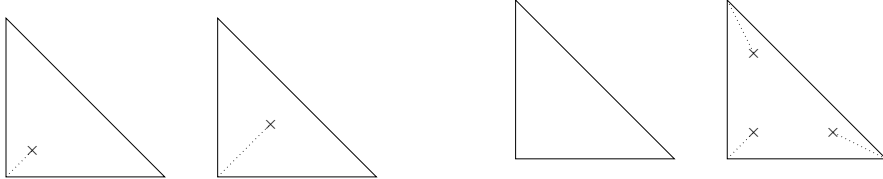
The Lagrangian fibers F_q of $X \rightarrow Q$ can be described by the points in the base diagram.

- If a point $q \in Q \setminus \mathbb{R}$ has a standard affine neighborhood, then F_q is a Lagrangian torus.
- If the point $q \in Q \setminus \mathbb{R}$ has an affine neighborhood modelled on $\mathbb{R} \times \mathbb{R}_{\geq 0}$ then fiber F_q is an elliptic fiber of corank 1, corresponding to an isotropic circle in X .
- If the point $q \in Q \setminus \mathbb{R}$ has an affine neighborhood modelled on $\mathbb{R}_{\geq 0} \times \mathbb{R}_{\geq 0}$, the fiber F_q is an elliptic fiber of corank 2, which is simply a point in X .
- If a point $q \in Q \setminus \mathbb{R}$ belongs to the discriminant locus, then the fiber is a Whitney sphere (if $k = 1$) or a plumbing of Lagrangians spheres (if $k > 1$).

There are several modifications of a base diagram Q which change the affine structure on Q but correspond to symplectomorphisms of $X \rightarrow Q$.

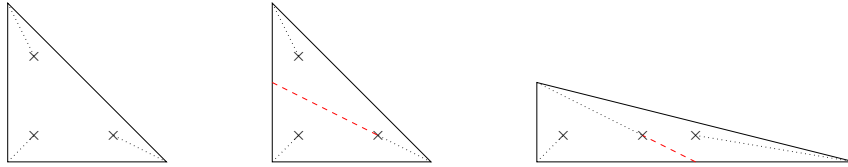
1. The *Nodal Slide* is an operation which moves a singular point of the base diagram in the direction of its eigenline. See fig. 26a.
2. The *Nodal Trade* operation modifies a base diagram by replacing an elliptic corank 2 fiber with a nodal fiber in the neighborhood of an elliptic corank 1 fiber. This replaces a corner with a nodal fiber whose eigenline points in the balancing direction to the corner. See fig. 26b.
3. The last operation we need to consider is *transferring the cut*, which corresponds to picking a different branch cut at a nodal point of the fibration. This reverses the eigenline of the singularity. See fig. 26c.

These three operations can be used to produce many different toric base representations of the same space.



(a) The Nodal Slide operation applied to a toric diagram. Note that the bottom corner is actually straight.

(b) The nodal trade applied three times to the toric diagram of \mathbb{CP}^2 . The toric divisor given by a nodal elliptic curve is transformed into a smooth elliptic.



(c) To transfer the cut, first extend an eigenline of the singular fiber in both directions. Then cut the base along this line, and identify the affine structures using the monodromy map.

Figure 26: Three modifications of toric base diagrams.

5.1.1 Some examples of tropical sections

A running example that we will use is the symplectic manifold $\mathbb{CP}^2 \setminus E$. One can construct an almost toric fibration for $\mathbb{CP}^2 \setminus E$ by starting with the toric base diagram for \mathbb{CP}^2 . By applying nodal trades at each corner, we obtain a toric fibration $\text{val} : \mathbb{CP}^2 \rightarrow Q_{\mathbb{CP}^2}$, where the boundary of $Q_{\mathbb{CP}^2}$ is an affine S^1 (see fig. 26b). The preimage of $\text{val}^{-1}(\partial Q_{\mathbb{CP}^2}) = E \subset \mathbb{CP}^2$, a symplectic submanifold isotopic to a smooth cubic. $\mathbb{CP}^2 \setminus E$ is an almost toric fibration over the interior of this set, $Q_{\mathbb{CP}^2 \setminus E} = Q_{\mathbb{CP}^2} \setminus \partial Q$. The monodromy around the three singular fibers allows us to construct some more interesting tropical sections of Q . We give three such examples of these sections and their associated tropical subvarieties below.

- Tropical sections which have critical locus close to the boundary of $Q_{\mathbb{CP}^2 \setminus E}$. Figure 27a gives an example of such a section. Even though the critical locus appears to have three corners, the affine coordinate change across the branch cuts means that this critical locus is actually an affine circle.
- The example given in fig. 27b is an example of a tropical section which does not arise as the differential of a globally defined tropical function. The critical locus terminates at the nodal point, and points in the direction of the eigenray of the nodal point.
- Tropical sections which meet the singular fibers coming from admissible tropical sections as in fig. 27c. This gives us an example of a compact tropical curve in Q of genus 1.

The examples above are typical of the kind of phenomenon which may occur for tropical curves in affine tropical surfaces.

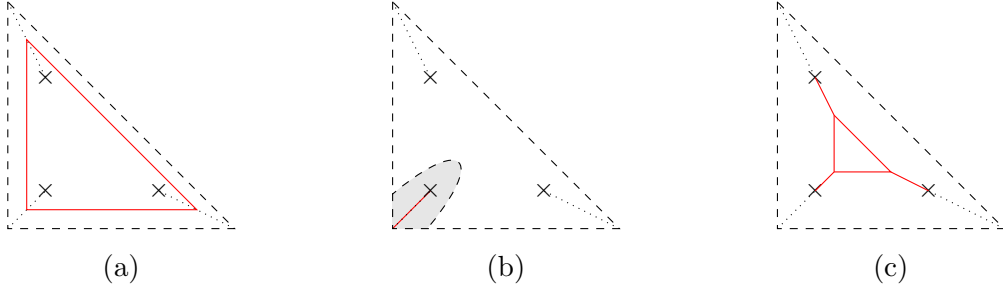


Figure 27: Tropical Subvarieties associated to some tropical sections on $\mathbb{CP}^2 \setminus E$.

Definition 5.1.5. Let $V \subset Q$ be a tropical curve in an affine tropical surface.

We say that V avoids the critical locus if V is disjoint from Δ and ∂Q .

We say that the interior of V avoids the critical locus if V is disjoint from ∂Q , and at each node $q \in Q \setminus \Delta$, there is a neighborhood $B_\epsilon(q)$ so that the restriction of $V \cap B_\epsilon(q)$ is a ray parallel to the eigenray of q .

5.2 Lifting to Tropical Lagrangian Submanifolds

Much of the machinery we have constructed for building Lagrangians lifts of tropical hypersurfaces in the fibration $(\mathbb{C}^*)^n \rightarrow \mathbb{R}^n$ carries over to building tropical Lagrangian hypersurfaces for $X \rightarrow Q$ with the dimension of the base $\dim Q = 2$. By abuse of notation, when we are given a tropical section $\phi \in d\text{Trop}(U)$ where $U \subset Q \setminus \Delta$, we will write $\sigma_\phi : U \rightarrow X|_U$ to mean the Lagrangian section defined over the bundle $X|_U \rightarrow U$ given by some choice of smoothing parameter. It is immediate that we can use the existing surgery lemma to build tropical Lagrangians away from the critical locus.

Claim 5.2.1. Let $\text{val} : X \rightarrow Q$ be an almost toric Lagrangian fibration. Suppose that $V(\phi) \subset Q$ is a tropical curve which is disjoint from the critical locus. Then there exists a Lagrangian submanifold $L(\phi) \subset X$ whose valuation projection lies in a small neighborhood of V . Furthermore, if Q has no boundary, there exists a tropical section ϕ so that $L(\phi) = \sigma_0 \# \sigma_{-\phi}$.

In the case where $\dim(Q) = 2$, we can find a Lagrangian lift when the interior of V avoids the critical locus. This is built on the following local model.

Claim 5.2.2. Let $X = \mathbb{C}^2 \setminus \{z_1 z_2 = 1\}$ be the symplectic manifold with symplectic fibration

$$\begin{aligned} W : \mathbb{C}^2 \setminus \{z_1 z_2 = 1\} &\rightarrow \mathbb{C} \setminus \{1\} \\ (z_1, z_2) &\mapsto z_1 z_2 \end{aligned}$$

and let $\text{val} : X \rightarrow Q$ be the almost toric Lagrangian fibration described in [Aur07, Section 5.1]. Then Q has a single node q_\times of multiplicity 1, and there exists a tropical Lagrangian lift of the eigenray of q_\times .

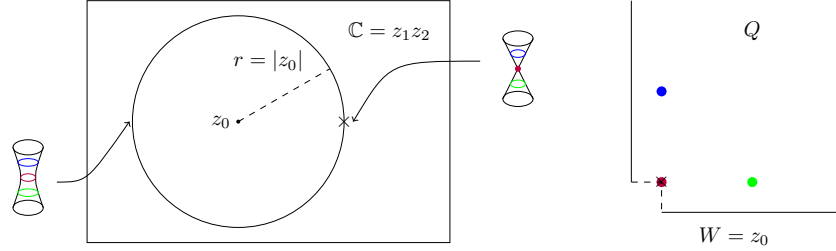


Figure 28: Lagrangian tori constructed from a Lefschetz fibration giving an almost toric fibration. The colored fibers correspond to cycles ℓ being parallel transported around a circle in the base.

Proof. The claim follows from considering the construction of the almost toric fibration arising from the Lefschetz fibration W . The rotation $(z_1, z_2) \mapsto (e^{i\theta}z_1, e^{-i\theta}z_2)$ is a global Hamiltonian S^1 symmetry which preserves the fibers of the fibration. Let $\mu : (\mathbb{C}^*)^2 \rightarrow \mathbb{R}$ be the moment map of this Hamiltonian action, which also descends to a moment map $\mu : W^{-1}(z) \rightarrow \mathbb{R}$. This map gives an SYZ fibration on the fibers of the Lefschetz fibration.

The base of the Lefschetz fibration $\mathbb{C} \setminus \{1\}$ comes with a standard SYZ fibration by circles $1 + re^{2\pi i\theta}$. The symplectic parallel transport map given by the Lefschetz fibration preserves the SYZ fibration on $W^{-1}(z)$; as a result, one can build an SYZ fibration for the total space $\{\mathbb{C}^2 \setminus z_1 z_2 = 1\}$ by taking the circles $\text{val}_{W^{-1}(z)}^{-1}(s)$ and parallel transporting them along circles $1 + re^{i\theta}$ of the second fibration to obtain Lagrangian tori

$$F_{r,s} = \{(z_1, z_2) \mid |z_1 z_2 - 1| = r, \mu(z_1, z_2) = s\}.$$

The nodal degeneration occurs from parallel transport of vanishing cycle through the path $1 + e^{i\theta}$. This corresponds to the single almost toric fiber of this fibration, a Whitney sphere, which occurs in the base when $q_x = (1, 0)$. Q comes with an affine structure by identifying the cotangent fiber at q with $H^*(F_q, \mathbb{R})$, and taking the lattice to be the integral homology classes. The monodromy of this fibration around the Whitney sphere acts by a Dehn twist on the vanishing cycle (i.e. for $s = 0$) of F_q . As a result, the coordinate s is a global affine coordinate on Q near q_x , but r is not. The eigenray is $s = 0$. The Lagrangian tori F_q with q in the eigenray of q_x are those tori which are built from parallel transport of the vanishing cycle. See fig. 28 for the correspondence between Lagrangians in the Lefschetz fibration and almost toric fibration.

We now consider the Lagrangian thimble τ drawn from the critical point $(z_1, z_2) = (0, 0)$. As the Lagrangian thimble is built from a parallel transport of the vanishing cycle, it only intersects the Lagrangians F_q with q on the eigenray of q_x . Therefore, this Lagrangian thimble has valuation projection travelling in the eigenray direction of q_x , proving the claim. \square

Corollary 5.2.3. *Let $\text{val} : X \rightarrow Q$ be an almost toric Lagrangian fibration over an integral tropical surface Q . Let V be a smooth tropical variety whose interior avoids the discriminant locus Δ . Then there exists a tropical Lagrangian lift $L \subset X$ of V .*

Proof. First, construct the lift of V to a Lagrangian \mathring{L} on $X \setminus X^0$. It remains to compactify \mathring{L} to a Lagrangian submanifold of X . At each point $q_i \in X^0$, we take a neighborhood B_i of q_i and model it on the standard neighborhood from claim 5.2.2. The portion of \mathring{L} with valuation over B_i is a Lagrangian cylinder given by the periodized conormal to the eigenray of q_i . Similarly, the thimble τ_i restricted to this valuation is a Lagrangian cylinder given by the periodized conormal to the eigenray of q_i . Therefore, we may compactify \mathring{L} to a Lagrangian $L \subset X$ by gluing the thimbles τ_i to L at each nodal point such that $q_i \in V$. \square

This allows us to build tropical Lagrangian lifts of the tropical curves described in figs. 27a to 27c. We may generalize the examples of compact Lagrangian tori in \mathbb{CP}^2 to more toric symplectic manifolds with $\dim_{\mathbb{C}}(X) = 2$. Let X_Σ be a toric surface, and let $\text{val} : X_\Sigma \rightarrow Q_\Sigma^{dz}$ be the standard moment map projection. The moment polytope Q^{dz} is an example of almost toric base diagram. Consider the almost toric fibration $\text{val} : X_\Sigma \rightarrow Q_\Sigma$ obtained by applying a nodal trade to each corner of the moment polytope. The boundary of Q is now an affine circle, corresponding to a symplectic torus $E \subset X_\Sigma$.

Example 5.2.4. *The neighborhood of ∂Q_Σ is topologically $\partial Q_\Sigma \times [0, \epsilon)_t$. For fixed real constant $0 < r < \epsilon$, we construct the tropical function $r \oplus t$, which only has dependence on collar direction t . This extends to a tropical function over Q_Σ , whose critical locus is an affine circle pushed off from the boundary ∂Q_Σ . The critical locus is a tropical curve which avoids the discriminant locus, so there is an associated Lagrangian torus $L_r^{\partial Q_\Sigma} \subset X_\Sigma$ corresponding to this tropical curve.*

This Lagrangian torus can also be constructed without using the machinery of Lagrangian surgery. Let $\gamma \subset E$ be a curve. There is a neighborhood D of $E \subset X_\Sigma$ which is a disk bundle $D \rightarrow E$. There is a standard procedure to take γ and lift it to a Lagrangian ∂D_γ , the union of real boundaries of this disk bundle along the curve γ . See fig. 29a.

As one increases the parameter r , the Lagrangian $L_r^{\partial Q_\Sigma}$ approaches the critical locus Δ_Σ . One can continue this family of Lagrangian submanifolds past the critical locus.

Example 5.2.5. *In the above example, each nodal point q_i corresponds to a corner of the Delzant polytope Q_Σ^{dz} . The index i is cyclically ordered by the boundary of the Delzant polytope. Let Σ_i be the fan generated by vectors v_i^-, v_i^+ given by the edges of the corner corresponding to q_i . Let v_i^λ be the eigenray of q_i . Then $\Sigma_i \cup \{v_i^\lambda\}$ is a balanced fan. At each nodal point q_i , consider the tropical pair of pants with legs in the directions $\Sigma_i \cup \{v_i^\lambda\}$.*

The legs of adjacent pairs of pants (from the cyclic ordering) match so that $v_i^- = -v_{i+1}^+$. This means that if the pairs of pants are properly placed (say so that the distance from the vertex of the pair of pants along the eigenray direction to the boundary ∂Q_Σ are all equal) these assemble into a tropical curve.

This is a tropical curve whose interior is disjoint from the critical locus, and thus lifts to a tropical Lagrangian with the topology of a torus in X_Σ . See fig. 29b

The two previous examples are related to each other via a Lagrangian isotopy which we will explore in section 7. A curious feature of these Lagrangian tori is that they seemingly

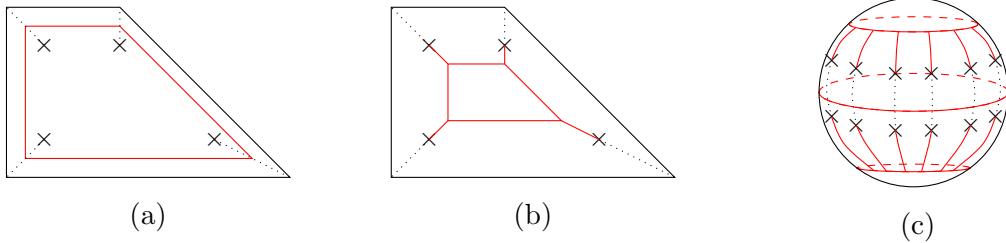


Figure 29: Some more examples of tropical sections

fiber a large portion of $X_\Sigma \setminus E$, and are quite different from the standard toric fibration on $X_\Sigma \setminus E$.

We now give two more examples of tropical Lagrangians which exist in compact symplectic manifolds and make some comments about their geometry as well.

Example 5.2.6 (K3 surface). *Consider a toric base diagram for a K3 surface, which is obtained from taking two copies of \mathbb{CP}^2 blown up 3 times along each edge, and then identifying the boundary elliptic curves. One can produce this Lagrangian torus fibration as the hyperKähler twist of an elliptic fibered K3 surface. The base is a sphere with 24 singular fibers, and one can select branch cuts between pairs of singular fibers. In fig. 29c, we have drawn 3 tori which are somewhat analogous to the tori constructed in figs. 29a and 29b. These Lagrangians also seemingly fiber a large portion of the K3 surface.*

Example 5.2.7. *One of the simplest examples to consider are tropical Lagrangian curves inside of Abelian varieties $X_{M_\mathbb{Z}}$. Here, Q is a given by the torus $\mathbb{R}^n / M_\mathbb{Z}$ for some choice of lattice $M_\mathbb{Z} \subset \mathbb{R}^n$. The tropical manifold Q has no discriminant locus. The global sections of $d\text{Trop}(Q)$ strongly depend on the choice of lattice. Given a global tropical section σ_ϕ , we may take the connect sum $\sigma_0 \#_{U_{v_i}} \sigma_{-\phi}$. Because $X_{M_\mathbb{Z}}$ is compact, this connect sum is Hamiltonian isotopic to the standard connect sum for some Hamiltonian θ making $\theta(\sigma_\phi)$ and σ_0 transverse (claim 3.3.17.) As a result, the same argument of unobstructedness (proposition 3.3.8) may be carried out to prove that $L(\sigma_\phi)$ is unobstructed. An upshot of this example is that the argument here is completely within the compact setting, so the surgery from proposition 3.1.1 matches the standard surgery after Hamiltonian isotopy, and the arguments using bottlenecked Lagrangians (definition 3.3.11) are no longer necessary.*

If the tropical hypersurface V is not smooth there is some additional complication in constructing an immersed Lagrangian lift of V , especially if V does not avoid the discriminant locus. In definition 6.1.3, we will discuss how construct embedded Lagrangian lifts corresponding to some non-smooth tropical curves in $(\mathbb{C}^*)^2$. These tropical curves are allowed to have edges with higher multiplicity. If it is possible to lift a non-smooth tropical curve to a embedded Lagrangian, the lift of an edge with multiplicity greater than one is a collection of Lagrangian cylinders with valuation over the edge. These Lagrangian cylinders are lifted to different arguments of the tori above the edge so that they do not intersect.

Suppose that $V \subset Q$ is a non-smooth tropical curve whose interior avoids the discriminant locus, which additionally admits an embedded tropical Lagrangian lift $L(V) \subset X \setminus X^0$. Then one may compactify $L(V)$ to an immersed Lagrangian in X by attaching Lagrangian thimbles to the non-compact Lagrangian cylinders which run off toward the discriminant locus. If the edge has higher multiplicity, this corresponds to a collection of thimbles constructed from the same intersection point, each of which mutually have pairwise intersection. From this immersed Lagrangian, one can produce an embedded Lagrangian submanifold by applying Lagrangian surgery at the transverse intersection points lying at the ends of the multiply covered edges meeting the discriminant locus. There is no guarantee that the resulting Lagrangian will be oriented, so the meaning of these Lagrangians as objects of the Fukaya category is slightly obscured.

5.3 Digression: Markov Triangles and Lagrangians

We now go on a small trip building many new immersed Lagrangians in \mathbb{CP}^2 using Markov triangles. This discussion is independent of the remainder of this paper.

Definition 5.3.1. *A Markov triangle is a triple of primitive vectors and numbers*

$$\begin{array}{ll} (a_1, a_2, a_3) & a_1, a_2, a_3 \in \mathbb{N}, \quad a_1^2 + a_2^2 + a_3^2 = 3a_1a_2a_3 \\ (\hat{u}_1, \hat{u}_2, \hat{u}_3) & \hat{u}_1, \hat{u}_2, \hat{u}_3 \in \mathbb{N}^2, \quad a_1^2\hat{u}_1 + a_2^2\hat{u}_2 + a_3^2\hat{u}_3 = 0 \end{array}$$

The eigenrays of a Markov triple are the (nonprimitive) vectors

$$\vec{v}_1 = \hat{u}_3 - \hat{u}_2 \quad \vec{v}_2 = \hat{u}_1 - \hat{u}_3 \quad \vec{v}_3 = \hat{u}_1 - \hat{u}_2$$

Claim 5.3.2 ([Via14]). *Let $\hat{u}_1, \hat{u}_2, \hat{u}_3$ be three primitive vectors so that*

$$a_1^2\hat{u}_1 + a_2^2\hat{u}_2 + a_3^2\hat{u}_3 = 0$$

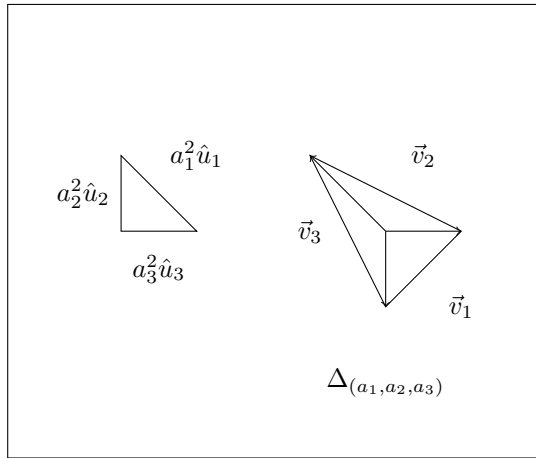
Then if we define

$$\begin{array}{lll} a'_1 = a_2 & a'_2 = 3a_2a_3 - a_1 & a'_3 = a_3 \\ \hat{u}'_1 = \hat{u}_1 & \hat{u}'_2 = \hat{u}_2 & \hat{u}'_3 = \frac{1}{(a'_3)^2}(-(a'_1)^2\hat{u}_1 - (a'_2)^2\hat{u}_2) \end{array}$$

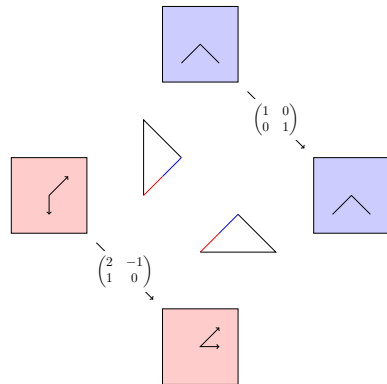
the collection $(a'_1, a'_2, a'_3), (\hat{u}'_1, \hat{u}'_2, \hat{u}'_3)$ is a Markov triangle.

The choice of coefficients may seem a bit strange; this notation relates the two Markov mutations by transferring the cut drawn in fig. 30.

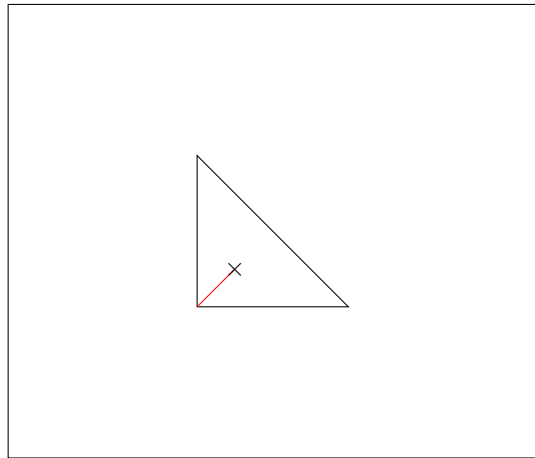
Theorem 5.3.3 ([Via14]). *For each (a_1, a_2, a_3) , a Markov triple, the base diagram obtained by performing nodal trades on the corresponding the Markov triangle is an almost toric base diagram for \mathbb{CP}^2 . The Lagrangian tori fiber above the barycenter of the triangle is monotone. However, no two of these Lagrangian tori can be identified by a symplectomorphism of \mathbb{CP}^2 .*



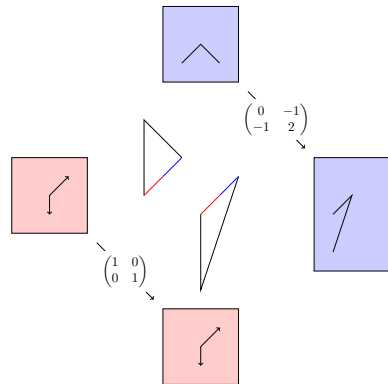
(a) Labeling of edges for Markov Triangle



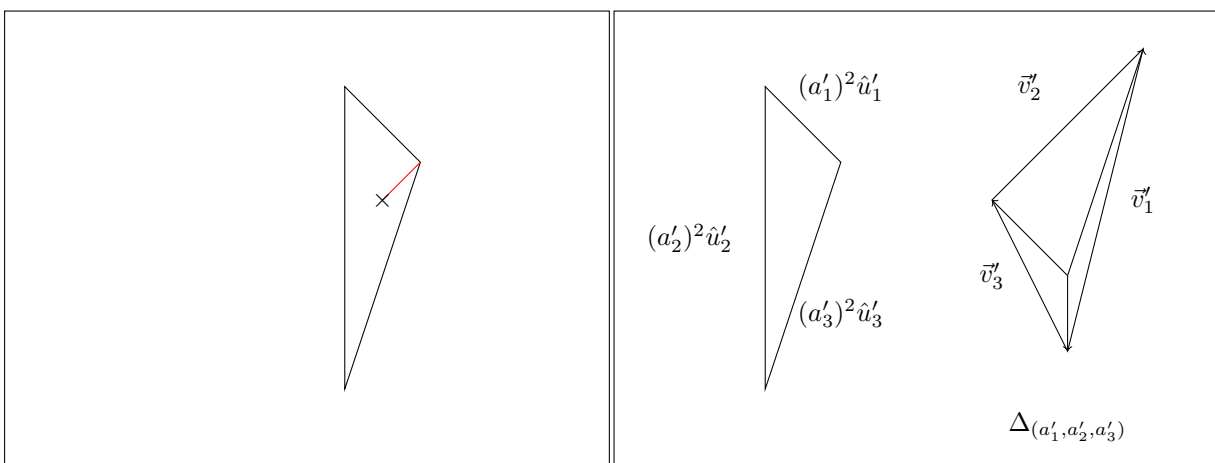
(c) Cutting the base into two pieces, and identifying either side of the node with matrix.



(b) Applying a nodal trade at the corner.



a- (d) Switching the branch cut so it points in the other direction.



(e) Gluing two charts back together
ray pointing in opposite direction.

(f) Applying another nodal trade. This completes the mutation of the Markov triangle.

Figure 30: Setting up Markov Mutations

We will use these almost toric base diagrams to construct tropical Lagrangians. From each node of the base diagram, take a_i copies of the eigenray, where a_i is the coefficient associated to the opposite edge. These eigenrays all meet at the barycenter. We'll use this tropical curve to build a tropical Lagrangian. Notice that this tropical Lagrangian will fail to be immersed, as the thimbles corresponding to a_i copies of the eigenrays will intersect each other at the critical point of the associated nodal fibers. In order to show that the vertex is balanced, and compute the genus of this tropical Lagrangian, we'll need the following computation.

Lemma 5.3.4. *Let $(a_1, a_2, a_3), (\hat{u}_1, \hat{u}_2, \hat{u}_3)$ be a Markov triangle.*

- *The affine length of \vec{v}_i is a_i .*
- *Let $\Delta_{(a_1, a_2, a_3)}$ be the convex hull of vectors $\hat{u}_1, \hat{u}_2, \hat{u}_3$. Then we can compute the area*

$$\text{Area}(\Delta_{(a_1, a_2, a_3)}) = \frac{3a_1 a_2 a_3}{2}.$$

Proof. We prove by showing the claim holds under the application of mutation.

Let $\{(a_1, a_2, a_3), (\hat{u}_1, \hat{u}_2, \hat{u}_3)\}$ and $\{(a'_1, a'_2, a'_3), (\hat{u}'_1, \hat{u}'_2, \hat{u}'_3)\}$ be Markov triangles related by mutation. Suppose that the claim holds for the first triangle. For the first claim, notice that $\vec{v}_3 = \vec{v}'_3$, and $a_3 = a'_3$, and \vec{v}'_1 is related to \vec{v}_2 by an element of $SL_2(\mathbb{Z})$, which can be seen from the transferring the cut process in fig. 30. We therefore only need to check for \vec{v}'_2 , which is shown by algebraic computation

$$\begin{aligned} \vec{v}'_2 &= \hat{u}'_1 - \hat{u}'_3 = \hat{u}_1 + \frac{1}{(a'_3)^2} \cdot ((a_2)^2 \cdot \hat{u}_1 + (a'_2)^2 \hat{u}_2) \\ &= \hat{u}_1 + \frac{1}{(a_3)^2} \cdot ((a_2)^2 \cdot \hat{u}_1 + (3a_2 a_3 - a_1)^2 \hat{u}_2) \\ &= \hat{u}_1 + \frac{1}{a_3^2} \left(a_2^2 \hat{u}_1 + (a_2^2 + a_3^2)^2 \frac{\hat{u}_2}{a_1^2} \right) \\ &= \frac{a_2^2 + a_3^2}{a_3^2} \left(\hat{u}_1 + \frac{a_2^2 + a_3^2}{a_1^2} \hat{u}_2 \right) \\ &= \frac{a_2^2 + a_3^2}{a_1^2} \left(\hat{u}_2 + \frac{a_1^2 \hat{u}_1 + a_2^2 \hat{u}_2}{a_3^2} \right) \\ &= \frac{a_2^2 + a_3^2}{a_1^2} (\hat{u}_2 - \hat{u}_3) \\ &= \frac{-3a_2 a_3 - a_1}{a_1} (\hat{u}_3 - \hat{u}_2) \\ &= \frac{-a'_2}{a_1} \vec{v}_1. \end{aligned}$$

For the second claim, we compute the area using the wedge product

$$2 \text{Area}(\Delta_{(a'_1, a'_2, a'_3)}) = \vec{v}'_2 \wedge \vec{v}'_3 = \frac{-a'_2}{a_1} \vec{v}_1 \wedge \vec{v}_3 = 3a'_1 a'_2 a'_3$$

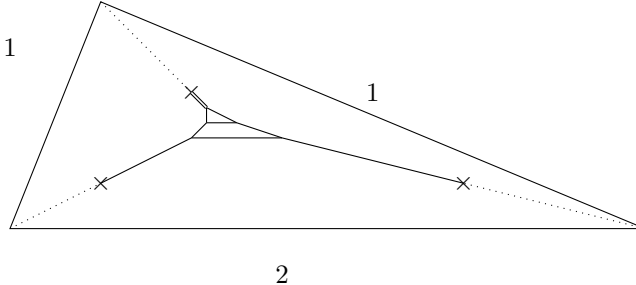


Figure 31: The immersed tropical Lagrangian associated to the Markov triple $(1, 1, 2)$. Notice that the top thimble is of multiplicity two. This Lagrangian has one self-intersection.

□

By an application of Pick's theorem, we get the following corollary:

Corollary 5.3.5. *Let $\Delta_{(a_1, a_2, a_3)}$ be the convex hull of associated vectors $\hat{u}_1, \hat{u}_2, \hat{u}_3$. Then $\Delta_{(a_1, a_2, a_3)}$ contains $\frac{3}{2}a_1a_2a_3 - \frac{a_1+a_2+a_3}{2} + 1$ lattice points.*

One can use this corollary to construct tropical Lagrangian submanifolds in \mathbb{CP}^2 by taking a Lagrangian lift of this tropical variety. The polytope $\Delta_{(a_1, a_2, a_3)}$ locally describes the Newton polytope of the tropical polynomial primitive at the vertex of this Lagrangian. The genus of the Lagrangian submanifold lift is determined by the number of interior lattice points.

Claim 5.3.6. *The tropical Lagrangian associated to the (a_1, a_2, a_3) base diagram of \mathbb{CP}^2 is well defined and has genus $\frac{3a_1a_2a_3 - (a_1 + a_2 + a_3)}{2} + 1$. This tentacles of this Lagrangian correspond to a_1, a_2, a_3 copies of thimbles which intersect at each corner, giving additional*

$$\binom{a_1}{2} + \binom{a_2}{2} + \binom{a_3}{2}$$

self-intersection points.

It is important to note that these are all immersed Lagrangians in \mathbb{CP}^2 unless we're using the Markov triple $(1, 1, 1)$. This must be the case as any embedded oriented Lagrangian in \mathbb{CP}^2 must have genus 1. If one tries to resolve the self-intersections on this Lagrangian, we necessarily will construct a non-orientable Lagrangian submanifold of \mathbb{CP}^2 . See fig. 31 for an example of a immersed genus 2 curve in \mathbb{CP}^2 .

6 Dimers, del Pezzos and Wall-Crossing

We now introduce a combinatorial framework tying together the stories from section 1.2 and definition 3.4.1, generalizing some of the ideas discussed in [Mat18, Section 5.2], and the previous work of [TWZ18; UY13; STWZ15; FHKV+08].

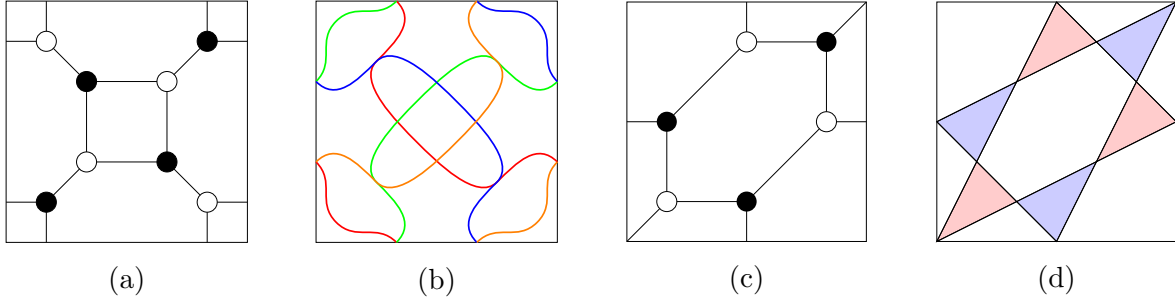


Figure 32: Two examples of dimers and their zigzag graphs. The second example is an affine dimer.

Definition 6.0.1. A dimer is an embedded bipartite graph G on T^2 so that $V(G) = V^\circ \sqcup V^\bullet$. A zigzag configuration for a dimer G is a set of transverse cycles $\Sigma \subset C_1(T^2)$ satisfying the following conditions:

- Each connected component in $T^2 \setminus \Sigma$ contains at most one vertex of G .
- Each edge of the dimer is transverse to every cycle. Each edge passes through exactly one intersection point between 2 cycles.
- The oriented normals of the cycles point outward on the V° dimer faces, and inward on the V^\bullet dimer faces.

We will now restrict to the setting of *affine dimers*, where Σ is a collection of affine cycles.¹² It is the case that for every $[\Sigma] \subset H_1(T^2)$ we can find a dimer whose zigzag collection is $[\Sigma]$, however, it is not necessarily the case that we can find an *affine* dimer with this property [Gul08], [For16, Section 4]. A dimer picks out an oriented two chain whose boundary is Σ . This is the data that we need to run the machinery from section 1.2, which we now generalize.

More generally, we will consider pairs of the following form:

Definition 6.0.2. A higher dimer or n -dimer is two collections of n -polytopes

$$\{\Delta_v^\circ\}, \{\Delta_w^\bullet\} \subset \mathbb{R}^n$$

which satisfy the following properties.

- Each vertex set $\{\Delta_v^{\bullet/\circ}\}^0$ is a set of distinct points on the torus in the sense that whenever $w_1, w_2 \in \{\Delta_v^\circ\}^0$ and $w_1 \equiv w_2 \pmod{\mathbb{Z}^n}$, then $w_1 = w_2$.
- We require that these two vertex sets match after quotienting by the lattice,

$$\{\Delta_v^\circ\}^0 / \mathbb{Z}^n = \{\Delta_w^\bullet\}^0 / \mathbb{Z}^n.$$

¹²Somewhat counterintuitively, an affine dimer is one whose zigzags are straight circles.

- Let $p_1 \in \Delta_v^\circ$ be a vertex, and let $p_2 \in \Delta_w^\bullet$ be the corresponding vertex so that $p_1 \equiv p_2 \pmod{\mathbb{Z}^n}$. Let $\{e_1, \dots, e_k\}$ be the edges of Δ_v° containing the vertex p_1 . We require that the edges of Δ_w^\bullet containing p_2 point in the opposite directions $\{-e_1, \dots, -e_k\}$.

If the interiors of the Δ_v° and Δ_w^\bullet are disjoint $\pmod{\mathbb{Z}^n}$, we say that the higher dimer configuration has no self-intersections.

From this data, we obtain a bipartite graph $G \subset T^n$, whose vertices are indexed by $\{\Delta_v^\circ\} \cup \{\Delta_w^\bullet\}$, and whose edges are determined by which polytopes in the higher dimer share a common vertex.

We will usually index the polytopes by the vertices $v^{\bullet/\circ} \in V^\circ \sqcup V^\bullet = V(G)$. The edges of the bipartite graph are in bijection with $\{\Delta_v^\circ\}^0 = \{\Delta_w^\bullet\}^0$. The graph G need not be embedded. If the polytopes $\{\Delta_v^{\bullet/\circ}\}$ are disjoint, then G can be chosen to be embedded. A higher dimer prescribes the data of a n -chain in T^n . Our requirement that G is bipartite guarantees that this n -chain is oriented.

We now briefly explore some of the combinatorics of these higher dimers to produce the data of a tropical hypersurface in \mathbb{R}^n .

Claim 6.0.3. *The edges of an affine dimer all have rational slope.*

Proof. Let e be an edge of Δ_v° , with ends on vertices $p_-, p_+ \in \{\Delta_v^{\bullet/\circ}\}^0$. From our definition of a higher dimer, there exists an edge e_- in some Δ_w^\bullet which also has end on p_- and is parallel to e . By concatenating e_- and e_+ , we obtain a line segment. By repeating this process, we obtain an affine representative of a cycle in $H_1(T^n, \mathbb{Z})$ associated to each edge e . \square

Claim 6.0.4. *Let $\{\Delta_v^\circ\}, \{\Delta_w^\bullet\}$ be a n -dimer. Let α be a facet of some Δ_v^\bullet . Consider $T^\alpha \subset T^n$, the affine $(n-1)$ subtorus spanned by α . The set of $(n-1)$ polytopes $\Delta_\beta^{\bullet/\circ}$ given by the facets of our original set of polytopes which satisfy*

$$\begin{aligned} & \{\Delta_\beta^\bullet \mid \beta \text{ is a facet of } \Delta^\bullet, \beta \subset T^\alpha\} \\ & \{\Delta_\beta^\circ \mid \beta \text{ is a facet of } \Delta^\circ, \beta \subset T^\alpha\} \end{aligned}$$

is the data of an $(n-1)$ dimer on T^α .

By induction, we get the same result for all faces.

Corollary 6.0.5. *Let α be a k -face of some Δ_v^\bullet . Consider $T^\alpha \subset T^n$, the affine sub-torus spanned by α . The set of k polytopes given by the k -faces satisfying*

$$\begin{aligned} & \{\Delta_\beta^\bullet \mid \beta \text{ is a } k\text{-face of } \Delta^\bullet, \beta \subset T^\alpha\} \\ & \{\Delta_\beta^\circ \mid \beta \text{ is a } k\text{-face of } \Delta^\circ, \beta \subset T^\alpha\} \end{aligned}$$

is a k -dimer of T^α .

Each of these k dimensional affine dimers gives the data of a k -chain in T^α . We denote these k -chains of T^n ,

$$\{\underline{U}^\beta \mid \beta \text{ is a } k\text{-facet}\} \subset C_k(T^n, \mathbb{Z}).$$

This can also be thought of an equivalence relation on the set of k -faces of the higher-dimer polytopes, where two faces are equivalent if they define the same k -dimer chain. A *cone* is the real positive span of a finite set of vectors. Given a cone $V \subset \mathbb{R}^n$, a subspace $U \subset \mathbb{R}^n$, the U -relative dual cone of V is

$$V^{\vee|U} := \{u \in U \mid \langle u, V \rangle \geq 0\}.$$

To each k -chain \underline{U}^β we can associate a cone in \mathbb{R}^n .

Definition 6.0.6. Let \underline{U}^β be a chain given by a facet $\beta \subset \Delta_v^{\bullet/\circ}$. Assume that we have translated $\Delta_v^{\bullet/\circ}$ so that the origin is an interior point of the face β . Let \mathbb{R}^β be the affine subspace generated by β . Let $(\mathbb{R}^\beta)^\perp$ be the corresponding perpendicular subspace. We define the dual cone to the facet \underline{U}^β to be

$$\underline{U}_\beta := \begin{cases} (\mathbb{R}_{\geq 0} \cdot \Delta_v^\bullet)^{\vee|(\mathbb{R}^\beta)^\perp} & \text{If } \beta \text{ belongs to a } \bullet \text{-polytope} \\ -(\mathbb{R}_{\geq 0} \cdot \Delta_v^\circ)^{\vee|(\mathbb{R}^\beta)^\perp} & \text{If } \beta \text{ belongs to a } \circ \text{-polytope} \end{cases}$$

Suppose that α and β are facets in the same k -dimer so that $U^\alpha = U^\beta$. Let $\alpha \subset \Delta_v^\bullet$, and suppose that $\beta \subset \Delta_w^\bullet$. After translating Δ_v^\bullet and Δ_w^\bullet so that $0 \in \alpha$ and $0 \in \beta$, we get an agreement of the cones $\mathbb{R}_{\geq 0} \cdot \Delta_v^\bullet = \mathbb{R}_{\geq 0} \cdot \Delta_w^\bullet$. Similarly, if $\gamma \subset \Delta_u^\circ$ and $\underline{U}^\gamma = \underline{U}^\alpha$, then $\mathbb{R}_{\geq 0} \cdot \Delta_v^\bullet = -\mathbb{R}_{\geq 0} \cdot \Delta_u^\circ$. It follows that:

Claim 6.0.7. If $\underline{U}^\alpha \subseteq \underline{U}^\beta$, then $\underline{U}_\alpha \supseteq \underline{U}_\beta$

This also shows that the definition of the cone is really only dependent on the data of the k -chain represented by the choice of facet α , in that $\underline{U}_\alpha = \underline{U}_\beta$ whenever $U^\alpha = U^\beta$. Consider the polyhedral complex containing the subset U^β . This complex satisfies the *zero tension condition*, and therefore describes a tropical subvariety of \mathbb{R}^n .

Of particular interest to us will be the case where the edges of G have the following compatibility condition with the affine structure from the higher dimer:

- Each edge of G is an affine line segment.
- For each edge $e \in E(G)$ connecting v and w , let $p \in \Delta_v^\bullet \cap \Delta_w^\circ$ be the mutual common vertex. Let e_1, \dots, e_k be the primitive edge vectors for Δ^\bullet at the corner p . We require e be parallel to $\sum_k e_k$.

If G satisfies these properties, we say that $\{\Delta_v^\circ\}, \{\Delta_w^\bullet\}$ is an *affine higher dimer*.

6.1 Dimer Lagrangians

Definition 6.1.1. Let $\Delta_v \subset \mathbb{R}^n$ be a polytope. The convex dual tropical function ϕ_v° is the convex piecewise linear function with Newton polytope Δ_v° . We choose the function which is maximally degenerate in the sense that each domain of linearity contains the origin. Similarly, define ϕ_v^\bullet to be the concave dual tropical function, $\phi_v^\bullet = -\phi_v^\circ$.

Given $\{\Delta_v^\circ\}, \{\Delta_w^\bullet\}$ a higher dimer, let $\{\phi_v^\circ\}, \{\phi_w^\bullet\}$ be the associated dual tropical functions. Similarly, let $\{\sigma_v^\circ\}, \{\sigma_w^\bullet\}$ be tropical sections constructed from the data of $\phi_v^{\bullet/\circ}$.

Claim 6.1.2. Let $\{\Delta_v^\circ\}, \{\Delta_w^\bullet\}$ be a higher dimer configuration without self-intersections. There is a decomposition of the intersections of the σ_v° and σ_w^\bullet into convex subsets of \mathbb{R}^n ,

$$\bigcup_{v,w \in G} \sigma_v^\bullet \cap \sigma_w^\circ = \bigcup_{e \in G} U_e.$$

Furthermore, the sections $\sigma_k^{\bullet/\circ}$ intersect convexly in the sense of proposition 3.1.1 at each of the U_e .

Definition 6.1.3. Let $\{\Delta_v^\circ\}, \{\Delta_w^\bullet\}$ be a dual-dimer configuration. The dimer Lagrangian is the Lagrangian connect sum

$$L(\phi_w^\bullet, \phi_v^\circ) := \sigma_v^\circ \#_{U_e | e \in G} \sigma_w^\bullet.$$

The set U_β is very close to the set U_e , where β is the common vertex of the two dimer polytopes corresponding to the edge e . As a result, the valuation of a dimer Lagrangian is close to the tropical hypersurface associated to the dimer.

We've already seen a preliminary version of this Lagrangian in definition 3.4.1.

Example 6.1.4. Consider the higher dimer model drawn in fig. 32d. The six triangles drawn are associated to the following six tropical functions.

$$\begin{aligned} \phi_1^\circ &= (x_1^{6/6} \odot x_2^{6/6}) \oplus (x_1^{5/6} \odot x_2^{4/6}) \oplus (x_1^{4/6} \odot x_2^{5/6}) \\ \phi_2^\circ &= (x_1^{2/6} \odot x_2^{4/6}) \oplus (x_1^{0/6} \odot x_2^{3/6}) \oplus (x_1^{1/6} \odot x_2^{2/6}) \\ \phi_3^\circ &= (x_1^{4/6} \odot x_2^{2/6}) \oplus (x_1^{2/6} \odot x_2^{1/6}) \oplus (x_1^{3/6} \odot x_2^{0/6}) \\ \phi_1^\bullet &= - (x_1^{0/6} \odot x_2^{0/6}) \oplus (x_1^{1/6} \odot x_2^{2/6}) \oplus (x_1^{2/6} \odot x_2^{1/6}) \\ \phi_2^\bullet &= - (x_1^{2/6} \odot x_2^{4/6}) \oplus (x_1^{3/6} \odot x_2^{6/6}) \oplus (x_1^{4/6} \odot x_2^{5/6}) \\ \phi_3^\bullet &= - (x_1^{4/6} \odot x_2^{2/6}) \oplus (x_1^{5/6} \odot x_2^{4/6}) \oplus (x_1^{6/6} \odot x_2^{3/6}) \end{aligned}$$

All six functions give the same nonlinearity stratification to Q ,

$$V(\phi_i^\bullet) = V(\phi_i^\circ) = V(x_1 \oplus x_2 \oplus (x_1 x_2)^{-1}).$$

There are nine Lagrangian surgeries that we need to perform in order to build $L(\phi_w^\bullet, \phi_v^\circ)$. Compare this to the eight surgeries that we need to build the Lagrangian $L(\phi_{T^2}^0)$ from fig. 18, which still has 1 immersed point.

These dimer Lagrangians serve as a generalization of tropical Lagrangians. We can recover tropical Lagrangians by considering the dimer Lagrangians

$$L(\phi) = L(\phi_v, 0),$$

and the “balanced” tropical Lagrangians (definition 3.4.1)

$$L^{\frac{1}{2}}(\phi) = L\left(\frac{1}{2} \cdot \phi, \frac{-1}{2} \cdot \phi\right).$$

6.2 Mutations of Tropical Lagrangians

Dimers provide us with a combinatorial framework to generalize the Lagrangian mutations discussed in fig. 19 and section 3.4.2. We now restrict to examples in dimension 2.

Definition 6.2.1. *Let $L(\phi_w^\bullet, \phi_v^\circ)$ be a dimer Lagrangian. Let G be the associated graph. Give G the structure of a directed graph with edges going from \circ to \bullet . To each edge e , let*

$$\gamma_e : [0, 1] \rightarrow L(\phi_w^\bullet, \phi_v^\circ)$$

be a lift of the edge e to the dimer Lagrangian. We define the weight of an edge e to be the integral

$$w_e := \int_{\gamma_e} \eta$$

where $\eta = p \cdot dq$ is the tautological one form on the cotangent bundle.

We say that a cycle $c \subset E(G)$ has zero weight if

$$\sum_{e \in c} w_e = 0.$$

Lemma 6.2.2. *Let $\{\Delta_v^\circ\}, \{\Delta_w^\bullet\}$ be a dimer model with graph G . For each face $f \in F(G)$, let $c = \partial_f$ be the boundary cycle of the face. Suppose that c has zero weight. Let $\gamma_c : S^1 \rightarrow L(\phi_w^\bullet, \phi_v^\circ)$ be a lift of the cycle to the dimer Lagrangian, in the sense that*

$$\arg(\gamma_c) = c.$$

There exists a Lagrangian disk D_f with $\partial D_f = c \subset L(\phi_w^\bullet, \phi_v^\circ)$.

Proof. Let $V_f \subset T^2$ be the subset of the Lagrangian torus $T^2 \subset T^*T^2$ corresponding to the face f . The zero weighting condition tells us that

$$\int_{\gamma_c} \eta = 0,$$

and so there is no obstruction to finding a closed one form over V_f whose value on the boundary matches $(\gamma_c)_q$. The Lagrangian disk D_f is defined by the graph of this one form. \square

The Lagrangian antisurgery $\alpha_{D_f} L(\phi_w^\bullet, \phi_v^\circ)$ is an immersed Lagrangian, which we now describe with a higher dimer model. Let $\partial f := \{v_1^\bullet, v_1^\circ, \dots, v_k^\bullet, v_k^\circ\}$ be the sequence of vertices of G corresponding to the boundary of f . Recall that Σ is the set of cycles in T^2 given by the boundary polygons of the higher dimer model. Let $\text{Im}(\Sigma) \subset T^2$ be the image of these cycles. After taking an isotopy of c , we may assume that $\arg(c) \subset \text{Im}(\Sigma)$. We can also require that $\arg(c)$ is a homeomorphism onto its image.

We now take a parameterization

$$h : S^1 \times [-1, 1] \rightarrow L(\{\Delta_v^\circ\}, \{\Delta_w^\bullet\})$$

for a neighborhood of $\gamma_c \subset L(\phi_w^\bullet, \phi_v^\circ)$, with $h(\theta, 0) = \gamma_c(\theta)$. The boundary components of the collar $h : S^1 \times [-1, 1]$ give two cycles in $L(\{\Delta_v^\circ\}, \{\Delta_w^\bullet\})$, which we will label

$$\begin{aligned}\gamma_c^\bullet &:= \gamma_c(\theta, -1) \\ \gamma_c^\circ &:= \gamma_c(\theta, 1)\end{aligned}$$

The path γ has argument contained within Σ , but we require the map $h(\theta, t) : S^1 \times [-1, 1] \rightarrow L(\{\Delta_v^\circ\}, \{\Delta_w^\bullet\})$ have argument

$$\begin{aligned}\text{Im}(\arg \circ \gamma_c^\bullet) &\subset \Sigma \cup \{\Delta_i^\bullet\} \\ \text{Im}(\arg \circ \gamma_c^\circ) &\subset \Sigma \cup \{\Delta_v^\circ\}\end{aligned}$$

which “alternates” between bleeding into the Δ_v° and Δ_w^\bullet polytopes. We now state this alternating condition. We require at each θ exactly one of the three following cases occur:

- That the \circ component bleeds out of Σ into the interior of the dimer so $\arg \circ h(\theta, 1) \notin \Sigma$
- That the \bullet component bleeds out of Σ into the interior of the dimer so $\arg \circ h(\theta, -1) \notin \Sigma$
- Neither boundary component bleeds out of Σ , but the collar h passes through the vertex connected to polytopes in our dimer model so $\arg \circ h(t, \theta)$ maps to a vertex of the $\Delta_i^{\bullet/\circ}$.

After performing the Lagrangian surgery, the band parameterized by h will be replaced with two disks D_f^\bullet and D_f° . The boundaries of $D_f^{\bullet/\circ}$ are the cycles $\gamma_{c^\bullet/\circ}$.

The disk D_f^\bullet glues the polygons $\Delta_{v_i}^\bullet$ which lie along the cycle γ_c^\bullet to each other. Similarly, the disk D_f° connects the $\Delta_{w_i}^\circ$ together. In summary, the polygons in the cycle c are replaced with two larger polygons in the antisurgery:

$$\begin{aligned}\Delta_{f^\bullet} &:= \text{Hull}_{v_i^\bullet \in \partial f}(\Delta_{v_i}^\bullet) \\ \Delta_{f^\circ} &:= \text{Hull}_{v_i^\circ \in \partial f}(\Delta_{v_i}^\circ).\end{aligned}$$

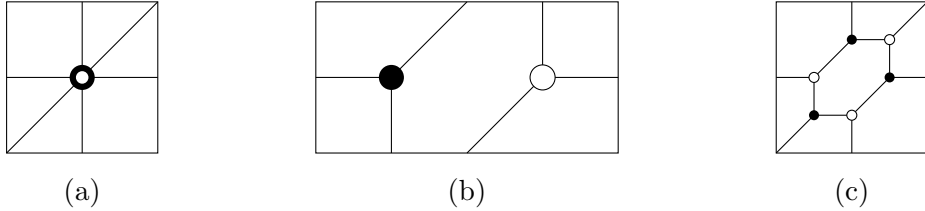


Figure 33: An immersed dimer on the torus, along with the corresponding immersed dimer on the double cover. The last figure draws the resolution of this immersed dimer into a non-immersed dimer.

Lemma 6.2.3. *Consider a dimer model $\{\Delta_v^\circ\}, \{\Delta_w^\bullet\}$. Let f be a face of G . Suppose that the boundary of f has zero weight. The antisurgery $\alpha_{D_f} L(\phi_w^\bullet, \phi_v^\circ)$ is again described by a higher dimer model, whose polygons are given by the collections*

$$\begin{aligned} & \{\Delta_v^\bullet \mid \text{for all } v^\bullet \notin \partial f\} \cup \{\Delta_{f^\bullet}\} \\ & \{\Delta_w^\circ \mid \text{for all } w^\circ \notin \partial f\} \cup \{\Delta_{f^\circ}\} \end{aligned}$$

The graph for this dimer is immersed. For example, the immersed Lagrangian $L^{1/2}(\phi_{T^2}^0)$ can be represented by the immersed graph in fig. 33.

This framework provides us with a generalization of the mutation story considered in section 3.4.2 which can be extended to the Lagrangians L_{inner} constructed in fig. 29b.

6.2.1 Seeds and Surgeries

Besides using antisurgery to modify Lagrangian submanifolds, we may use the presence of antisurgery disks for $L(\phi_w^\bullet, \phi_v^\circ)$ to construct a Lagrangian seed in the sense of [PT17].

Definition 6.2.4 ([PT17]). *A Lagrangian seed $(L, \{D_i\})$ is a monotone Lagrangian torus $L \subset X$ along with a collection of antisurgery disks $\{D_i\}$ for L with disjoint interiors, and an affine structure on L making ∂D_i affine cycles. Should the $\partial D_i \subset L$ be the edges of an affine zigzag diagram, we say that this seed gives a dimer configuration on L .*

Whenever we have a mutation seed giving a dimer configuration on L , we can build a dual Lagrangian using the same surgery techniques used to construct tropical Lagrangians. We start by taking a Weinstein neighborhood $B_\epsilon^* L$ of L . Let $\{\Delta_v^\circ\}, \{\Delta_w^\bullet\}$ be the dimer model on L induced by the Lagrangian seed structure. Using definition 6.1.3, we can construct $L(\{\phi_v^\circ\}, \{\phi_w^\bullet\})$ in the neighborhood $B_\epsilon^* L$. The boundary of $L(\{\phi_v^\circ\}, \{\phi_w^\bullet\})$ is contained in the ϵ -cotangent sphere $S_\epsilon^* L$ and consists of the ϵ -conormals Legendrians $N_\epsilon^*(\partial D_i)$. After taking a Hamiltonian isotopy, the disks $\{D_i\}$ can be made to intersect $S_\epsilon^* L$ along $N_\epsilon^*(\partial D_i)$. By gluing the dimer Lagrangian to these antisurgery disks, we compactify $L(\{\phi_v^\circ\}, \{\phi_w^\bullet\}) \subset B_\epsilon^* L$ to a Lagrangian $L^* \subset X$.

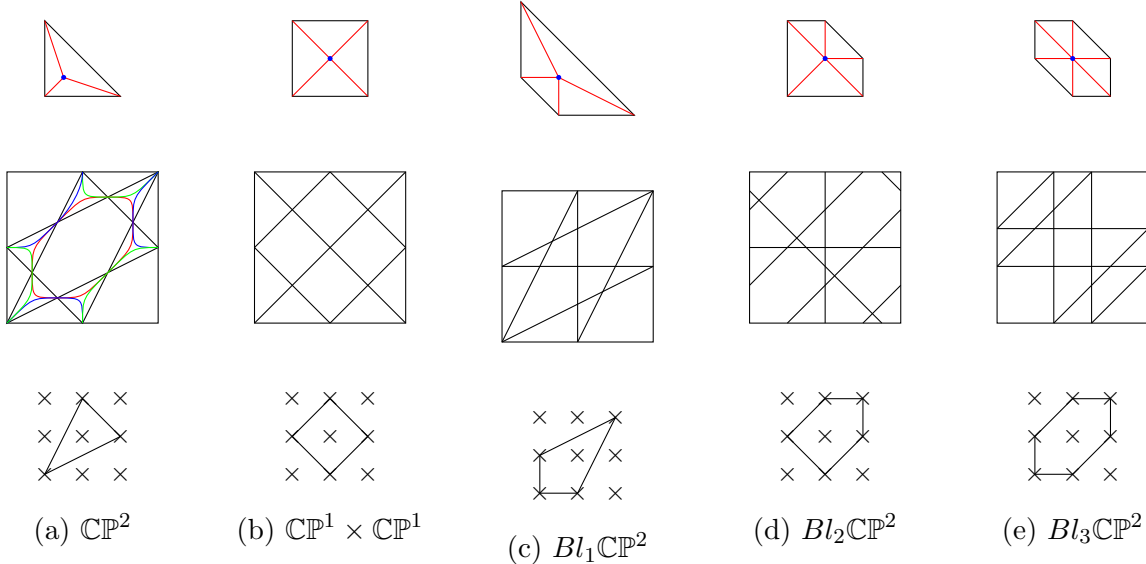


Figure 34: **Top:** Lagrangian seeds in toric del Pezzo surfaces. The antisurgery disks are drawn in red. **Middle:** The corresponding affine dimer models associated the Lagrangian seeds. In the first example of $\mathbb{C}\mathbb{P}^2$, we additionally draw the classes of the cycles $\partial D_{f_i, \Sigma} \subset F_\Sigma^*$. **Bottom:** Cycle classes of the zigzag diagram, corresponding to mutation directions.

Definition 6.2.5. Let $(L, \{D_i\})$ be a Lagrangian seed giving a dimer configuration on L . We call the Lagrangian $L^* \subset X$ the dual Lagrangian to (L, D_i) .

One way to interpret this construction is that a Lagrangian seed has a small symplectic neighborhood which may be given an almost toric fibration. The dual Lagrangian L^* is a compact tropical Lagrangian built inside of this almost toric fibration.

By lemma 6.2.3 the Lagrangian L^* possesses a set of antisurgery disks given by the faces of the dimer graph on L . Should the antisurgery disks D_f with boundary on L^* form a mutation configuration, we call $(L^*, \{D_f\})$ the dual Lagrangian seed.

Remark 6.2.6. The geometric portion of this construction does not require L or L^* to be tori, although statements about mutations of Lagrangians from [PT17] and relations to mirror symmetry use that L is a torus.

6.2.2 Examples from Toric del-Pezzos

Monotone Lagrangian tori and Lagrangian seeds in del-Pezzo surfaces have been studied in [Via17; PT17]. Let X_Σ be a toric del-Pezzo. There exists a choice of symplectic structure on X_Σ so that the monotone Lagrangian torus F_Σ at the barycenter of the moment polytope has a Lagrangian seed structure $\{D_{i, \Sigma}\}$ given by the Lagrangian thimbles extending from the corners of the moment polytope. The Lagrangian thimbles and corresponding dimers are drawn in figs. 34a to 34e. In these 5 examples, the dimer Lagrangian F_Σ^* constructed

from the data of $(F_\Sigma, D_{i,\Sigma})$ again has the topology of a torus. This can be checked from the computation of the Euler characteristic of the dual Lagrangian,

$$\chi(L^*) = |V(G)| - |E(G)| + |\Sigma|,$$

where $|\Sigma|$ is the number of antisurgery disks with boundary on L .

One method of distinguishing Lagrangians is to compute their open Gromov-Witten potentials. In the case of toric Fano, it was proven in [Ton18] that all Lagrangian tori have the potentials given by one of those in [Via17]. A computation shows that the Lagrangians F_Σ and F_Σ^* have the same mutation configuration.

Claim 6.2.7. *Let X_Σ be a toric Fano, F_Σ the standard monotone Clifford torus in X_Σ , and F_Σ^* be the dual torus constructed using the Lagrangian seed structure on F_Σ . There is a set of coordinates for $H_1(F_\Sigma^*)$ and $H_1(F_\Sigma)$ so that the mutation directions determined by their Lagrangian seed structures are the same.*

Proof. This is done by an explicit computation of the homology classes of the disk boundaries in F_Σ^* . \square

Remark 6.2.8. *In the example fig. 34c, there are more faces of G than mutation directions. However, some of the disks represent the same homology classes.*

As a corollary, the wall and chamber structure on the moduli space of Lagrangians F_Σ obtained by mutations may be replicated in a similar fashion on the moduli space of the Lagrangians F_Σ^* .

Corollary 6.2.9. *In the setting of toric Fano, the Landau-Ginzburg potential of F_Σ is the same as F_Σ^* .*

In both figs. 34a and 34b we may mutate the diagram to give us a dimer model with two polygons, which is the balanced tropical Lagrangian for some tropical polynomial. As a result, the Lagrangians figs. 34a and 34b are Lagrangian isotopic to tropical Lagrangians constructed in section 5.1. It is unclear how much of this story extends beyond the toric case.

Question 6.2.10. *Is there a relation between (L, D_i) and (L^*, D_f^*) that can be stated in the language of mirror symmetry?*

6.3 Preliminary Floer Theory computations, and some mirror symmetry predictions.

We return to the setting of $(\mathbb{C}^*)^2 = T^*F_0$. The dimer gives us a combinatorial approximation of

$$CF^\bullet(L(\phi_w^\bullet, \phi_v^\circ), F_0),$$

the Floer theory of our tropical Lagrangian against fibers of the SYZ fibration.

Definition 6.3.1. Let $\{\Delta_v^\circ\}, \{\Delta_w^\bullet\}$ be a affine dimer configuration with affine bipartite graph G . Let ∇ be a \mathbb{C}^* local system on T^n . The Kasteleyn complex with weighting ∇ is the 2-term chain complex $C^\bullet(G, \nabla)$ which as a graded vector space is

$$\mathbb{C}\langle v_i^\circ \rangle \oplus \mathbb{C}\langle w_j^\bullet \rangle[1].$$

The differential d_∇ is determined by the structure coefficients

$$\langle d_\nabla^\Sigma(v^\circ), v^\bullet \rangle = \sum_{\substack{e \in E(G) \\ e = v^\circ v^\bullet}} \nabla_e T^{w(e)}.$$

The support of $\{\Delta_v^\circ\}, \{\Delta_w^\bullet\}$ is the set of local systems

$$\text{Supp}(\{\Delta_v^\circ\}, \{\Delta_w^\bullet\}) := \{\nabla \mid H^1(G, \nabla) \neq 0\}.$$

In dimension 2, G is exactly a dimer, and the support is the zero locus of the polynomial

$$Z^G(\nabla) := \det(d_\nabla).$$

The terminology comes from literature on dimers [KOS06]. By letting the local system ∇ determine a weight for each edge of the dimer, the terms of the determinant corresponds to the product of weights of a maximal disjoint set of edges (called its Boltzmann weight). A maximal disjoint set of edges in a dimer is called a *dimer configuration*, and the sum of Boltzmann weights over all configurations gives the partition function $Z^G(\nabla)$ of the dimer.

We now explain the relation between the Kasteleyn complex $C^\bullet(G, \nabla)$ and the Lagrangian intersection Floer complex $CF(L(\phi_w^\bullet, \phi_v^\circ), (F_0, \nabla))$. These complexes are isomorphic as vector spaces, as the intersection points of F_0 and $L(\phi_w^\bullet, \phi_v^\circ)$ are in bijection with the vertices of the dimer. The Lagrangian $L(\phi_w^\bullet, \phi_v^\circ)$ is built from taking a surgery of the pieces $\sigma_{v^\bullet/\circ}$. An expectation from [Fuk10] is that holomorphic strips contributing to the differential $\mu^1 : CF(L_0 \#_p L_1, L_2)$ are in correspondence with holomorphic triangles contributing to $\mu^2 : CF(L_0, L_1) \otimes CF(L_1, L_2)$. In our construction of $L(\phi_w^\bullet, \phi_v^\circ)$ we smoothed regions larger than intersection points between the sections $\sigma_{v^\bullet/\circ}$, however we expect a similar result to hold. These intersections are in correspondence with the edges of the dimer G , and so we predict that the differential on $CF(L(\phi_w^\bullet, \phi_v^\circ), (F_0, \nabla))$ should be given by weighted count of edges in the dimer. The local system ∇ on F_0 determines the weight of the holomorphic strips corresponding to each edge.

Conjecture 6.3.2. The isomorphism of vector spaces

$$CF^\bullet(L(\phi_w^\bullet, \phi_v^\circ), F_0) \rightarrow C^\bullet(G, \nabla)$$

is a chain homomorphism.

If this conjecture holds, we have a new tool for computing the support of the Lagrangian $L(\phi_w^\bullet, \phi_v^\circ)$, which will be determined by the zero locus of $Z^G(\nabla)$.

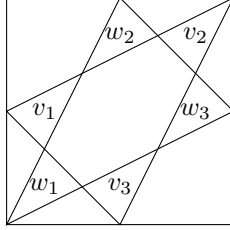


Figure 35: The labelling of faces for the dimer model

Example 6.3.3. *A first example to look at is the Kasteleyn complex of example 6.1.4. We give the polygons of the dimer the labels from example 6.1.4. We can rewrite $Z^G(\nabla)$ as a polynomial by picking coordinates on the space of connections. Let z_1 and z_2 be the holonomies of a local system ∇ along the longitudinal and meridional directions of the torus. The differential on the complex $C^\bullet(G, \nabla)$ in the prescribed coordinates is*

$$d_\nabla^\Sigma = \begin{pmatrix} z_2^{\frac{1}{3}} & (z_1 z_2)^{\frac{-1}{3}} & z_1^{\frac{1}{3}} \\ (z_1 z_2)^{\frac{-1}{3}} & z_1^{\frac{1}{3}} & z_2^{\frac{1}{3}} \\ z_1^{\frac{1}{3}} & z_2^{\frac{1}{3}} & (z_1 z_2)^{\frac{-1}{3}} \end{pmatrix}.$$

The determinant of d_∇^Σ is $Z^G(z_1, z_2) = 3 - (z_1 + z_2 + \frac{1}{z_1 z_2})$.

This polynomial is a reoccurring character in the mirror symmetry story of \mathbb{CP}^2 ; for example, it is the superpotential \tilde{W}_Σ determining the mirror Landau-Ginzburg model. This computation motivates section 7.

7 The example of \mathbb{CP}^2 .

We conclude our discussion with a collection of observations for mirror symmetry of $\mathbb{CP}^2 \setminus E$ and the elliptic surface \check{X}_{9111} . Here, \check{X}_{9111} is the extremal elliptic surface in the notation of [Mir89]. This elliptic surface $W_{9111} : \check{X}_{9111} \rightarrow \mathbb{CP}^1$ has 3 singular fibers of type I_1 , and one singular fiber of type I_9 . We can present this elliptic surface [AGL16, Table Two] as the blowup of a pencil of cubics on \mathbb{CP}^2 ,

$$(z_1^2 z_2 + z_2^2 z_3 + z_3^2 z_1) + t \cdot (z_1 z_2 z_3) = 0.$$

From this pencil, we get a map $\check{\pi}_{bl} : \check{X}_{9111} \rightarrow \mathbb{CP}^2$, which has nine exceptional divisors. Three of the exceptional divisors correspond to the base points of the pencil giving us three sections of the fibration $\check{W}_{9111} : \check{X}_{9111} \rightarrow \mathbb{CP}^1$. We've already looked at homological mirror symmetry for tropical Lagrangians when we place the A -model on $X_{9111} \setminus (I_9 \cup \{D_i\}_{i=1}^3) = (\mathbb{C}^*)^2$, and the B model on \mathbb{CP}^2 . We now switch the model used to study each space, and instead study the A -model on \mathbb{CP}^2 . Of principle interest will be the Lagrangian discussed in fig. 27c, which we will call $L_{inner} \subset \mathbb{CP}^2$. The Lagrangian discussed in fig. 27a will be called $L_{outer} \subset \mathbb{CP}^2$.

In section 7.1, we relate the geometry of tropical Lagrangians to the geometry of Lefschetz fibrations, which will give us another way to manipulate these tropical Lagrangians. In section 7.2, we use these methods to compare the Lagrangian L_{T^2} to a fiber $F_q \subset \mathbb{CP}^2$ of the moment map. Finally, we make a homological mirror symmetry statement for L_{T^2} and the fibers of the elliptic surface \check{X}_{9111} in section 7.3.

7.1 Lagrangians from Lefschetz Fibrations

In section 3.3.3, we discussed tropical symplectic fibrations, and how Lagrangian thimbles for tropical symplectic fibrations are related to tropical sections for a given monomial admissibility condition. The goal of this section is to build some geometric intuition for interchanging these two different perspectives. We now describe three Lagrangian submanifolds which will serve as building blocks to build other Lagrangian submanifolds, similar to those considered in [BC15]. See fig. 36.

The first piece is suspension of Hamiltonian isotopy. Given a path $e : [0, 1] \rightarrow \mathbb{C}$ avoiding the critical values of $W : X \rightarrow \mathbb{C}$, and Hamiltonian isotopic Lagrangians ℓ_0 and ℓ_1 in $W^{-1}(e(0))$ and $W^{-1}(e(1))$, we can create a Lagrangian L_e^ℓ which is the suspension of Hamiltonian isotopy along the path e . We assume that this Hamiltonian isotopy is small enough so that the trace of the isotopy similarly avoids the critical fibers. This Lagrangian has two boundary components, one above $e(0)$ and one above $e(1)$. In practice, we will simply specify the Lagrangian ℓ_0 and assume that the Hamiltonian isotopies are negligible.

The second building block that we consider are the *Lagrangian thimbles*, which are the real downward flow spaces of critical points in the fibration. These can also be characterized by taking a path $e : [0, 1] \rightarrow \mathbb{C}$ with $e(0)$ a critical value of $W : X \rightarrow \mathbb{C}$, and letting ℓ be a vanishing cycle for a critical point in $W^{-1}(e(1/2))$. The Lagrangian thimble, also denoted L_e^ℓ , has single boundary component above $e(1)$.

The third building block we will use comes from Lagrangian cobordisms. In any small contractible neighborhood $U \subset C$ of \mathbb{C} which does not contain a critical value of $W : X \rightarrow \mathbb{C}$, we can use symplectic parallel transport to trivialize the fibration so it is $W^{-1}(p) \times D^2$ for some $p \in U$. We then consider cycles $\ell_1, \ell_2, \ell_3 \subset W^{-1}(p)$ so that $\ell_1 \# \ell_2 = \ell_3$ with neck size ϵ . There is the trace cobordism of the Lagrangian surgery between these three cycles which produces a Lagrangian cobordism in the space $W^{-1}(p) \times \mathbb{C}$. Given paths $e_1, e_2, e_3 \subset D^2$ indexed in clockwise order, with $e_i(1) = p$, we let $L_{e_i}^{\ell_i}$ be the trace cobordism of the surgery between the ℓ_i with support living in a neighborhood of the edges e_i . This Lagrangian has three boundary components, which live above $e_i(0)$.

These pieces glue together to assemble smooth Lagrangian submanifolds of X whenever the ends of the pieces (determined by their intersection with the fiber) agree with each other.

Definition 7.1.1. *Let $W : X \rightarrow \mathbb{C}$ be a symplectic fibration. A Lagrangian glove $L \subset X$ is a Lagrangian submanifold so that for each point $z \in \mathbb{C}$, there exists a neighborhood $U \ni z$ so that $W^{-1}(U) \cap L$ is one of the three building blocks given above.*

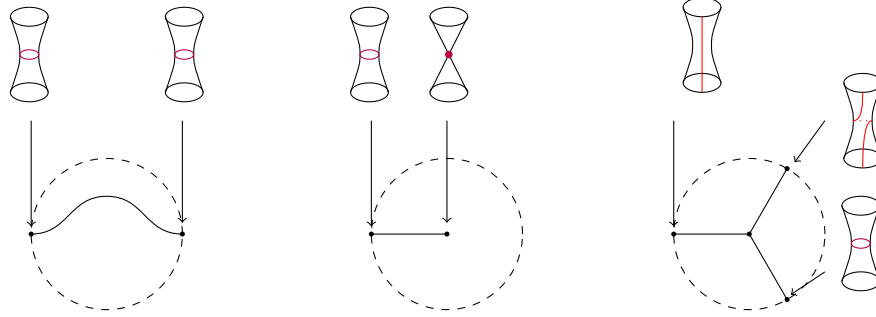


Figure 36: The three different building blocks for a Lagrangian glove: parallel transport, thimbles, and trace of a surgery.

The reason that we look at Lagrangian gloves is that they can be specified by the following pieces of data:

- A planar graph $G \subset \mathbb{C}$. This graph is allowed to have semi-infinite edges and loops.
- A Lagrangian submanifold $\ell_e \subset W^{-1}(e(0))$ labelling each edge $e \in G$.

This data will correspond to a Lagrangian glove if it satisfies the following conditions:

- The interior of each edge is disjoint from the critical values of W .
- Outside of a compact set, the semi-infinite edges are parallel to the positive real axis.
- All vertices of G have degree 1 or degree 3.
- Every vertex of degree 1 must lie at a critical value. Furthermore, the incoming edge e to the vertex v is labelled with a vanishing cycle of the corresponding critical fiber.
- Every vertex of degree 3 with incoming edges e_1, e_2, e_3 must have corresponding Lagrangian labels ℓ_1, ℓ_2 and ℓ_3 which satisfy the relation $\ell_1 \# \ell_2 = \ell_3$ for a surgery of neck size small enough that there exists a disk $D \supset v$ containing the trace of this surgery.

Such a collection of data gives us a Lagrangian $L_G^{\ell_e} \subset X$.

We will diagram these Lagrangians by additionally picking a choice of branch cuts b_i for \mathbb{C} so that $W : (X \setminus W^{-1}(b_i)) \rightarrow (\mathbb{C} \setminus \{b_i\})$ is a trivial fibration. We can then consistently label the edges of the graph $G \subset \mathbb{C}$ with Lagrangians in $\ell_e \in W^{-1}(p)$ for some fixed non-critical value p . Graph isotopies which avoid the critical values correspond to isotopic Lagrangians; furthermore, as long as the label of an edge does not intersect the vanishing cycle of a critical value, we are allowed to isotope an edge over a critical value.

There is another type of isotopy which comes from interchanging Lagrangian cobordisms with Dehn twists [MW15; AS18], which we now describe. Let v be a trivalent vertex with edges $e_1 = vw_1, e_2 = vw_2, e_3 = vw_3$. Suppose that the degree of w_2 is one. Suppose additionally that the Lagrangians ℓ_1 and ℓ_2 , the labels above e_1 and e_2 , intersect at a single

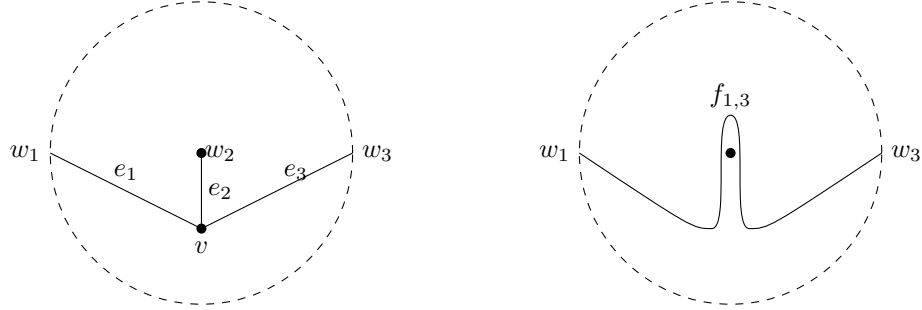


Figure 37: One can add or remove Lagrangian thimbles by exchanging them for Dehn twists.

point so that the surgery performed is the standard one at a single transverse intersection point. Let G be the graph obtained by replacing e_1, e_2, e_3 with a new edge $f_{1,3}$ which has vertices w_1, w_3 , and is obtained travelling along e_1 , out along e_2 and around the critical value w_2 , and returning along e_2 and e_3 (See fig. 37.) Then the graph $H = G \cup \{f_{1,3}\} \setminus \{e_i\}$ equipped with Lagrangian labelling data inherited from G (with the additional label $\ell_{f_{1,3}} = \ell_{e_1}$) is again a Lagrangian glove. We call the Lagrangian obtained via this exchanging operation $\tau_w L_G^{\ell_e}$. In summary:

Proposition 7.1.2. *The following operations produce Lagrangian isotopic Lagrangian gloves.*

- Any isotopy of the graph G where the interior of the edges stay outside the complement of the critical values of W .
- Any isotopy of the graph G where an edge passes through a critical value, but the Lagrangian label of the edge is disjoint from the vanishing cycles of the critical fibers.
- Exchanging the Lagrangian $L_G^{\ell_e}$ with $\tau_w L_G^{\ell_e}$ at some vertex w .

Proof. The first two types of modifications are clear. For the third kind of modification, see [AS18, Lemma A.25]. \square

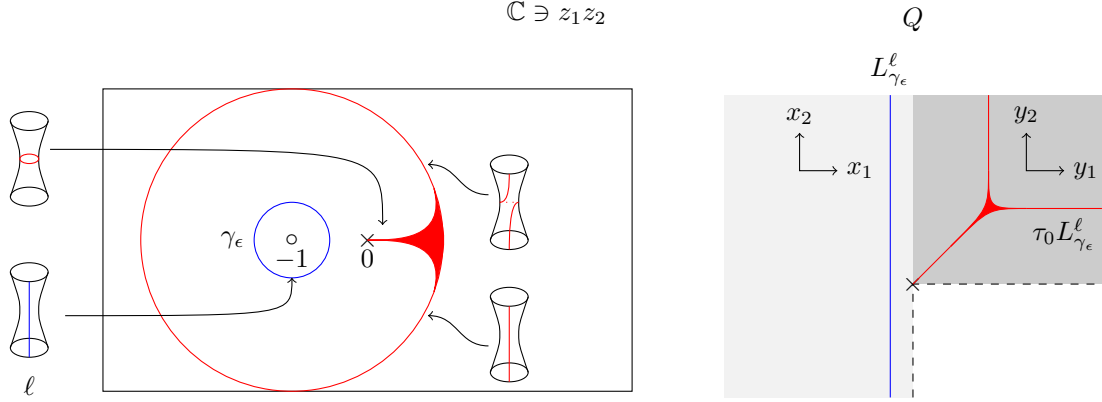
7.1.1 Comparisons between Tropical and Lefschetz: Pants

We now will provide a construction of a Lagrangian pair of pants in the setting of $(\mathbb{C}^2 \setminus \{z_1 z_2 = 1\})$ from the perspective of the Lefschetz fibration considered in section 5.2:

$$\begin{aligned} W : \mathbb{C}^2 \setminus \{z_1 z_2 = 1\} &\rightarrow \mathbb{C} \\ (z_1, z_2) &\mapsto z_1 z_2 \end{aligned}$$

See fig. 28 for the correspondence between Lagrangian tori in the Lefschetz fibration and almost toric fibration.

In this setting we build a Lagrangian glove. We start with the Lagrangian $\ell = \mathbb{R} \subset W^{-1}(1)$. For small $\epsilon < 1$, we consider the loop $\gamma_\epsilon = \epsilon e^{i\theta} - 1$. The parallel transport of ℓ



(a) Two Lagrangian gloves for the Lefschetz fibration $z_1 z_2 : \mathbb{C}^2 \setminus \{z_1 z_2 = 1\} \rightarrow \mathbb{C}$.

(b) The valuation projection of these Lagrangian gloves.

Figure 38

along this loop builds a Lagrangian $L_{\gamma_\epsilon}^\ell$. The Lagrangian $L_{\gamma_\epsilon}^\ell$ only pairs against tori $F_{\epsilon,s}$, so its support in the almost toric fibration will be a line. See the blue Lagrangian as drawn in fig. 38.

By exchanging a Dehn twist for an additional vertex in the glove (proposition 7.1.2), we can build a new Lagrangian $\tau_0 L_{\gamma_\epsilon}^\ell$ (drawn in red in fig. 38.) This description provides us with another construction of the Lagrangian pair of pants. These local models are compatible with the discussion from section 5.1. Let Q_\times be the integral tropical manifold which is the base of $X = \mathbb{C}^2 \setminus \{z_1 z_2 = 1\}$. Q_\times can be covered with two affine charts. Call the charts

$$\begin{aligned} Q_0 &= \{(x_1, x_2)\} \setminus \{(x, x) \mid x > 0\} \\ Q_1 &= \{(y_1, y_2)\} \setminus \{(y, y) \mid y < 0\}. \end{aligned}$$

The charts are glued with the change of coordinates

$$(y_1, y_2) = \begin{cases} (x_1, x_2) & x_2 > x_1 \\ (2x_1 - x_2, x_1) & x_2 < x_1 \end{cases}$$

We now consider two tropical curves inside of Q_\times . The first is an affine line, which is given by the critical locus of a tropical polynomial defined over the Q_0 chart

$$\phi_0(x_1, x_2) = 1 \oplus x_1.$$

The second tropical curve we consider is a pair of pants with a capping thimble (as described in section 5.1,) given by the critical locus of a tropical polynomial defined over the Q_1 chart,

$$\phi_1(y_1, y_2) = y_1 \oplus y_2 \oplus 1.$$

From proposition 7.1.2, we get the following corollary:

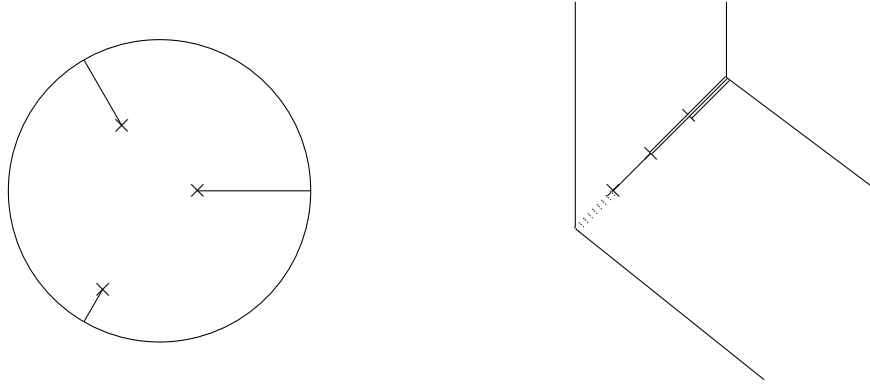


Figure 39: The resolved A_3 singularity, a Lagrangian glove, and its associated tropical curve.

Corollary 7.1.3 (Nodal Trade for Tropical Lagrangians). *Consider the tropical curves $V(\phi_0)$ and $V(\phi_1)$ inside of Q_\times . The Lagrangians $L(\phi_0)$ and $L(\phi_1)$ are Lagrangian isotopic in $\mathbb{C}^2 \setminus \{z_1 z_2 = 1\}$.*

This corollary allows us to manipulate tropical Lagrangians by manipulating the tropical diagrams in the affine tropical manifold instead.

Example 7.1.4. *Consider the Lefschetz fibration with fiber \mathbb{C}^* given by the smoothed A_n singularity as in fig. 39. We construct the Lagrangian glove where we parallel transport the real arc $\ell = \mathbb{R} \subset \mathbb{C}^*$ around the loop of the glove. The monodromy of the symplectic connection from travelling around the large circle corresponds to n twists of the same vanishing cycles. By attaching n vanishing cycles to this arc, we get a Lagrangian glove. In the moment map picture, all of the singularities lie on the same eigenray, and we get the tropical Lagrangian which is a $n+2$ punctured sphere with n of the punctures filled in with thimbles. Though it appears that the n thimbles of the Lagrangian coincide with each other in the moment map picture, they differ by some amount of phase in the fiber direction, which is easily seen in the Lefschetz fibration.*

7.1.2 Tropical Lagrangians and gloves in $(\mathbb{C}^*)^2$

The remainder of this subsection will be devoted to the Landau-Ginzburg model

$$((\mathbb{C}^*)^2, W_{\mathbb{CP}^2} := z_1 + z_2 + (z_1 z_2)^{-1}).$$

The mirror symmetry story that we've presented so far for \mathbb{CP}^2 has used the monomial admissible Fukaya category from [Han18] to build a category mirror to coherent sheaves on \mathbb{CP}^2 . However, using the story presented in section 3.3.3 the tropical Lagrangian sections of the monomial admissible Fukaya-category may be reinterpreted as thimbles of the tropical symplectic fibration (See also [AKO06].) It is expected that these categories are the same, with some interpolation given by the tropical Lefschetz fibration considered in [Abo09]. For purpose of exposition, we restrict ourselves to the setting of \mathbb{CP}^2 , and the mirror Landau-Ginzburg model ($X = (\mathbb{C}^*)^2, W_{\mathbb{CP}^2} = z_1 + z_2 + (z_1 z_2)^{-1}$).

The general fiber of W is a complex torus with 3 punctures. This Lefschetz fibration has three singular fibers. Each singular fiber has one critical point, giving us 3 distinct vanishing cycles. Pick $b \in \mathbb{C}$, some point of large valuation. We look at thimbles with ends on the fiber $W^{-1}(b)$. The fiber $W^{-1}(b)$ has valuation projection which lies near the tropical curve $x_1 \oplus x_2 \oplus (x_1 x_2)^{-1} \oplus (-b)$. The interior “chamber” of this tropical curve corresponds to the region where [Abo09] constructs tropical sections.

After picking a basis of thimbles, we can draw the vanishing cycles of the Lefschetz fibration $W : X \rightarrow \mathbb{C}$ in the fiber $W^{-1}(b)$. These three cycles are drawn for reference in fig. 41. In the Lefschetz fibration language, the Lagrangians τ_0, τ_1 , and τ_2 drawn from the three singular fibers are mirror to $\mathcal{O}, \mathcal{O}(1)$, and $\mathcal{O}(2)$ respectively.

Our intuition for the construction of tropical Lagrangians was instructed by the exact sequence on the B -model presenting a sheaf supported on a divisor:

$$\mathcal{O}(-D) \rightarrow \mathcal{O} \rightarrow \mathcal{O}_D.$$

Our construction of tropical Lagrangians is the replication of this exact-sequence on the A -model via Lagrangian surgery. We now use the tropical symplectic fibration setup instead and surger together the generating thimbles. The result surgery that we obtain will be a Lagrangian glove.

Thimbles, like monomially admissible Lagrangian sections, rarely intersect transversely due to the requirement that they be parallel to the real axis in a neighborhood of b . We may apply proposition 3.1.1 to obtain a well defined surgery of two Lagrangians which are admissible for a symplectic fibration.

Claim 7.1.5. *Let L_1, L_2 be two admissible Lagrangians of the Lefschetz fibration $W : X \rightarrow \mathbb{C}$. Suppose that outside of a compact region, the Lagrangians L_1 and L_2 are given by parallel transport of Lagrangians $\ell_1, \ell_2 \subset W^{-1}(b)$ over curves γ_0 and γ_1 as drawn in fig. 40. Furthermore, suppose that ℓ_1 and ℓ_2 intersect transversely in $W^{-1}(b)$. There is a Lagrangian connect sum $L_1 \#_{\ell_i} L_2$, and a admissible Lagrangian surgery cobordism,*

$$K : (L_1, L_2) \rightsquigarrow L_1 \#_{\ell_i} L_2$$

Furthermore, the Lagrangian connect sum $L_1 \#_{\ell_i} L_2$ is a parallel transport of $\ell_1 \# \ell_2$ in a neighborhood of b .

This gives us a Lagrangian glove as drawn in fig. 40.

Remark 7.1.6. *There is a risk of confusion when comparing drawings which represent the tropical Lagrangians via Lefschetz fibrations as opposed to SYZ fibrations. Namely, the cycles ℓ_i drawn in the fiber $W^{-1}(b)$ are not the cycles considered in the dimer model discussion from fig. 32a. The ℓ_i belong to a symplectic fiber, not a Lagrangian fiber.*

In figs. 42 and 43 we give two examples of Lagrangian gloves. These Lagrangian gloves give us a collection of boundary cycles inside of $W^{-1}(b)$, which we draw in the valuation projection. The valuations of these cycles match with the boundary of an associated tropical Lagrangian.

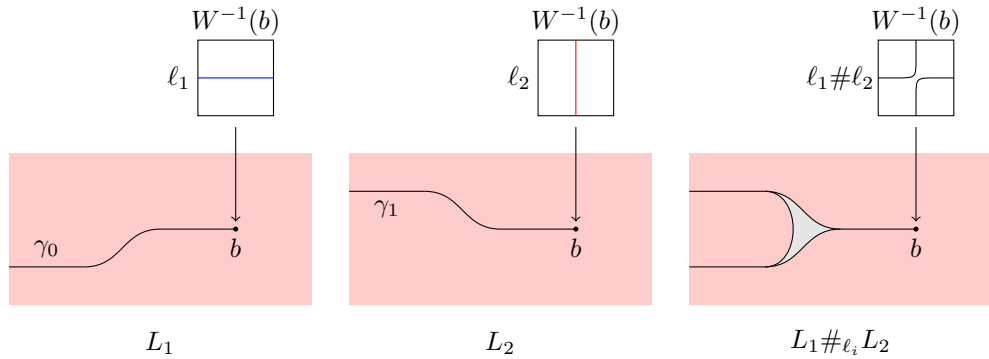


Figure 40: Taking the connect sum of two thimbles

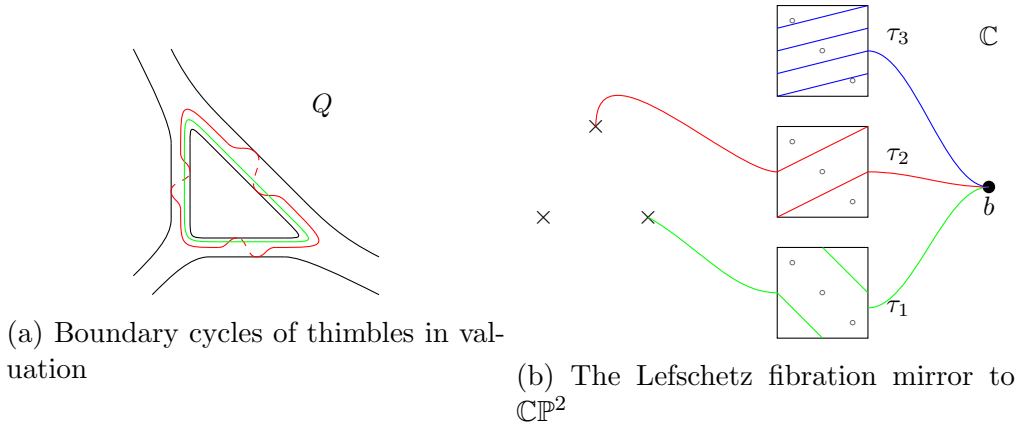


Figure 41: Thimbles and Tropical Sections for $(\mathbb{C}^*)^2, W_{\mathbb{CP}^2}$

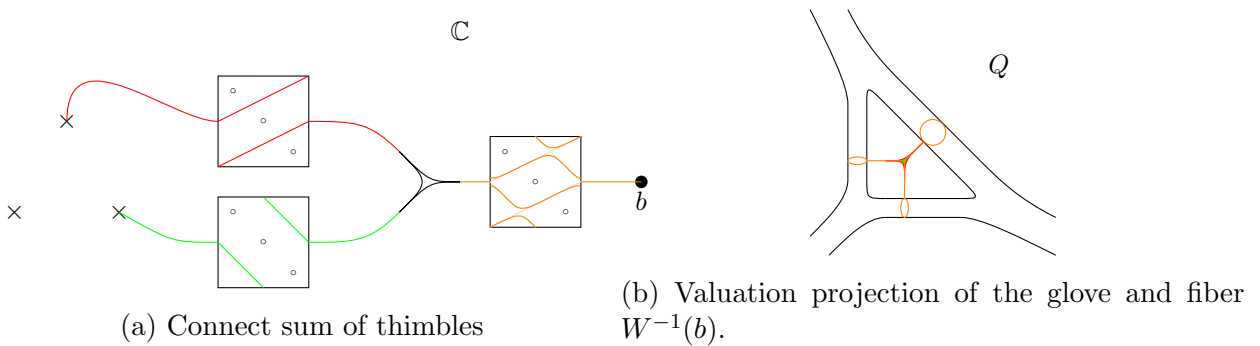
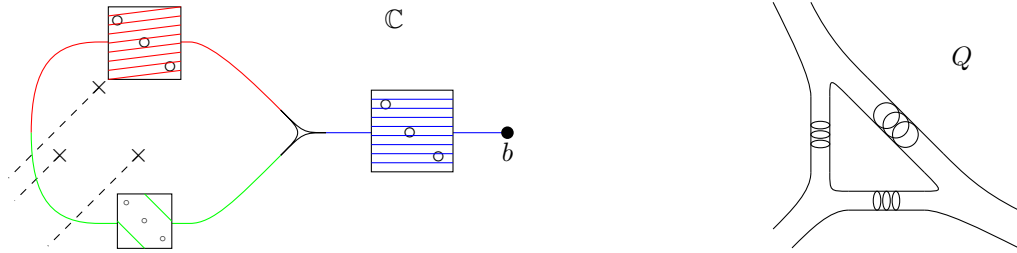


Figure 42: The pair of pants as a Lagrangian glove



(a) Lagrangian Glove. The dashed lines depict (b) Valuation projection of fiber $W^{-1}(b)$, with the branch cuts for the Lefschetz fibration. boundary of the Lagrangian glove drawn in.

Figure 43: The Lagrangian glove representing the mirror to the elliptic curve is the connect sum of the Lagrangian thimbles mirror to \mathcal{O} and $\mathcal{O}(3)$.

7.2 Tropical Lagrangian tori in \mathbb{CP}^2 .

We now apply the tools from Lefschetz fibrations to give us a better understanding of the tropical Lagrangians in \mathbb{CP}^2 from section 5.1.

Proposition 7.2.1. *The Lagrangian L_{inner} drawn in fig. 27c is Lagrangian isotopic to the moment map fiber F_p of \mathbb{CP}^2 .*

This relation is already somewhat expected. [Via14] provides an infinite collection of monotone Lagrangian tori which are constructed by mutating the product monotone tori along different mutation disks. It is conjectured that these are all of the monotone tori in \mathbb{CP}^2 . From section 3.4.2 we know that the Lagrangian L_{T^2} has the same Lagrangian mutation seed structure as $T_{prod,mon}^2$, so if this conjecture on the classification of Lagrangian tori in \mathbb{CP}^2 holds, these two tori must be Hamiltonian isotopic.

Proof. The outline is as follows: we first show that there exists a Lagrangian isotopy between L_{inner} and L_{outer} . We then compare the Lagrangians L_{outer} to a Lagrangian glove for the Lefschetz fibration. This Lefschetz fibration chosen is constructed from a pencil of elliptic curves with a large amount of symmetry. Finally, we compare F_p to the Lagrangian constructed via a Lefschetz fibration. The Lagrangians F_p and L_{outer} are matched via an automorphism of the pencil of elliptic curves.

We first will talk about the geometry of the pencil and the automorphism we consider. The Hesse pencil of elliptic curves is the one parameter family described by

$$(z_1^3 + z_2^3 + z_3^3) + t \cdot (z_1 z_2 z_3) = 0$$

which has four degenerate I_3 fibers at equidistant points $p_1, p_2, p_3, p_4 \in \mathbb{CP}^1$. Let $E_{12} \subset \mathbb{CP}^2$ be the member of the pencil whose projection to the parameter space \mathbb{CP}^1 is the midpoint p_{12} between p_1 and p_2 . The generic fiber of the projection $W_{3333} : \mathbb{CP}^2 \setminus E_{12} \rightarrow \mathbb{CP}^1$ is a 9-punctured torus. From each I_3 fiber we have three vanishing cycles. After picking paths from these degenerate fibers to a fixed point $p \in \mathbb{CP}^1$, we can match the vanishing cycles to the cycles in E_p as drawn in fig. 44.

Remark 7.2.2. *A small digression, useful for geometric intuition but otherwise unrelated to this discussion, concerning the apparent lack of symmetry in the vanishing cycles of X_{3333} . One might expect that the configuration of vanishing cycles which appear in fig. 44 to be entirely symmetric. While the Hesse pencil has symmetry group which acts transitively on the I_3 fibers, to construct the vanishing cycles one must pick a base point p and a basis of paths from E_p to the critical fibers of the Hesse configuration, which breaks this symmetry. Each path from a point p to one of the four critical values p_i gives us 3 parallel vanishing cycles. The 4 critical fibers of the Hesse configuration lie at the corners of an inscribed tetrahedron on \mathbb{CP}^1 . By choosing $p = p_{123}$ to be the center of a face spanned by three of these critical values, 3 paths (say, $\gamma_1, \gamma_2, \gamma_3$) from p to the critical values are completely symmetric. From such a choice, we obtain vanishing cycles $\ell_1^j, \ell_2^j, \ell_3^j$, where $j \in \{1, 2, 3\}$. The homology classes (and in fact, honest vanishing cycles)*

$$|\ell_1^j| = \langle 01 \rangle \quad |\ell_2^j| = \langle 1, 0 \rangle \quad |\ell_3^j| = \langle 1, 1 \rangle$$

are indistinguishable after action of $SL(2, \mathbb{Z})$, reflecting the overall symmetry of both the X_{3333} configuration and the symmetry of the paths. The action of $SL(2, \mathbb{Z})$ which interchanges these cycles also permutes the 9 points of $E_{p_{123}}$ which are the base points of this fibration.

However, the introduction of the last path from the fourth critical fiber to p_{123} breaks this symmetry. At best, this path can be chosen so that there remains one symmetry, which exchanges ℓ_1 and ℓ_2 . In this setup, the vanishing cycles ℓ_4^i lies in the class $\langle 1, -1 \rangle$. Correspondingly, the class $\langle 1, -1 \rangle$ distinguishes the class ℓ_3 from the other classes by intersection number.

This pencil is sometimes called the *anticanonical pencil of \mathbb{CP}^2* . The automorphism group of the Hesse pencil is called the Hessian Group [Jor77]. This group acts on \mathbb{CP}^1 by permuting the critical values by even permutations. Consider a pencil automorphism $g : \mathbb{CP}^2 \rightarrow \mathbb{CP}^2$ which acts on the 4 critical values via the permutation $(p_1 p_2)(p_3 p_4)$. The point p_{12} is fixed under this action, therefore $g(E_{12}) = E_{12}$. While the fiber E_{12} is mapped to itself, the map is a non-trivial automorphism of the fiber, swapping the vanishing cycles for p_1 and p_2 :

$$\begin{aligned} g(\ell_1) &= \ell_2 \\ g(\ell_2) &= \ell_1. \end{aligned}$$

We can use the Lefschetz fibration to associate to each cycle ℓ in E_{12} a Lagrangian in \mathbb{CP}^2 by taking the Hamiltonian suspension cobordism of ℓ in a small circle $p_{12} + \epsilon e^{i\theta}$ around the point p_{12} in the base of the Lefschetz fibration. Call the Lagrangian torus constructed this way $T_{\epsilon, \ell}$. The automorphism of the pencil $g : \mathbb{CP}^2 \rightarrow \mathbb{CP}^2$ interchanges the Lagrangians T_{ϵ, ℓ_1} and T_{ϵ, ℓ_2} .

The standard moment map $\text{val}_{dz} : \mathbb{CP}^2 \rightarrow Q_{\mathbb{CP}^2, dz}$ can be chosen so that one of the I_3 fibers of the Hesse configuration projects to the boundary of the Delzant polygon $Q_{\mathbb{CP}^2}$. We choose the moment map so that $\text{val}_{dz}^{-1}(\partial Q_{\mathbb{CP}^2, dz}) = E_1$, the I_3 fiber lying above the point p_1 .

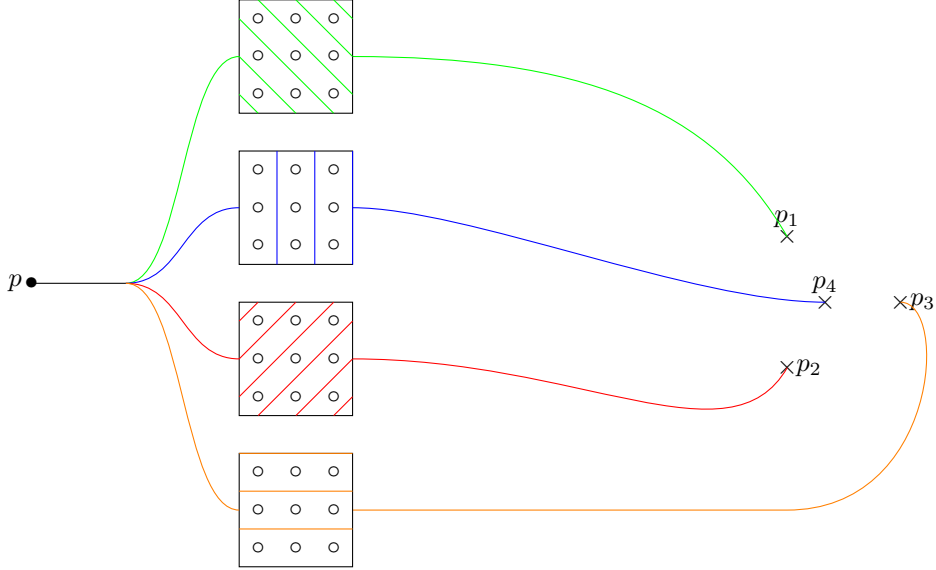


Figure 44: A basis for the vanishing cycles for X_{3333} given in [Sei17].

When one performs a nodal trade exchanging the corners of the moment map for interior critical fibers, we obtain a new toric base diagram, $Q_{\mathbb{CP}^2}$. The boundary of the base of the almost toric fibration $\text{val} : \mathbb{CP}^2 \rightarrow Q_{\mathbb{CP}^2}$ corresponds to a smooth symplectic torus. We arrange that

$$\text{val}^{-1}(\partial Q_{\mathbb{CP}^2}) = E_{12} \subset \mathbb{CP}^2.$$

By comparison to the standard moment map, one sees that the cycle $\ell_1 \subset E_{12}$ projects to a point in the boundary of the moment map, while the cycle $\ell_2 \subset E_{12}$ projects to the whole boundary cycle. This gives us an understanding of the valuation projections of Lagrangian T_{ϵ, ℓ_1} and T_{ϵ, ℓ_2} . T_{ϵ, ℓ_1} has valuation projection which roughly looks like a point, and T_{ϵ, ℓ_2} has valuation projection which is a cycle that travels close to the boundary of $Q_{\mathbb{CP}^2}$. As a result we have Hamiltonian isotopies identifying the Lagrangians

$$\begin{aligned} T_{\epsilon, \ell_1} &\sim F_p \\ T_{\epsilon, \ell_2} &\sim L_{\text{outer}}. \end{aligned}$$

See fig. 45, where L_{outer} is drawn in red, and F_p is drawn in blue.

We conclude $g(L_{\text{outer}}) \sim F_p$. As the projective linear group is connected, the morphism g is symplectically isotopic to the identity, and since $H^1(\mathbb{CP}^2)$ is trivial, all symplectic isotopies are Hamiltonian isotopies. Therefore the Lagrangians L_{outer} and F_p are Hamiltonian isotopic.

By corollary 7.1.3, the Lagrangians L_{inner} and F_p are Lagrangian isotopic. \square

This shows that L_{inner} is obtained from a Lagrangian that we've seen before, but presented from a very different perspective. By taking a Lagrangian isotopy, L_{outer} can be moved to L_{inner} . We obtain the following relationships between Lagrangian submanifolds. Here,

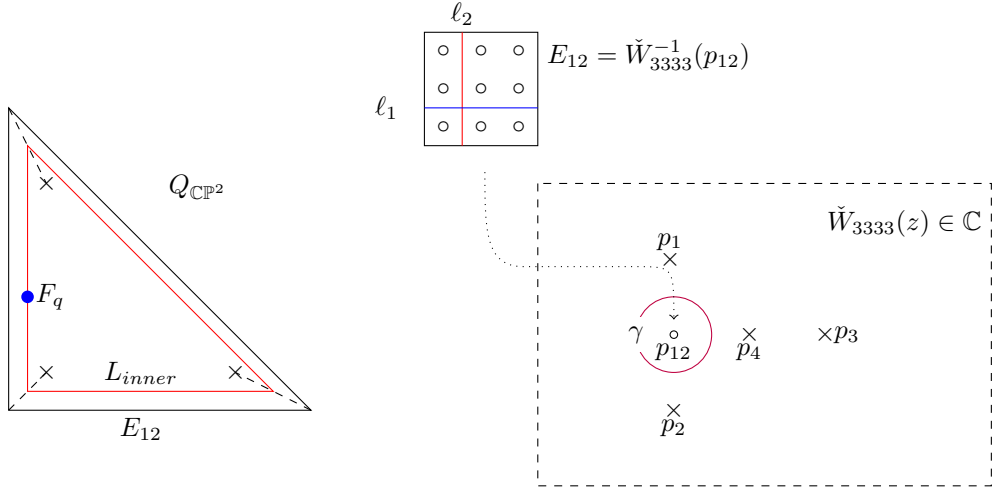


Figure 45: Relating Tropical Lagrangians to Thimbles

the equalities are taken up to Hamiltonian isotopy, and the dashed lines are Lagrangians which we expect to be Hamiltonian isotopic.

$$\begin{array}{ccccc}
 L_{T^2} & \xrightarrow{\text{mutation}} & L_{inner} & \xrightarrow{\text{Lag. Isotopy}} & L_{outer} \\
 \parallel & & \parallel & & \parallel \\
 T_{prod,mon}^2 & \xrightarrow{\text{mutation}} & T_{chek,mon}^2 & \xrightarrow{\text{Lag. Isotopy}} & F_p.
 \end{array}.$$

These tori are isomorphic objects of the Fukaya category, but this is a consequence of $\text{Fuk}(\mathbb{C}\mathbb{P}^2)$ having so few objects.

7.3 A-model on $\mathbb{C}\mathbb{P}^2 \setminus E$.

We now study the map $g : \mathbb{C}\mathbb{P}^2 \rightarrow \mathbb{C}\mathbb{P}^2$ given by the automorphism of the Hesse configuration. The category $\text{Fuk}(\mathbb{C}\mathbb{P}^2)$ does not contain many objects, so the automorphism of the Fukaya category induced by g is not so interesting. By removing an anticanonical divisor $E = E_{12}$ we obtain a much larger category. For example, the Lagrangians L_{outer} and F_q are no longer Hamiltonian isotopic in $\mathbb{C}\mathbb{P}^2 \setminus E$.

Claim 7.3.1. L_{outer} and F_q are not isomorphic objects of $\text{Fuk}(\mathbb{C}\mathbb{P}^2 \setminus E)$

Proof. The symplectic manifold $\mathbb{C}\mathbb{P}^2 \setminus E$ contains a Lagrangian thimble τ_1 which is constructed from the singular fiber of the almost toric fibration and extends out towards the removed curve E (see fig. 27b). This thimble τ_1 intersects L_{outer} at a single point, and therefore $CF^\bullet(L_{outer}, \tau_1)$ is nontrivial. However, τ_1 is disjoint from the fiber F_q , so $CF^\bullet(F_q, \tau_1)$ is trivial. As a result, F_q and L_{outer} are not isomorphic objects of the Fukaya category.¹³ \square

¹³In fact, the same argument shows that L_{outer} and F_q are not topologically isotopic.

Since E_{12} was fixed by the symplectomorphism $g : \mathbb{CP}^2 \rightarrow \mathbb{CP}^2$, the restriction to the complement $g : \mathbb{CP}^2 \setminus E_{12} \rightarrow \mathbb{CP}^2 \setminus E_{12}$ is still defined.

Corollary 7.3.2. *The automorphism of the Fukaya category induced by the symplectomorphism g*

$$g^* : \text{Fuk}(\mathbb{CP}^2 \setminus E) \rightarrow \text{Fuk}(\mathbb{CP}^2 \setminus E)$$

acts nontrivially on objects.

This section of the paper is a series of observations and conjectures outlining homological mirror symmetry with the A -model on $\mathbb{CP}^2 \setminus E$, and B -model on \check{X}_{9111} which hope to shed light on the following conjecture.

Conjecture 7.3.3. *The symplectomorphism $g : \mathbb{CP}^2 \rightarrow \mathbb{CP}^2$ is mirror to fiberwise Fourier Mukai transform on the elliptic surface \check{X}_{9111} which interchange the points of \check{X}_{9111} with line bundles supported on the fibers of the elliptic fibration.*

7.3.1 Homological Mirror Symmetry for $\mathbb{CP}^2 \setminus E$

To that end, we study $L_{T^2} \subset \mathbb{CP}^2 \setminus E$.

An intermediate Blowup and Base Diagrams for X_{9111} : We will begin with a description of the elliptic surface X_{9111} as an iterated blow up of \mathbb{CP}^2 along the base points of an elliptic pencil following [AKO06]. Consider the pencil

$$(z_1^2 z_2 + z_1 z_2^2 + z_3^3) + t z_1 z_2 z_3 = 0.$$

This elliptic fibration has 3 base points of degree 4, 4, and 1. Let $\check{W}_{9111} : \check{X}_{9111} \rightarrow \mathbb{CP}^1$ be projection to the parameter of the pencil. We can arrange for 6 of the blowups (3 on the two base points of degree 4) to be toric. We therefore obtain an intermediate step between $\check{\mathbb{CP}}^2$ and \check{X}_{9111} which is the toric symplectic manifold $\check{X}_{\Sigma^{int}}$. The toric diagram $Q_{\Sigma^{int}}$ is the Delzant polytope with 9 edges. The remaining 3 blowups introduce nodal fibers in the toric base diagram \check{Q}_{9111} for \check{X}_{9111} which has 9 edges and 3 nodal fibers. The 9 edges of the toric base correspond to the nine \mathbb{CP}^1 's making the I_9 fiber of the fibration. The eigenray at each cut in the diagram is parallel to the boundary curves. See fig. 46 for the base diagrams of these different blowups.

B -model of X_{9111} : Let $\check{\pi} : \check{X}_{9111} \rightarrow \check{X}_{\Sigma^{int}}$ be the projection of the blowup. By [BO95] have a semiorthogonal decomposition of the category of the blowup as

$$D^b \text{Coh}(\check{X}_{9111}) = \langle \check{\pi}^{-1} D^b \text{Coh}(\check{X}_{\Sigma^{int}}), \mathcal{O}_{D_1}, \mathcal{O}_{D_2}, \mathcal{O}_{D_3} \rangle.$$

For sheaves $\mathcal{O}_H \in D^b \text{Coh}(\check{X}_{\Sigma^{int}})$ with support on a hypersurface H , this semiorthogonal decomposition states that there is a corresponding sheaf in X_{9111} whose support is on the total transform of H . Should H avoid the points of the blow-up, the total transform will

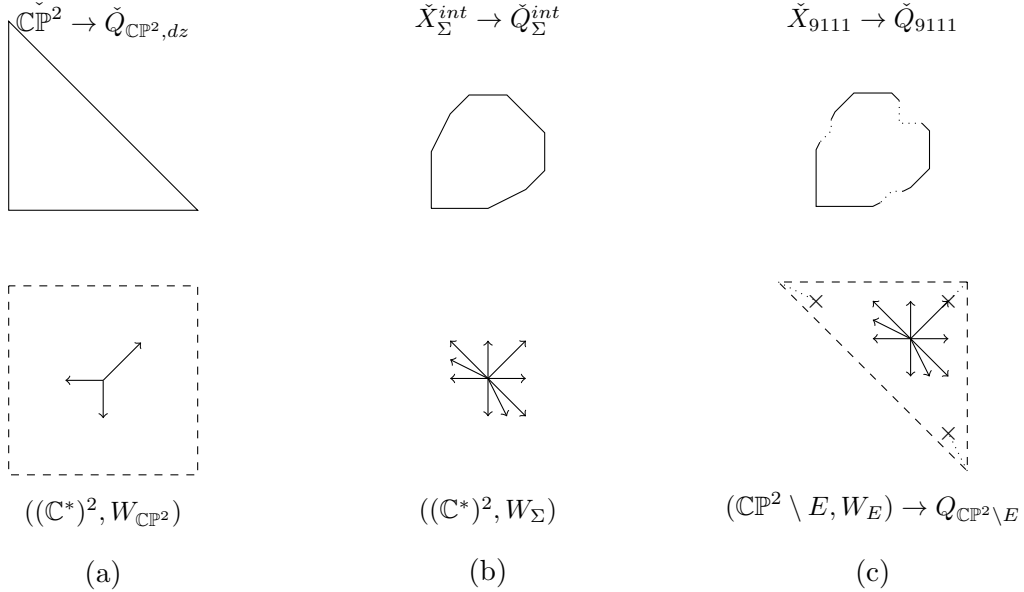


Figure 46: On the top: obtaining \check{X}_{9111} as a toric base diagram by first blowing up $\mathbb{C}\mathbb{P}^2$ 6 times, then blowing up 3 more times. On the bottom: admissibility conditions for the A -model mirrors.

have the same valuation projection as H . Should H contain the point of the blowup, the total transform includes the exceptional divisor of the blow-up. A fiber of the elliptic surface $W_{9111}^{-1}(p)$ is the proper transform of $E_p \subset X_{\Sigma^{int}}$, a member of the pencil. On sheaves, we have an exact sequence:

$$\left(\bigoplus_{i=1}^3 \mathcal{O}_{D_i} \right) \rightarrow \pi^{-1}(\mathcal{O}_{E_p}) \rightarrow \mathcal{O}_{W_{9111}^{-1}(p)}. \quad (7)$$

We will now set up some background necessary to state a similar story for the A -model, summarized in conjecture 7.3.6.

Base for $\mathbb{C}\mathbb{P}^2 \setminus E$: Running the machinery of [GS03] on \check{Q}_{9111} , the SYZ base for \check{X}_{9111} , will yield the SYZ base $Q_{\mathbb{C}\mathbb{P}^2 \setminus E}$ for $\mathbb{C}\mathbb{P}^2 \setminus E$. The base diagram $Q_{\mathbb{C}\mathbb{P}^2 \setminus E}$ can also be constructed by first constructing the mirror to the space $\check{X}_{\Sigma^{int}}$. As $\check{X}_{\Sigma^{int}}$ is a toric variety, the mirror space is a Landau Ginzburg model $(X_{\Sigma^{int}}, W_{\Sigma^{int}}) = ((\mathbb{C}^*)^2, W_{\Sigma^{int}})$, where the superpotential $W_{\Sigma^{int}}$ yields a monomial admissibility condition $\Delta_{\Sigma^{int}}$ on $Q_{\Sigma^{int}} = \mathbb{R}^2$.

Conjecture 7.3.4 (Monomial Admissible Blow-up). *There is notion of monomial admissibility condition for $\mathbb{C}\mathbb{P}^2 \setminus E$. This monomial admissibility condition is constructed from the data of the monomial admissibility condition $((\mathbb{C}^*)^2, W_{\Sigma^{int}})$.*

We now provide some motivation for this conjecture. Recall, a monomial admissibility

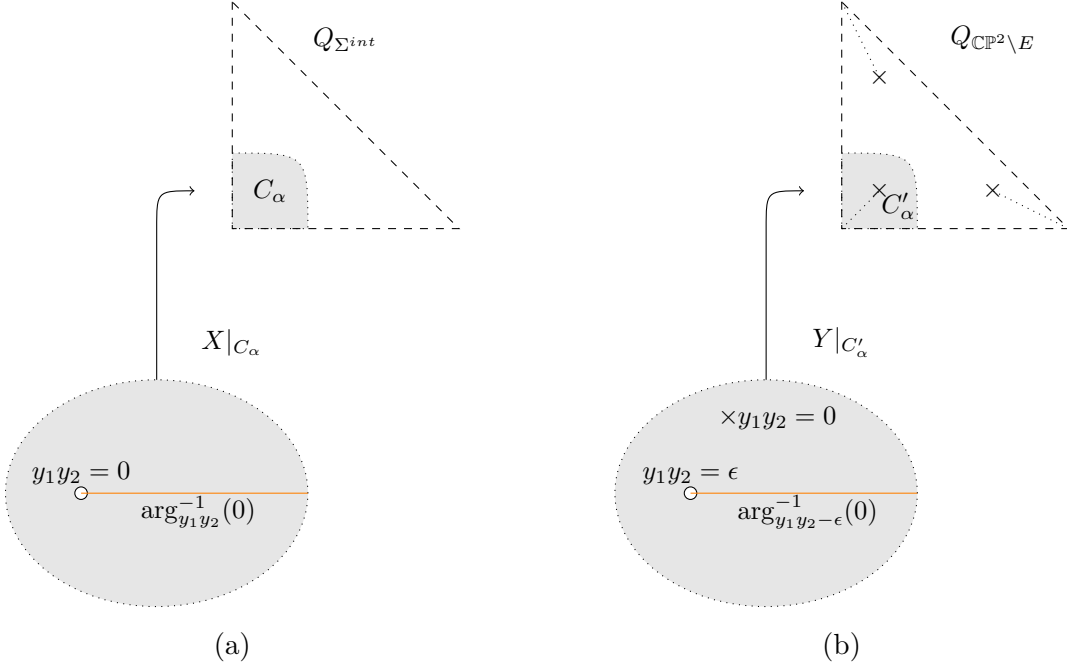


Figure 47: Relating Lagrangians and Admissibility conditions between $(\mathbb{C}^*)^2$ and $\mathbb{CP}^2 \setminus E$ with local Lefschetz models near corners.

condition assigns to each monomial $c_\alpha z^\alpha$ a closed set C_α on which $\arg_{c_\alpha z^\alpha}(L|_{C_\alpha}) = 0$. For a set C_α , denote by $X|_{C_\alpha}$ to be the portion of the SYZ valuation with valuation lying inside of C_α . The restriction of admissible Lagrangians $L|_{C_\alpha}$ are contained within $\arg_{c_\alpha z^\alpha}^{-1}(0)$. The projection $\arg_{c_\alpha z^\alpha}^{-1}(0) \rightarrow C_\alpha$ is an S^1 subbundle of the SYZ fibration $X|_{C_\alpha} \rightarrow C_\alpha$.

To obtain $Q_{\mathbb{CP}^2 \setminus E}$ from $Q_{\Sigma^{int}}$, we add in three cuts mirror to the three blowups. These three cuts are added by replacing the regions $C_{z_1 z_2}$, $C_{z_1 z_2^{-2}}$ and $C_{z_1^{-2} z_2}$ with affine charts $C'_{z_1 z_2}$, $C'_{z_1 z_2^{-2}}$ and $C''_{z_1^{-2} z_2}$ each containing a nodal fiber. The charts C_α can be locally modelled on $\mathbb{C}^2 \setminus \{y_1 y_2 = 0\}$ with monomial admissibility condition $(y_1 y_2)^{-1}$. We replace these with charts containing a nodal fiber modeled on $Y := \mathbb{C}^2 \setminus \{y_1 y_2 = \epsilon\}$ and admissibility condition controlled by the monomial $(y_1 y_2 - \epsilon)^{-1}$. The valuation map $Y|'_{C_\alpha} \rightarrow C'_\alpha$ is an almost toric fibration. We still have an S^1 subbundle $\arg_{y_1 y_2 - \epsilon}^{-1}(0) \subset Y|'_{C_\alpha}$ of the SYZ fibration $Y|'_{C_\alpha} \rightarrow C'_\alpha$ whenever ϵ is not negative real. This S^1 -subbundle, and the monomial $(y_1 y_2 - \epsilon)^{-1}$, should be used to construct a monomial admissibility condition on $\mathbb{CP}^2 \setminus E$. See figs. 47 and 48

In terms of the almost toric base diagrams, this compatibility can be stated as a matching between the eigendirection of the introduced cuts and the ray of the fan corresponding to the controlling monomial over the region including the cut.

A-model on $\mathbb{CP}^2 \setminus E$ We now conjecture the existence of a mirror to the inverse-image functor on the *B*-model. Lagrangian submanifolds which lie in the S^1 subbundle $\arg_{c_\alpha z^\alpha}^{-1}(0) \rightarrow C_\alpha$ should be in correspondence with Lagrangians which lie in the subbundle $\arg_{y_1 y_2 - \epsilon}^{-1}(0) \subset Y|'_{C_\alpha}$. In particular monomial admissible Lagrangians of X give us monomial admissible

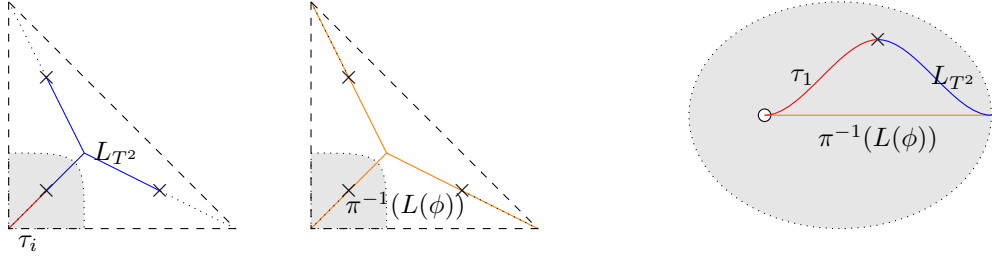


Figure 48: The Lagrangians in $\mathbb{CP}^2 \setminus E$ relevant to our homological mirror symmetry statement.

Lagrangians of $\mathbb{CP}^2 \setminus E$. This allows us to transfer Lagrangians L in $\text{Fuk}((\mathbb{C}^*)^2, W_{\Sigma^{int}})$ to Lagrangians $\pi^{-1}(L) \in \text{Fuk}(\mathbb{CP}^2 \setminus E, W_E)$.

Remark 7.3.5. $\pi^{-1}(L)$ does not arise from a map between the spaces $\mathbb{CP}^2 \setminus E$ and $(\mathbb{C}^*)^2$. The symplectic manifold $\mathbb{CP}^2 \setminus E$ is constructed from $(\mathbb{C}^*)^2$ by handle attachment. We keep the notation π^{-1} so that it is consistent with the inverse image functor from our earlier discussion on the B -model.

We observe that the thimbles of the newly introduced nodes (as in fig. 48) do not arise as lifts of Lagrangians in $(\mathbb{C}^*)^2$. When constructing the Lagrangian thimble, there is a choice of argument in the invariant direction of the node. We take the convention that in the local model $Y|_{C_\alpha}$, the argument of the constructed thimble is positive and decreasing to zero along the thimble. With this choice of argument an application of the wrapping Hamiltonian will separate the τ_i and $\pi^{-1}(L)$ so that

$$\pi^{-1}(L) \cap \theta(\tau_i) = \emptyset,$$

and $\text{hom}(\pi^{-1}(L), \tau_i) = 0$. In summary: see figs. 47 and 48

Conjecture 7.3.6 (Monomial Admissible Blow-up II). *There exists a Lagrangian correspondence between $((\mathbb{C}^*)^2, W_\Sigma)$ and (\mathbb{CP}^2, W_E) , giving us a functor*

$$\pi^{-1} : \text{Fuk}_\Delta((\mathbb{C}^*)^2, W_\Sigma) \rightarrow \text{Fuk}_\Delta(\mathbb{CP}^2 \setminus E, W_E).$$

This functor gives us a semi-orthogonal decompositions of categories:

$$\langle \pi^{-1} \text{Fuk}_\Delta((\mathbb{C}^*)^2, W_\Sigma), \tau_1, \tau_2, \tau_3 \rangle.$$

We furthermore conjecture that this is mirror to the decomposition:

$$\langle \check{\pi}^{-1} D^b \text{Coh}(X_{\Sigma^{int}}), \mathcal{O}_{D_1}, \mathcal{O}_{D_2}, \mathcal{O}_{D_3} \rangle.$$

Remark 7.3.7. While to our knowledge this has not been proven for the monomial admissibility condition, this statement is understood by experts in the symplectic Lefschetz fibration admissibility setting [HK; AKO06]. We give a translation of our statement into the Lefschetz viewpoint. Consider the pencil of elliptic curves

$$p(z_1, z_2, z_3) + t \cdot (z_1 z_2 z_3).$$

where $p(z_1 z_2 z_3) = 0$ is homogeneous degree 3 polynomial defining a generic elliptic curve E meeting $z_1 z_2 z_3 = 0$ at 9 distinct points. Consider the elliptic fibration $W_{E3} : X_{E3} \rightarrow \mathbb{CP}^1$ obtained by blowing up the 9 base points of this elliptic pencil, with exceptional divisors $P_1, \dots, P_9 \subset X_{E3}$. Let $z_\infty \in \mathbb{CP}^1$ be a critical value so that $W_{E3}^{-1}(z_\infty) = I_3$. Then

$$(\mathbb{C}^*)^2 \simeq X_{E3} \setminus (I_3 \cup P_1 \cup \dots \cup P_9),$$

and we may look at the restriction

$$\begin{aligned} W_{E3}|_{(\mathbb{C}^*)^2} : (\mathbb{C}^*)^2 &\rightarrow \mathbb{CP}^1 \setminus \{z_\infty\} = \mathbb{C} \\ (z_1, z_2) &\mapsto \frac{p(z_1, z_2, 1)}{z_1 z_2} \end{aligned}$$

By construction, this is a rational function which expands into 9 monomial terms, and has 9 critical points. The nine monomial terms correspond to the 9 directions in the fan drawn in fig. 46b. The Fukaya-Seidel category constructed with $W_{E3}|_{(\mathbb{C}^*)^2} \rightarrow \mathbb{CP}^1$ is mirror to $X_{\Sigma^{int}}$, where the 9 thimbles drawn from these critical points are mirror to a collection of 9 line bundles generating $D^b \text{Coh}(\check{X}_{\Sigma^{int}})$. These 9 thimbles correspond to 9 tropical Lagrangian sections $\sigma_\phi : Q_{\Sigma^{int}} \rightarrow (\mathbb{C}^*)^2$ in the monomial admissible Fukaya category with fan fig. 46b.

We now consider $X = (\mathbb{CP}^2 \setminus E) = (X_{E3} \setminus (E \cup P_1 \cup \dots \cup P_9))$. The restriction

$$W_{E3}|_X : X \rightarrow (\mathbb{CP}^1 \setminus \{0\}) = \mathbb{C}$$

has 12 critical points, 9 of which may be identified with the critical points from the example before. Conjecturally, this is mirror to X_{9111} , where the thimbles from the three additional critical points are mirror to the exceptional divisors introduced in the blowup $X_{9111} \rightarrow X_{\Sigma^{int}}$. In the monomial admissible picture, the three additional thimbles are matched to the tropical Lagrangian thimbles introduced from the nodes appearing in the toric base diagram $Q_{\mathbb{CP}^2 \setminus E}$ drawn in fig. 46c

7.3.2 A return to the Lagrangian $L_{T^2} \subset \mathbb{CP}^2 \setminus E$.

We finally return to the three punctured torus $\mathring{L}_{T^2} := \mu_0(L^{1/2}(\phi_{T^2}^c)) \subset (\mathbb{C}^*)^2 = \mathbb{CP}^2 \setminus I_3$ as described in section 3.4.2 and fig. 48. In order to make a homological mirror symmetry statement, we need to use the non-Archimedean mirror \check{X}_{9111}^Λ , however as in the case of homological mirror symmetry for toric varieties, the intuition should be independent of the use of Novikov coefficients.

Let $\phi_{T^2} = x_1 \oplus x_2 \oplus (x_1 x_2)^{-1}$ be the tropical polynomial whose critical locus passes through the rays of the nodes added in the modification of $Q_{\Sigma^{int}}$ to Q_{9111} .

A-side		B-side	
$(\mathbb{C}^*)^2, W_{\Sigma^{int}}$		$X_{\Sigma^{int}}$	
9 Thimbles of $W_{\Sigma^{int}}$		9 Line Bundles	
$L(\phi_{T^2})$		Member of 9111-pencil	
(a)			
A-side		B-side	
$\mathbb{CP}^2 \setminus E, W_E$		X_{9111}	
Thimbles τ_i		Exceptional Divisors D_i	
$\pi^{-1}(L(\phi_{T^2}))$		Total transform of member of 9111 Pencil	
L_{T^2}		Fiber of $X_{9111} \rightarrow \mathbb{CP}^1$.	
(b)			

Table 1: A summary of the mirror correspondences that we use for this section.

Theorem 7.3.8. *There exists a Lagrangian cobordism with ends*

$$(L_{T^2}, \tau_1 \cup \tau_2 \cup \tau_3) \rightsquigarrow \pi^{-1}(L_\phi).$$

Provided that conjecture 7.3.6 holds and the cobordism is unobstructed, the Lagrangian L_{T^2} is mirror to a divisor Chow-equivalent to a fiber of the elliptic fibration $\check{W}_{9111} : \check{X}_{9111} \rightarrow \mathbb{CP}^1$.

Proof. We first construct the Lagrangian cobordism. At each of the 3 nodal points in the base of the SYZ fibration $Q_{\mathbb{CP}^2 \setminus E}$ the Lagrangian L_{T^2} meets τ_i at a single intersection point. In our local model for the nodal neighborhood, this is the intersection of two Lagrangian thimbles. The surgery of those two thimbles is a smooth Lagrangian whose argument in the eigendirection of the node avoids the node. This was our local definition for $\pi^{-1}(L(\phi_{T^2}))$ in a neighborhood of the node.

Recall that in this setting, we have an exact sequence of sheaves

$$\left(\bigoplus_{i=1}^3 \mathcal{O}_{D_i} \right) \rightarrow \pi^{-1}(\mathcal{O}_{E_p}) \rightarrow \mathcal{O}_{W_{9111}^{-1}(p)}. \quad (8)$$

In the event that the cobordism constructed above is unobstructed, we have a similar exact triangle on the *A*-side,

$$\bigsqcup_{i=1}^3 \tau_i \rightarrow \pi^{-1}(L(\phi_{T^2})) \rightarrow L_{T^2}.$$

Provided that assumption A.3.2 holds as well, the first and third term in these exact triangles are mirror to each other. This identifies the mirror of the middle term in the Chow group, proving the theorem. \square

This mirror symmetry statement ties together several lines of reasoning. To each fiber $F_q \subset \mathbb{CP}^2 \setminus E$ equipped with local system ∇ , we can associate a value $OGW(F_q, \nabla)$ which is

a weighted count of holomorphic disks with boundary F_q in the compactification $F_q \subset \mathbb{CP}^2$. By viewing X_{9111} as the moduli space of pairs (F_q, ∇) , we obtain a function

$$W_{OGW} : X_{9111} \setminus I_9 \rightarrow \mathbb{C}.$$

This function matches the restriction $W_{9111}|_{X_{9111} \setminus I_9}$. In the previous discussion we conjectured that sheaves supported on $W_{OGW}^{-1}(0)$ are mirror to L_{T^2} . Recall that L_{T^2} can also be constructed as the dual dimer Lagrangian (definition 6.2.5) to the mutation configuration for the monotone fiber F_0 . In this example, these two constructions of L_{T^2} suggest that the dual dimer Lagrangian for a mutation configuration is mirror to the fiber of the Open Gromov-Witten superpotential.

A A -model on $((\mathbb{C}^*)^n, W_\Sigma)$

In [Abo09], the mirror to the B -model on the toric manifold \check{X}_Σ was constructed as the Landau-Ginzburg A -model $((\mathbb{C}^*)^n, W_\Sigma)$. We will use the version of the A -model described in [Han18] rather than the one constructed by Abouzaid, as it is the same category in the setting where \check{X} is Fano, and is easier for us to work with geometrically. In this section, $X := (\mathbb{C}^*)^n$.

The primary difficulty of setting up Lagrangian Floer theory in the non-compact setting is holomorphic strips escaping to infinity. To control this kind of behavior, one can introduce different taming conditions on the non-compact portion of Lagrangians. We use the notion of a *monomial division* as a taming condition for its particularly clean description in X .

Definition A.0.1 ([Han18]). *Let $W : X \rightarrow \mathbb{C}$ be a Laurent polynomial whose monomials are indexed by the rays of a fan Σ . A monomial division Δ for $W = \sum_{\alpha \in A} c_\alpha z^\alpha$ is an assignment of a closed set $C_\alpha \subset Q$ to each monomial in W such that the following conditions hold:*

- The C_α cover the complement of a compact subset of $Q = \mathbb{R}^n$
- There exist constants $k_\alpha \in \mathbb{R}_{>0}$ so that the maximum of

$$\max_{\alpha \in A} (|c_\alpha z^\alpha|^{k_\alpha})$$

is always achieved by $|c_\alpha z^\alpha|^{k_\alpha}$ for an α such that $\text{val}(z) \in C_\alpha$.

- C_α is a subset of the open star of the ray α in the fan Σ .

A Lagrangian $L \subset X$ is Δ -monomially admissible if over $\text{val}^{-1}(C_\alpha)$ the argument of $c_\alpha z^\alpha$ restricted to L is zero outside of a compact set.

Given W_Σ , there is often a preferred type of monomial subdivision, the *tropical division*, with covering regions defined by

$$C_\alpha := \{|c_\alpha z^\alpha| \geq (1 - \delta) \max_{\beta \in A} (|c_\beta z^\beta|)\}$$

for some fixed $\delta \in [0, 1]$. The data of a monomial division allows the construction of a *monomial admissible Fukaya-Seidel category*.

Theorem A.0.2 ([Han18]). *Given Δ a monomial division for W , there exists an A_∞ category $\text{Fuk}_\Delta(X, W)$ whose objects are Δ -admissible Lagrangians, and whose morphism spaces are defined by localizing an A_∞ pre-category $\text{Fuk}^\rightarrow(X)$ with morphisms:*

$$\text{hom}(L_0, L_1) = CF^\bullet(L_0, \theta(L_1)).$$

Here θ is an admissible Hamiltonian perturbation. The higher composition maps m^d in this precategory are given by counts of punctured holomorphic disks.

The Lagrangians considered in the setting of [Han18] do not bound holomorphic disks. The purpose of this appendix is to review the relevant pieces of machinery to define bounding cochains, and to outline an extension of the monomial admissible Fukaya category to contain Lagrangians which are unobstructed in the sense of [Fuk10]. This is only a “path to a proof,” where we describe how one may join together some existing technologies for different models of the Fukaya category to build a monomial admissible Fukaya category with bounding cochains. However, as each of these pieces are constructed with slightly different techniques, we expect that giving a completely rigorous description of this category will require substantial analytic work, and is beyond the scope of this paper. In appendix A.1, we review the so-called “pearly model,” a curved A_∞ algebra associated to each Lagrangian L arising as the deformation of the Morse complex through disk insertions. This allows us to define what bounding cochains are, giving us a notion of unobstructed Lagrangians. In appendix A.2, we define Lagrangian intersection Floer homology between two Lagrangians which are unobstructed by bounding cochain. This allows us to define an A_∞ precategory $\text{Fuk}^\rightarrow(X)$ which includes unobstructed Lagrangian branes. Finally, appendix A.3 uses Lagrangian cobordisms to define the quasi-units needed to localize $\text{Fuk}^\rightarrow(X)$.

A.1 Pearly Model

Out of the different models that exist for pearly A_∞ algebras and Fukaya category, we choose the “treed-disk” model or pearly model described in [CW15; CL06; LW14]. This section is a discussion to fix conventions and geometric intuitions. The technical details of setting up such a model are beyond the scope of this thesis, and the following outline of framework is largely based on notes from [Pol]. The pearly A_∞ algebra is a deformation of the cohomology ring of a Lagrangian L by counting contributions of holomorphic disks with boundary in L . Constructing the pearly A_∞ algebra involves picking a model for the chain complex of L , as well as an interpretation of how holomorphic disks deform the differential (and higher products) of L . Our model for the pearly A_∞ algebra will be using treed-disks, which are a deformation of the Morse cochain complex.

Definition A.1.1. *A Lagrangian $L \subset X$ is relatively spin if the Stiefel-Whitney class of $w_2(TL) \in H^2(L; \mathbb{Z}_2)$ arises as the restriction of a cohomology class from X . A tuple (L_0, \dots, L_k) is relatively spin if the classes $w_2(TL_i) \in H^2(L; \mathbb{Z}_2)$ mutually arise as restrictions of some class in $H^2(X, \mathbb{Z})$.*

Definition A.1.2. A geometric Lagrangian brane of X is a Lagrangian L equipped with a relative spin structure and admissible Morse function $h : L \rightarrow \mathbb{R}$.

In the setting of non-compact Lagrangians, we must choose Morse functions $h : L \rightarrow \mathbb{R}$ in such a way that the flow of the Morse function is admissible with respect to W_Σ . We say that a Morse function $h : L \rightarrow \mathbb{R}$ is *monomially admissible* if h is a pullback of the wrapping Hamiltonian outside of a compact region [Han18]. The outward directed flow of these functions will later ensure compactness of the moduli space of treed disks. For this choice of Morse function, $CM^\bullet(L; h)$ computes the cohomology of L ; an inward choice of flow of the Morse function at the boundary would compute the Morse cohomology of L relative its boundary as collared by the function h .

Definition A.1.3. Given a Lagrangian brane L_0 , we define the Floer Cochain Complex

$$CF^\bullet(L_0; h) := \bigoplus_{x \in \text{Crit}(h)} \Lambda \cdot x.$$

We will usually simply write (L, h) for the data of a Lagrangian brane, or sometimes even just L .

A.1.1 Treed Disks

We outline the construction of the moduli space of treed disks. The domain of a treed disk is a tuple of data

$$\mathcal{T} = \{T, \underline{\ell}, \underline{p} \mid (*)\} / \sim$$

which are:

- T , a rooted tree. We use T to encode the adjacency relations between the different components of a flow tree. We give a decomposition of its vertex set into interior vertices and critical vertices,

$$V = V^c \sqcup V^i$$

where the critical vertices are the root, and a subset of the leaves of T . Furthermore, we fix an embedding of T into the disk which sends the leaves to the boundary of the disk. Starting at the root, and proceeding counterclockwise, we obtain an ordering of the critical vertices V^c as $(v_0; v_1, \dots, v_k)$.

- Each edge will represent a Morse flow line. We assign to each edge a normalized length $\ell_e \in [0, 1]$ and set the vector $\bar{\ell} = (\ell_e)_{e \in E}$. Edges adjacent to critical vertices must have normalized length 1.
- Every interior vertex v will represent a (potentially constant) disk. For each vertex v , let $N(v)$ be the edges adjacent to v . We have an assignment $\underline{p}_v : N(v) \rightarrow \partial D^2$ telling us how to glue the Morse flow lines to the disks. This assignment must respect the ordering of the edges around v inherited from the planar embedding of T .

The *valence* of a tree is its number of critical vertices, and is denoted $\text{val}(\mathcal{T})$. Let $L \subset X$ be a submanifold. A map from the domain data of a disked tree is:

$$u : \mathcal{T} \rightarrow (X, L)$$

consist of the following data:

- For each edge e , a path $u_e : [0, \ell_e] \rightarrow L$.
- For each interior vertex v , a disk $u_v : (D^2, \partial D^2) \rightarrow (X, L)$.

satisfying the following incidence conditions:

- For each incidence between an edge e and interior vertex v , it is either the case that

$$u_v(p_v(e)) = u_e(0) \quad \text{or} \quad u_v(p_v(e)) = u_e(\ell_e)$$

depending on whether v is the vertex of e which closer to the root or not.

Fix a tree \mathcal{T} . Given a submanifold $L \subset X$, a choice of disk classes $\beta_v \in \pi_2(X, L)$ for each $v \in V^i$, and a tuple of points in L , $(x_0; x_1, \dots, x_{\text{val}(\mathcal{T})})$ we say that a map $u : \mathcal{T} \rightarrow (X, L)$:

- Has flow lines limiting to $(x_0; \underline{x})$ if each edge e limiting to a critical vertex v_i , we have $u_e(0) = x_i$. Similarly, at the root e limiting to root vertex w , we have $u_e(1) = x_0$.
- Is in the class $\underline{\beta}$ if for each v , there is an agreement of disk classes $[u_v] = \beta_v$.
- Is *stable* if each *ghost vertex*, that is vertex v such that $\omega(\beta_v) = 0$, has degree at least 3.

After fixing a class $\beta \in H_2(X, L)$, we let $\mathcal{X}_\beta(L, x_0, \underline{x})$ be the set of stable trees with flow lines limiting to $(x_0; \underline{x})$, and is in the class $\underline{\beta}$ where

$$\sum_{v \in V^i} \beta_v = \beta.$$

Finally, the analytic portion of the problem comes into play by requiring that these disks satisfy the following partial differential equations:

- We require each edge to be a gradient Morse flow line $\frac{du_e}{dt} = \nabla h$.
- We require at each interior vertex the disk $u_v : D^2 \rightarrow X$ be a J -holomorphic disk, $\bar{\partial}_J u_v = 0$.

The space of maps $u \in \mathcal{X}_{\underline{\beta}}(L, x_0, \underline{x},)$ satisfying the above equations will be denoted a $\{u \mid \bar{\partial}_J u = 0\}$. There is little reason for this space to be cut out transversely. There are different approaches to regularizing this space of treed disks– by either using abstract

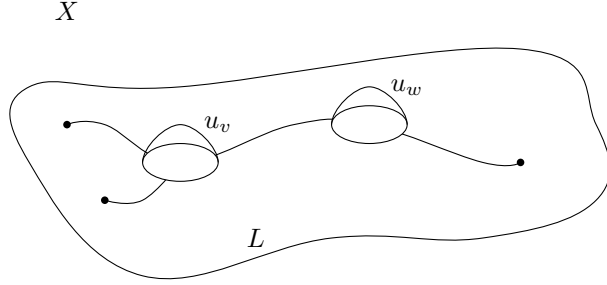


Figure 49: A flow tree-disk.

perturbations (from polyfolds or Kuranishi structures), or by using geometric perturbations from stabilizing divisors.

The moduli space is taken up to reparameterization of flow lines by translations and disks by holomorphic reparameterization. A feature of the moduli space of treed disks is that M does not have boundary components arising from the bubbling of disks. When a disk bubble is visible from the domain, it is identified with a treed disk with internal edge of length zero between the two bubbled components. As a result, the only boundary components in the moduli of treed disks occur when the length of a flow line goes to infinity and we get breaking in the Morse sense. This is comparable to the quantum bubble tree picture for Legendrian contact homology [AENV+14].

Assumption A.1.4. *Let $x_0; x_1, \dots, x_k$ be critical points of h . Fix $\beta \in H_2(X, L)$. There is a regularization set up that produces a smooth moduli space*

$$\mathcal{M}_\beta(L, x_0; x_1, \dots, x_k)$$

which admits a compactification by broken treed disks $\overline{\mathcal{M}}_\beta(L, x_0; x_1, \dots, x_k)$.

The codimension 1 components of the boundary of $\overline{\mathcal{M}}_\beta(L, x_0; x_1, \dots, x_k)$ are

$$\partial \overline{\mathcal{M}}_\beta(L, x_0; x_1, \dots, x_k) = \bigsqcup_{\substack{\beta_1 + \beta_2 = \beta \\ 0 \leq i \leq j \leq k}} \overline{\mathcal{M}}_{\beta_1}(L, x_0; x_1, \dots, x_i, y, x_{j+1}, \dots, x_k) \times \overline{\mathcal{M}}_{\beta_2}(L, y; x_{i+1}, \dots, x_j).$$

A.1.2 Floer Complex $CF^\bullet(L, h)$

We will review curved A_∞ algebras, their morphisms and deformations.

In order to ensure convergence of the deformations we develop, we work with *filtered A_∞* algebras. This will mean working over the Novikov field.

Definition A.1.5 ([Fuk10]). *Let R be a commutative ring with unit. The universal Novikov ring over R is the set of formal sums*

$$\Lambda_{\geq 0} := \left\{ \sum_{i=0}^{\infty} a_i T^{\lambda_i} e^{n_i} \mid \lambda_i \in \mathbb{R}_{\geq 0}, n_i \in \mathbb{Z}, \lim_{i \rightarrow \infty} \lambda_i = \infty. \right\}$$

Let k be a field. The Novikov Field is the set of formal sums

$$\Lambda := \left\{ \sum_{i=0}^{\infty} a_i T^{\lambda_i} \mid \lambda \in \mathbb{R}, n_i \in \mathbb{Z}, \lim_{i \rightarrow \infty} \lambda_i = \infty \right\}$$

This is a non-Archimedean field with the same valuation. An energy filtration on a graded Λ -module A^\bullet is a filtration $F^{\lambda_i} A^k$ so that

- Each A^k is complete with respect to the filtration, and has a basis with zero valuation over Λ .
- Multiplication by T^Λ increases the filtration by λ .

It's hard to motivate these additional pieces of data without some intuition from application to the Fukaya category. The energy filtration T_i^λ will encode the amount of symplectic area of disks contributing to the differential in Lagrangian intersection Floer theory. The energy filtration will still play an important role in the algebraic setting where many of our constructions will either induct on the energy filtration, or construct maps as sequences which converge in the Novikov field.

Definition A.1.6. Let A^\bullet have an energy filtration. A filtered A_∞ structure (A, m^k) is an enhancement of A^\bullet with $\Lambda_{\geq 0}$ linear graded higher products for each $k \geq 0$

$$m^k : A^{\otimes k} \rightarrow A[2 - k]$$

satisfying the following properties:

- Energy: The product respects the energy filtration in the sense that :

$$m^k(F^{\lambda_1} A, \dots, F^{\lambda_k} A) \subset F^{\sum_{i=1}^k \lambda_i} A$$

- Non-Zero Energy Curvature The obstructing curvature term has positive energy, $m^0 \in F^{\lambda > 0} C$.
- The quadratic A_∞ relations for each $k \geq 0$,

$$\sum_{j_1+i+j_2=k} (-1)^{\clubsuit} m^{j_1+j_2+1} (\text{id}^{\otimes j_1} \otimes m^i \otimes \text{id}^{\otimes j_2}) = 0.$$

The value of \clubsuit is determined on an input element $a_1 \otimes \dots \otimes a_k$ by

$$\clubsuit = |a_{k-j_1}| + \dots + |a_k| - i.$$

We say that A^\bullet is unital if there exists an element e_A such that

$$m^2(e_A, a) = m^2(a, e_A) = a.$$

For the purposes of exposition, we will work up to signs from here on out. From a Lagrangian brane, we can construct such a filtered A_∞ algebra.

Definition A.1.7. *Let $L \subset X$ be an admissible Lagrangian brane equipped with admissible Morse function $h : L \rightarrow \mathbb{R}$. Define the chains of the Floer complex to be*

$$CF^\bullet(L, h) = \Lambda \langle (\text{Crit}(h)) \rangle$$

as the Λ -module generated on critical points of h . For each homology class $\beta \in H_2(X, L)$, we define the contribution of the class β to the higher product homologically graded in β by structure coefficients counting treed disks:

$$m_\beta^k : CF^\bullet(L, h)^{\otimes k} \rightarrow CF^\bullet(L, h)[2 - k]$$

$$\langle x_0, m_\beta^k(x_1, \dots, x_k) \rangle := \left(\int_T dh \right) \cdot T^{\omega(\beta)} \cdot \# \bar{\mathcal{M}}_{\beta T}(L, x_0; x_1, \dots, x_k).$$

We define the pearly higher products as

$$m^k(x_1, \dots, x_k) := \sum_{\beta \in H_2(X, L)} m_\beta^k(x_1, \dots, x_k).$$

We call the pair $(CF^\bullet(L, h), m^k)$ the pearly algebra of L .

Due to the presence of disks, the maps m^k do not have the appropriate A_∞ grading; instead, they give $(CF^\bullet(L, h), m^k)$ the structure of a *filtered A_∞ algebra*. The grading of m_β^k is determined by the Maslov index, causing a shift:

$$m_\beta^k : CF^\bullet(L, h) \rightarrow CF^\bullet(L, h)[2 - k - \mu(\beta)].$$

Theorem A.1.8 ([Fuk96]). *The algebra $CF^\bullet(L, h)$ is a filtered A_∞ algebra.*

A.1.3 Bounding Cochains and corrected strips

The presence of additional product structures in A_∞ algebras gives us a very rich deformation theory. As the theory of curved A_∞ algebras is substantially more difficult to work with than the uncurved case, we will turn our curved A_∞ algebras into uncurved A_∞ algebras via deformation of the product structure when possible.

Definition A.1.9. *Let $a \in A^\bullet$ be an element of homological degree 1 and positive Novikov valuation. The a -deformed product structure on A is the multiplication*

$$m_a^k := \sum_n \sum_{j_0 + \dots + j_k = n} m^{k+n}(a^{\otimes j_0} \otimes \text{id} \otimes a^{\otimes j_1} \otimes \text{id} \otimes \dots \otimes a^{\otimes j_{k-1}} \otimes \text{id} \otimes a^{\otimes j_k})$$

In order for this deformation to remain graded, the element a should have homological degree 1. If A^\bullet is a DGA and a represents a class of $H^1(A)$, the resulting homology theory we recover is the homology of A^\bullet twisted by a . If a is not closed, then m_a^1 will not necessarily square to zero, however, we can still recover some meaningful algebraic structure.

Claim A.1.10. (A^\bullet, m_a^k) is again a filtered A_∞ algebra.

When the A_∞ structure on A^\bullet is already clear, we will write A_a^\bullet to denote the algebra with product deformed by $a \in A^\bullet$. We are interested in the cases where A_a^\bullet gives us a well defined homology theory even though A^\bullet itself may be curved.

Definition A.1.11. We say that $b \in A^\bullet$ is a *bounding cochain* or *Maurer-Cartan Solution* if $m_b^0 = 0$. If $CF^\bullet(L, H)$ posses a *bounding cochain*, we say that the *Lagrangian* L is *unobstructed*.

Notation A.1.12. Unless otherwise stated, from here on all *Lagrangians* will be *unobstructed by bounding cochain*. When we say a *unobstructed Lagrangian brane*, we will mean a *Lagrangian brane* equipped with choice of *bounding cochain*, and when we write a *Lagrangian with index* L_i , its corresponding *bounding cochain* will be denoted b_i . When we write $CF^\bullet_b(L)$, we will mean the *pearly algebra* deformed by the *bounding cochain* b .

A.2 Lagrangian Intersections and Treed Strips

When $\{L_i\}$ are a collection of *unobstructed compact Lagrangian branes* with *bounding cochains* \underline{b} , there is a well defined *Lagrangian intersection Floer cochain complex* $CF^\bullet_{\underline{b}}(L_i, L_j)$ whose differential counts *treed strips* (weighted by *bounding cochain*) between intersection points of the *Lagrangians*. More generally, given a sequence of *Lagrangians* L_k , we may look at *treed disks* with multiple strip-like ends to obtain product maps.

Definition A.2.1. The domain of a treed strip is the data $\mathcal{S} := \{D, \underline{z}, \underline{\mathcal{T}}, \underline{\ell}\} / \sim$ where

- the \underline{z} is an ordered set of boundary marked points $z_i \subset \partial D^2$. These marked points obtain two kinds of labels: the critical marked points z_i^c , and the tree attachment points z_i^t
- for each tree attachment point z_i^t , a choice $\mathcal{T}_{z_i^t}$ of treed disk domain with k_i leaves. We additionally pick a root length $\ell_{z_i^t} \in [0, 1]$ for the length of the root edge of the tree.

A map $u : \mathcal{S} \rightarrow (X, \bigcup_i L_i)$ consists of the following data

- a map $u_D : D^2 \rightarrow X$, which maps the boundary arc between the points z_i^c, z_{i+1}^c to the *Lagrangian* L_{i+1} .
- For each z_i^t , a treed disk $u_{z_i^t} : \mathcal{T}_{z_i^t} \rightarrow X$ with edges and disk boundaries contained in L_i , with root mapped to the attachment point $u_D(z_i^t)$.

Given *Lagrangian branes* $\{L_i\}_{i=1}^k$, a sequence of intersection points $z_i \in L_i \cap L_{i+1}$, and a sequence of critical points $\{x_{i,j}\}_{j=1}^{k_i}$ for each i , we say that $u : \mathcal{S} \rightarrow (X, \bigcup_i L_i)$

- has strip like ends limiting to z_i if arcs of D_i limit to the intersection points z_i .
- has flow lines limiting to $\{x_{i,j}\}$ if the leaves of $u_{z_i^t} : \mathcal{T}_{z_i^t} \rightarrow (X, L)$ are flow lines limiting to $\{x_{i,j}\}$.

We define the space of maps $\mathcal{X}(\underline{L}, \underline{x}, \underline{z}_i)$ consisting of maps $u : \mathcal{S} \rightarrow X$ to be the set of all such maps with appropriate limiting conditions. We can then impose on the space of maps the following conditions given by partial differential equations:

- The map $u_D : D^2 \rightarrow X$ be a J -holomorphic disk.
- The maps $u_i^t : \mathcal{T}_{z_i^t} \rightarrow X$ satisfy the conditions $\bar{\partial}_J u_i^t = 0$.

The space of maps $u \in \mathcal{X}(\underline{L}, \underline{x}, \underline{z}_i)$ satisfying the above equations will be denoted as $\{u \mid \bar{\partial}_J u = 0\} \subset \mathcal{X}(\underline{L}, \underline{x}, \underline{z}_i)$. As in the setting of treed disks, we assume the existence of a regular moduli space of disks with boundary stratification:

Assumption A.2.2. *Let $(z_0; \underline{z})$ be the data of intersection points in a collection of Lagrangian branes (L, h) , and let \underline{x}^t be a collection of critical points. We assume that there is a well define moduli space of treed strips*

$$\mathcal{M}_\beta(z_0; \underline{z}, \underline{x}^t) := \{u : \mathcal{S} \rightarrow X \mid (*)\}, \bar{\partial}_J u = 0\} / \sim.$$

where the conditions $(*)$ are that the strips are stable, and limit to the intersection points $(z_0; z_1, \dots, z_k)$ and have flow lines limiting to $\{x_i^t\}$. Furthermore, we assume that this moduli space is compact, with boundary strata by strip breaking, and breaking along flow lines of the attached treed disks.

So far, the data of the bounding cochain has not entered the definitions of these disks.

Definition A.2.3. *Let $u : \mathcal{S} \rightarrow X$ be a treed strip. The bounding cochain corrected weight of this strip is*

$$T^{w_b(u)} := \left(T^{\omega(u_D)} \cdot \prod_{z_i^t} T^{w(\mathcal{T}_{z_i^t})} \right) \cdot \prod \langle b_i, x_{i,k}^t \rangle.$$

Between two Lagrangians (L_0, H_0, b_0) and (L_1, H_1, b_1) we have a bounding cochain corrected Floer intersection complex

$$CF^{\bullet}_{\underline{b}}(L_0, L_1) := \bigoplus_{z \in L_0 \cap L_1} \Lambda \cdot z$$

whose differential is given by a weighted count of strips defined by the structure coefficients

$$\langle \mu^1(z_1), z_0 \rangle := \sum_{\beta, \underline{x}} T^{w_b(u)} \mathcal{M}_\beta(z_0; z_1, \underline{x}^t).$$

This gives a chain complex. More generally, we have the following algebraic structure:

Definition A.2.4. *Let X be a symplectic manifold. The Fukaya precategory is the precategory whose:*

- Objects are a fixed collection of Lagrangian branes L_α with bounding cochains b_α

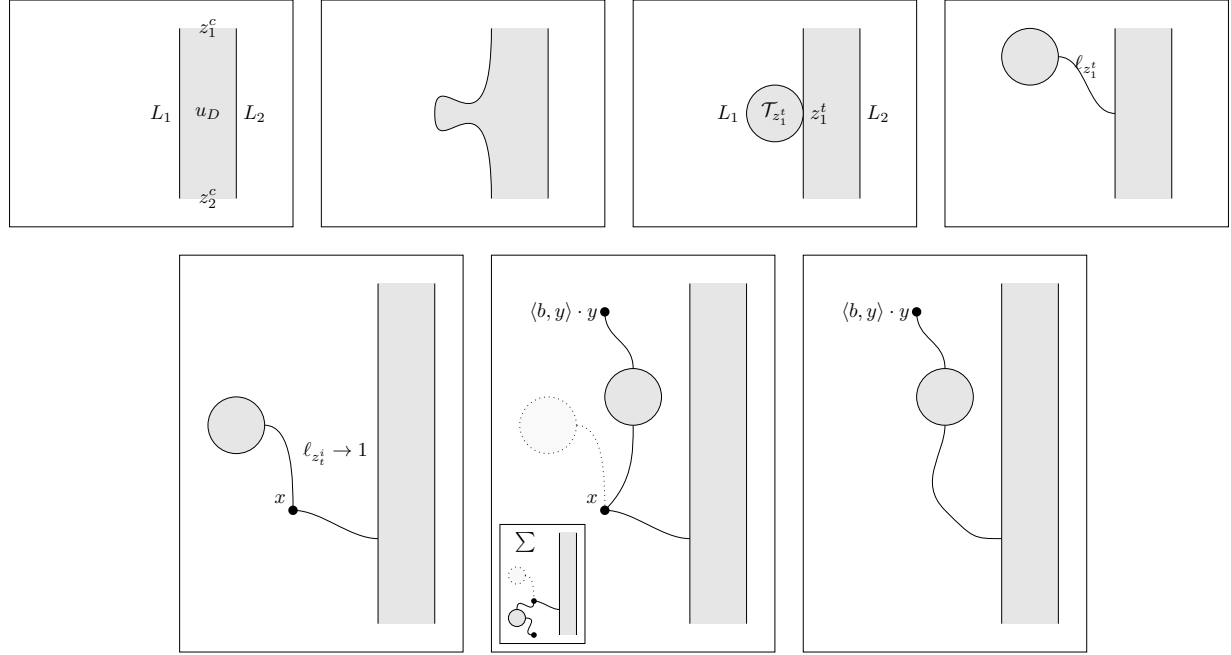


Figure 50: How bounding cochains correct for disk bubbling. First, the possible bubbling off on a disk is geometrically extended by connecting the bubbled disk to our strip with a Morse flow line of H_1 . As this Morse flowline breaks, we can algebraically continue the count by attaching on the flow from the bounding cochain of L_1 . Note that this *does not* necessarily give us a geometric continuation of the space, as there may be many terms of the bounding cochain which when simultaneously counted cancel out this contribution (as represented by the sum over the inset figure.)

- *Morphism spaces are the graded vector spaces defined for $L_i \neq L_j$ which intersect transversely*

$$\hom(L_i, L_j) := CF^{\bullet}_{\underline{b}}(L_i, L_j) := \Lambda \langle L_i \cap L_j \rangle.$$

- *Products are defined by counts of corrected flow strips,*

$$\begin{aligned} \mu_{\underline{b}}^k : \hom(L_0, L_1) \otimes \hom(L_1, L_2) \otimes \cdots \otimes \hom(L_{k-1}, L_k) &\rightarrow \hom(L_0, L_k) \\ \langle \mu_{\underline{b}}^k(z_1 \otimes \cdots \otimes z_k), z_0 \rangle &:= \sum_{\beta, \underline{x}} T^{w_{\beta}(u)} \mathcal{M}_{\beta}(z_0, \underline{z}, \underline{x}^t). \end{aligned}$$

Theorem A.2.5. *Provided that assumption A.2.2 holds, the Fukaya precategory is a uncurved A_{∞} precategory.*

When checking the computation for $(\mu_{\underline{b}}^1)^2$, the bubbling of disks which previously obstructed the differential squaring to zero is now exactly cancelled out by the bounding cochain contributions (See fig. 50.)

A.3 Localization and Quasi-Units

In the compact setting there is a description of the Fukaya category, where we use Lagrangian intersection Floer theory to define the morphisms between distinct Lagrangians, and we use the pearly algebra to define the endomorphisms of an object. However, in the non-compact setting, we are required to take an admissible Hamiltonian perturbation of our Lagrangians before computing their Floer theory; in particular, the self-Floer theory of a Lagrangian is not described with the pearly A_{∞} algebra. As such, we can only geometrically define a directed pre-category. In [Han18], this pre-category is upgraded to a category by choosing the following additional data:

- A sequence of admissible Hamiltonian isotopies $\theta_0, \theta_1, \dots$ which make $\theta_i(L)$ transverse to $\theta_j(L')$ whenever $i \neq j$ for all L, L' . Here, admissibility means that the argument of $z^{\alpha}(\theta_i(\sigma_0))$ is a non-zero constant a_i on the region of admissibility U_{α} . We require that the sequence of constants a_i are increasing.
- This determines a set of *quasi-units* in $c_{ij} \in CF^{\bullet}(\theta_i(L), \theta_j(L))$ for all $i < j$. The element c_{ij} is defined to be the count of disks $u : D^2 \setminus z_0 \rightarrow X$ with a single output and a moving Lagrangian boundary condition which interpolates between $\theta_i(L)$ and $\theta_j(L)$. Multiplication with the quasi-unit corresponds to the first order term of the continuation map associated to the Hamiltonian isotopy $\theta_j \theta_i^{-1}$.

The category is then defined by taking a directed pre-category $\text{Fuk}^{\rightarrow}(X)$ whose objects are pairs (L, θ_i) , and where the graded morphisms defined by

$$\hom((L, \theta_i), (L', \theta_j)) = \begin{cases} CF^{\bullet}(\theta_i(L), \theta_j(L')) & i < j \\ \Lambda \cdot \text{id} & \text{if } i = j \text{ and } L = L' \\ \text{Undefined} & \text{Otherwise} \end{cases}$$

The Fukaya category is then recovered by localizing $\text{Fuk}^\rightarrow(X)$ at the set of quasi-units.

To extend this to the setting of unobstructed Lagrangians branes, we need to know two things: which Hamiltonian isotopic Lagrangians equipped with bounding cochains are supposed to be equivalent, and how to define quasi-units between these equivalent Lagrangians. The choices of bounding cochains is given by the pushforward map associated to a Hamiltonian isotopy, which we describe in appendix A.3.1.

The more difficult problem is defining the quasi-units, which is complicated by the presence of disk bubbling. In the setting where there is no disk bubbling, one defines the quasi-unit by taking a count of disks with one output and moving boundary condition interpolating between $\theta_i(L)$ and $\theta_j(L)$. A geometric approach to constructing quasi-units in the setting of corrected strips would be to accessorize the domain to include these bubbles by counting disks treed disks $u : \mathcal{S} \rightarrow X$, where the domain \mathcal{S} has no inputs on the main component, and the map $u_D : D^2 \setminus z_0 \rightarrow X$ has a moving boundary condition. These treed disks would need the additional condition that each $u_i^t : \mathcal{T}_i \rightarrow X$ is a treed disk for the Lagrangian $\theta_i(L)$, where θ_i is the value of the moving boundary condition at the attachment point of the root of \mathcal{T}_i to \mathcal{S} . We believe that this is indeed the moduli space that one should count to obtain a quasi-unit in $\mathcal{S} \rightarrow X$, however the need to work with disked trees in a 1-parameter family is problematic due to the possible occurrence of index -1 disks in the family [LW14].

We sketch how one can use Lagrangian cobordisms as a way to avoid this complication and construct quasi-units. In appendix A.3.1 we give an interpretation of continuation maps for Hamiltonian isotopies in Lagrangian Floer theory from the perspective of cobordisms. In appendix A.3.2, we use Lagrangian cobordisms to construct quasi-units in Lagrangian intersection Floer theory. Finally, in appendix A.3.3 we construct the Fukaya-Seidel category for unobstructed Lagrangian branes by localizing at these quasi-units.

A.3.1 Continuation maps from Lagrangian Cobordisms

We implicitly will use many of the results from [BC14]. Theorem 2.2.7 tells us that Hamiltonian isotopies give us equivalences in the monotone Fukaya category via the suspension cobordism. This section gives an extension of that result to unobstructed Lagrangian branes. Given H_t , a time dependent Hamiltonian with compact support in the t -variable, and $L \subset X$ a Lagrangian brane, the *suspension* of H_t is the Lagrangian cobordism $K_{H_t} = L \times \mathbb{R} \subset X \times T^*\mathbb{R}$ with embedding parameterized by

$$(x, t) \mapsto (\theta_{H_t}(x), t + iH_t(x))$$

where $\theta_{H_t}(x)$ is the time t flow of H_t . Denote $\theta = \theta_{H_t}$ for $t \gg 0$.

Definition A.3.1. *Let $K \subset X \times \mathbb{C}$ be a Lagrangian cobordism which is cylindrical on the regions $\text{Re}(z) \leq b^-$ and $\text{Re}(z) \geq b^+$, so that outside of these regions K is modeled on $L^- \times \mathbb{R}_-$ and $L^+ \times \mathbb{R}_+$. A Morse function $h^t : K \rightarrow \mathbb{R}$ is cobordism admissible if there exist Morse functions $h^\pm : L^\pm \rightarrow \mathbb{R}$ and constants $\epsilon^\pm \in \mathbb{R}_\pm$ and $c^\pm \in \mathbb{R}$ so that*

$$h|_{\substack{\text{Re}(z) < b^- \\ \text{or } \text{Re}(z) > b^+}} = h^\pm + (\text{Re}(z) - (b^\pm - \epsilon^\pm))^2 + c^\pm.$$

With this choice of Morse function the Morse complex $CM^\bullet(K_H)$ becomes a mapping cylinder between the Morse complex of $CM^\bullet(L)$ and $CM^\bullet(\theta(L))$, in that there are projection maps

$$\begin{array}{ccc} & CM^\bullet(K_H, h^t) & \\ \pi^- \swarrow & & \searrow \pi^+ \\ CM^\bullet(L, h^-) & & CM^\bullet(\theta(L), h^+) \end{array}$$

We expect that the projections for Morse theory extend to A_∞ homomorphism on the pearly algebra. To prove this statement, one would need to show that the treed disks in this cobordism either have image over $[b^-, b^+] \times i\mathbb{R}$, or lie completely inside a fiber. In the case where we work with a split complex structure, this follows from the open mapping principle. Although we expect that the perturbations we've introduced to regularize the moduli space of treed disks can be done so in such a way which preserves this split-complex structure in a neighborhood of b_- and b_+ , to our knowledge this has not yet been proven for this particular setup of pearly algebra.

Assumption A.3.2. *We assume that the maps $\pi^- : CF^\bullet(K_H) \rightarrow CF^\bullet(L)$ and $\pi^+ : CF^\bullet(K_H) \rightarrow CF^\bullet(\theta(L))$ are filtered A_∞ morphisms.*

We now take a short aside to talk about A_∞ mapping cylinders.

Definition A.3.3. *Let A^+ and A^- be two filtered A_∞ algebras. A cylinder from A^+ to A^- is a filtered A_∞ algebra B which as a vector space is isomorphic to $A^- \oplus A^+[1] \oplus A^+$, and satisfies the following properties.*

- *The chain differential on B is the chain complex mapping cylinder:*

$$\begin{pmatrix} m_{A^-}^1 & 0 & 0 \\ f^1 & m_{A^+}^1 & h \\ 0 & 0 & m_{A^+}^1 \end{pmatrix}.$$

where $h : B \rightarrow B[1]$ is an isomorphism.

- *The projections of chain complexes*

$$\begin{array}{ccc} & B & \\ \pi^- \swarrow & & \searrow \pi^+ \\ A^- & & A^+ \end{array}$$

can be extended to A_∞ homomorphisms $(\pi_\pm^\pm)^k$, with $(\pi^\pm)^k = 0$ for all $k \neq 1$.

A mapping cylinder is chain homotopic to its negative end. One can prove that the chain-level homotopy inverse $i^- : A^- \rightarrow B$ can be extended to a map of filtered chain complexes.

Theorem A.3.4 (Curved Homological Perturbation Lemma). *Let B be a (curved) A_∞ algebra, and A a chain complex.*

Suppose there exist maps $\pi : B \rightarrow A$ and $i : A \rightarrow B$ so that

- $\pi \circ i = \text{id}_A$
- *There exists a weakly-filtered chain homotopy h between $i \circ \pi$ and the identity on B .*

Then we can extend the chain structure on A to an A_∞ structure so that π is a homotopy equivalence of (curved) A_∞ algebras with explicit weakly filtered A_∞ morphism

$$\hat{i} : A \rightarrow B.$$

If A already had an A_∞ structure so that π is an A_∞ map making A^\bullet a quotient of B^\bullet , then the extended A_∞ structure on A can be chosen to match the original structure.

From the curved homological perturbation lemma, we can build the following A_∞ homomorphisms

$$\begin{array}{ccc} & B & \\ \hat{i}^- \nearrow & \downarrow & \searrow \pi^+ \\ A^- & \xleftarrow{\pi^-} & A^+ \end{array}$$

By taking the composition $\pi^+ \circ \hat{i}^-$, we get a new map from $A^- \rightarrow A^+$ called the *pullback-pushforward map*, which we will denote

$$\Theta_B = \pi^+ \circ \hat{i}^-.$$

Returning to symplectic geometry, the chain complex $CM^\bullet(K_H, h_t)$ is a mapping cylinder between the chain complexes $CM^\bullet(L, h^-)$ and $CM^\bullet(\theta(L), h^+)$. One can then show that $CF^\bullet(K_H, h^t)$ is an A_∞ mapping cylinder between $CF^\bullet(L, h^-)$ and $CF^\bullet(\theta(L), h^+)$. This gives us an A_∞ homomorphism $\hat{i}^- : CF(L, h^-) \rightarrow CF(K_H, h^t)$ and the composition

$$\Theta_H := \pi^+ \circ \hat{i}^- : CF^\bullet(L, h^-) \rightarrow CF^\bullet(\theta(L), h^+)$$

is our continuation map of A_∞ algebras.

Corollary A.3.5. *If the Lagrangian L is unobstructed, so are K_H and $\theta(L)$.*

Proof. More generally, let $f : A^\bullet \rightarrow B^\bullet$ be a weakly filtered A_∞ morphism. Then there exists a *pushforward* map between the bounding cochains on A^\bullet and the bounding cochains of B^\bullet given by

$$f_*(b) := \sum_{k \geq 0} f^k(b^{\otimes k})$$

Let b be our bounding cochain on L . Then the pushforwards $(\hat{i}^-)_*b$ and $(\pi^+ \circ \hat{i}^-)_*b$ are bounding cochains on $CF^\bullet(K_H)$ and $CF^\bullet(\theta(L))$ respectively. \square

This construction can be extended to prove the following invariance property of the pearly algebra.

Theorem A.3.6. *If L is unobstructed, then $CF^\bullet(L)$ and $CF^\bullet(\theta(L))$ are quasi-isomorphic.*

In particular, the quasi-isomorphism class of $CF^\bullet(L; h)$ is independent of Morse function chosen.

Remark A.3.7. *We will now make the following simplifications for the purposes of exposition. We say that two cobordisms K_1 and K_2 intersect cleanly in the cobordism parameter if whenever $p \in K_1 \cap K_2$, there exists a neighborhood of the parameter space of the cobordism around p so that K_1 and K_2 are modelled on parallel transport along a curve in that neighborhood. We will say that K_1 and K_2 are equipped with clean intersection admissible Morse functions if near each point $p \in T^*\mathbb{R}$ where $K_1 \cap K_2$ intersect under projection to the base, the Morse function for K_i is a fiberwise perturbation of a Morse-Bott function for K_i which has a maximum on the fiber $\pi^{-1}(p) \cap K_i$. For the remainder of this section, we will assume that our Lagrangian cobordisms always intersect cleanly in the cobordism parameter, and are equipped with clean-intersection admissible Morse functions. As $CF^\bullet(K, h)$ is independent of Morse function up to quasi-isomorphism, we will not explicitly write these Morse functions, as they become rather unwieldy. In general, the Morse portion of the differential on $CF^\bullet(K, h)$ will be a ‘‘telescoped mapping cylinder;’’ for example, the Morse portion of the homology for K_{H_t} as drawn in fig. 52 is*

$$\begin{array}{ccccccc}
 & & CF^\bullet(L; h_2)[1] & & CF^\bullet(L; h_3)[1] & & CF^\bullet(\theta(L); h_4)[1] \\
 & \swarrow & \parallel & \swarrow & \parallel & \swarrow & \parallel \\
 CF^\bullet(L; h_1) & & CF^\bullet(L; h_2) & & CF^\bullet(L; h_3) & & CF^\bullet(\theta(L); h_4)
 \end{array}$$

where the downward arrows are isomorphisms. Clearly, the complex is quasi-isomorphic to $CF(L; h_1)$, and presence of this squiggly Morse function is a technicality needed to make the restriction maps from Fukaya category of cobordisms to the Fukaya category of X work. Similarly, see the profile function h' in [BC14, Figure 10].

The Lagrangian cobordism K_H also allows us to define continuation maps between $CF^\bullet(L, T)$ and $CF^\bullet(\theta(L), T)$ for some test Lagrangian T . Consider the Lagrangians K_{H_t} and $T \times \gamma$ as drawn in fig. 51. The complex $CF^\bullet(K_{H_t}, T \times \gamma)$ has the structure of a mapping cone between $CF^\bullet(L, T)$ and $CF^\bullet(\theta(L), T)$. We define the map $\Theta_{H_t} : CF^\bullet(L, T) \rightarrow CF^\bullet(\theta(L), T)$ to be the connecting morphism of this mapping cone.

Remark A.3.8. *The Lagrangians L that we will be considering will be non-compact, and the Hamiltonian isotopies θ_i are the flows of unbounded Hamiltonian functions. As a result, the diagrams we have drawn for our Lagrangians will not honestly have a compact projection (as in fig. 51). However, as all intersection points, critical values of H , and treed disks on L and the suspension cobordism K_{H_t} will be contained within a compact subset, these pictures still provide an intuition for the geometry of our Lagrangian cobordisms.*

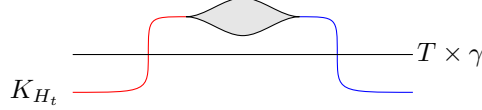


Figure 51: The suspension cobordism for H_t intersecting cleanly in the cobordism parameter with $T \times \gamma$, a parallel transport of T .

Proposition A.3.9. *The connecting map Θ_{H_t} is a quasi-isomorphism.*

Proof. This comes from considering a more elaborate setup of Lagrangian cobordisms, as drawn in fig. 52. The four intersection points in the base give us a decomposition of $CF^\bullet(K_{H_t}, T \times \gamma_{cont})$ as a vector space into 4 components.

- The intersections above the point c are in correspondence with the generators of $CF^\bullet(L, T)$.
- The intersections above the point b are in correspondence with the generators of $CF^\bullet(L, T)[1]$.
- The intersections above the point d are in correspondence with the generators of $CF^\bullet(\theta_H(L), T)[2]$.
- The intersections above the point a are in correspondence with the generators of $CF^\bullet(L, T)[2]$.

The complex $CF^\bullet(K_{H_t}, T \times \gamma_{cont})$ can be filtered by grading in the projection to the base. The differential splits into a graded portion which counts holomorphic strips confined to a fiber of the cobordism parameter, and 5 other components which count strips passing between intersections in different fibers.

$$\begin{array}{ccc}
 CF^\bullet(L, T) & \xrightarrow{m_{cb}^1} & CF^\bullet(L, T)[1] \\
 \downarrow m_{cd}^1 & \searrow m_{ca}^1 & \downarrow m_{ba}^1 \\
 CF^\bullet(\theta(L), T)[1] & \xrightarrow{m_{da}^1} & CF^\bullet(L, T)[2]
 \end{array}$$

The maps $m_{cb}^1, m_{cd}^1, m_{da}^1, m_{ba}^1$ and m_{ca}^1 are given by counts of holomorphic disks with projection over the regions drawn in fig. 52. Comparing to the regions of the suspension cobordism, the map m_{cd}^1 is seen to match the connecting homomorphism from the suspension cobordism, and our candidate for continuation map. The morphisms m_{ba} and m_{cb} are isomorphisms. The map m_{ca} provides a chain homotopy

$$m_{da} \circ m_{cd} \sim m_{ba} \circ m_{cb}$$

showing that we've constructed a 1-sided homotopy inverse. Making the same argument with the cobordism where everything is reflected, we conclude that m_{cd} is a quasi-isomorphism. \square

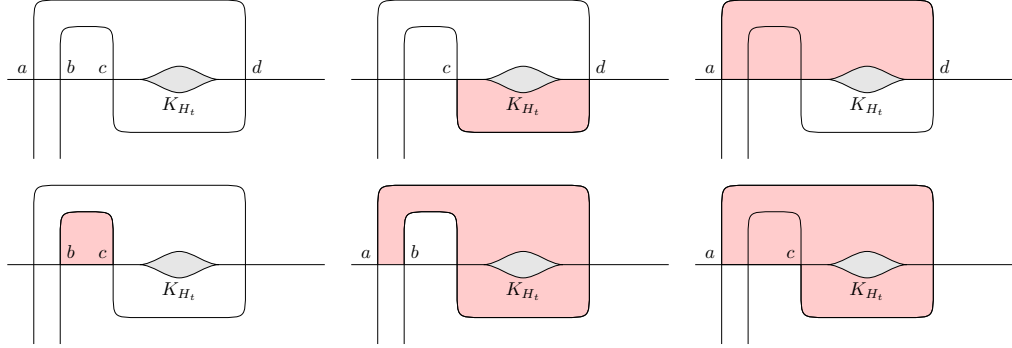


Figure 52: Showing that continuation by the trace of Hamiltonian isotopy is a quasi-isomorphism. The 5 different regions correspond to non-graded components of the differential on $CF^\bullet(K_{H_t}, T \times \gamma_{cont})$

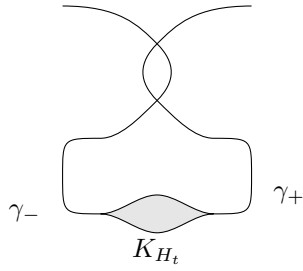


Figure 53: The quasi-unit cobordism

A.3.2 Quasi-Units for Hamiltonian isotopy

The goal of this section is to construct a quasi-unit c_{H_t} associated to a time dependent Hamiltonian H_t . Let $\theta(L)$ be the Lagrangian submanifold obtained by applying the Hamiltonian flow of H_t to L . Assume that $\theta(L)$ is transverse to L .

Definition A.3.10. *Let $H_t : L \times [0, 1] \rightarrow \mathbb{R}$ be a smooth time dependent Lagrangian Hamiltonian isotopy with $H_0(L) = H_1(L) = 0$. We define the quasi-unit cobordism associated to H_t to be the Lagrangian $K_{H_t}^{qu} \subset X \times \mathbb{C}$ which is topologically $L \times \mathbb{R}$, and is parameterized by the following pieces:*

- $L \times (-\infty, 0]$ is the \mathfrak{L} -shaped Lagrangian cobordism $L \times \gamma_-$ for the path γ_- drawn in fig. 53.
- $L \times [0, 1]$ is a restriction of suspension cobordism K_{H_t} of the Hamiltonian H_t .
- $\theta(L) \times [1, \infty)$ is the S -shaped Lagrangian cobordism $L \times \gamma_+$ for the path γ_+ drawn in fig. 53.

This is an immersed Lagrangian, so the generators of its Floer complex are the critical points of a Morse function $f : K \rightarrow \mathbb{R}$, as well as a pair of generators for each self-intersection of K . These self-intersection points are transverse and correspond to generators

of $CF^\bullet(L, \theta(L))$ and $CF^\bullet(\theta(L), L)$, shifted in homological degree corresponding to whether they lie in the upper or lower self-intersection. The product maps $m^k : CF^\bullet(K_{H_t}^{qu})^{\otimes k} \rightarrow CF^\bullet(K_{H_t}^{qu})$ count treed strips with boundary on $J_{H_t}^{qu}$, whose strip-like ends limit to inputs and/or outputs corresponding to the self-intersections of $K_{H_t}^{qu}$. The Morse function for $CF^\bullet(K_{H_t}^{qu})$ is chosen to be clean intersection compatible with the self-intersections of this Lagrangian. As a vector space, we have a decomposition of $CF^\bullet(K_{H_t}^{qu})$,

$$\begin{aligned} CF^\bullet(K_{H_t}^{qu}) &= CM^\bullet(K_{H_t}^{qu}) \\ &\oplus CF^\bullet(L, \theta(L)) \oplus CF^\bullet(L, \theta(L))[1] \\ &\oplus CF^\bullet(\theta(L), L) \oplus CF^\bullet(\theta(L), L)[1], \end{aligned}$$

where $CM^\bullet(K_{H_t}^{qu})$ is the portion of the complex generated by critical points of the Morse complex. The remaining subspaces are generated by critical points lying at the “upper” or “lower” self-intersection drawn in fig. 53. In addition possibility of holomorphic disks obstructing our Floer theory, there are holomorphic teardrops with outputs on $CF^\bullet(L, \theta(L))$ which may obstruct the differential from squaring to zero. We expect that these teardrops can be accounted for via bounding cochain, as the output of the teardrops lie in the “upper intersections” as drawn in fig. 53, and are therefore in the boundary of the differential arising from the “lower intersections.” These teardrops provide our candidate for the quasi-unit, and have boundaries which interpolate between L and $\theta(L)$. However, the attached flow trees to these teardrops are not constrained to lie in a single time-slice of the Hamiltonian, and thereby avoiding the regularization problem.

Claim A.3.11. *Whenever the Lagrangian L is unobstructed by bounding cochain b , the Lagrangian cobordism $K_{H_t}^{qu}$ is unobstructed by bounding cochain.*

Proof. The idea of proof is similar to showing that the suspension cobordism K_{H_t} is unobstructed: first we show that the pearly algebra is homotopic to the end, and then we apply the curved homological perturbation lemma. First, we note that the Morse portion $CF^\bullet_m(K_{H_t}^{qu})$ as a vector space splits as

$$CF^\bullet(L) \oplus (\text{Additional Terms}) \oplus CF^\bullet(L)[1] \oplus CF^\bullet(\theta(L))$$

where the additional terms are “telescoped mapping cylinder” terms discussed in remark A.3.7. As the only flow trees/strips with output on $CF^\bullet(L)$ must have input from $CF^\bullet(L)$, there exists an A_∞ projection

$$\pi_- : CF^\bullet(K_{H_t}^{qu}) \rightarrow CF^\bullet(L).$$

To construct an A_∞ homotopy between $CF^\bullet(K_{H_t}^{qu})$ and $CF^\bullet(L)$, we look at the low-energy portion of the structure. The lowest energy portion of the differential on $CF^\bullet(K_{H_t}^{qu})$ comes from counts of

- Pure Morse strips with input and output on $CF^\bullet_m(K_{H_t}^{qu})$
- The visible strip from $CF^\bullet(L, \theta(L)) \rightarrow CF^\bullet(L, \theta(L))[1]$

- The visible strip from $CF^\bullet(\theta(L), L) \rightarrow CF^\bullet(\theta(L), L)[1]$.

Therefore, there exists a valuation λ so that $CF^\bullet(K_{H_t}^{qu}) \bmod T^\lambda$ is chain homotopic to $CM^\bullet(L)$, and one can induct on the filtration to produce a homotopy equivalence between $CF^\bullet(K_{H_t}^{qu})$ and $CF^\bullet(L)$.

With the curved homological perturbation lemma we produce a homotopy inverse $i_{qu}^- : CF^\bullet(L) \rightarrow CF^\bullet(K_{H_t}^{qu})$ to the projection $\pi^- : CF^\bullet(K_{H_t}^{qu}) \rightarrow CF^\bullet(L)$. By pushing bounding cochains along this inverse, we obtain a bounding cochain $(i_{qu}^-)_* b$ for $CF^\bullet(K_{H_t}^{qu})$. \square

The bounding cochain lives in $CF^\bullet(L, \theta(L))$, the subspace generated by the self-intersections of $K_{H_t}^{qu}$ away from the teardrop. The projection from

$$\pi_{out} : CF^\bullet(K_{H_t}^{qu}, (i_{qu}^-)_* b) \rightarrow CF^\bullet((L, b), (\theta(L), (\Theta_*)_b))$$

is similarly well defined, as all strips with outputs on $CF(L, \theta(L))$ must similarly have inputs in that fiber of the cobordism parameter. There is an additional subtlety here, which is that the restriction of the bounding cochain $(i_{qu}^-)_* b$ to $CF^\bullet(\theta(L))$ matches $(\Theta_*)_b$. This allows us to pushforward the bounding cochain b from $CF^\bullet(K_{H_t}^{qu})$ to an element of Lagrangian intersection cohomology.

Definition A.3.12. *Given a Hamiltonian H_t of (L, b) we define the quasi-unit of H_t via the pushforward*

$$c_{H_t} := (\pi_{out})_*(i_{qu}^-)_* b \in CF^\bullet(L, \theta(L)).$$

Geometrically, this bounding cochain cancels out the count of holomorphic teardrops on the Lagrangian K_{H_t} , and should represent the image of the identity under the continuation map.

Example A.3.13. *In the case where $K_{H_t}^{qu}$ bounds no holomorphic disks, then L is tautologically unobstructed and $b = 0$. The pushforward of the zero deformation is the curvature term of the quasi-isomorphism, so*

$$b = (i_{qu}^-)_*(0) = (i_{qu}^-)^0,$$

where $(i_{qu}^-)^0$ is the curvature term

$$(i_{qu}^-)^0 : \Lambda \rightarrow CF^\bullet(K_{H_t}^{qu})$$

This term can be determined by a composition of $m^0 : \Lambda \rightarrow CF^\bullet(K_{H_t}^{qu})$, the homotopy h between $i^{qu-} \circ \pi_- \sim \text{id}$, and the products m_{qu}^k on $CF^\bullet(K_{H_t}^{qu})$. The lowest order contribution of this is given by the composition $h \circ m_{qu}^0$. The only terms contributing to m_{qu}^0 in this scenario are the teardrops with output on $CF^\bullet(L, \theta(L))[1]$, and the portion of the homotopy h we must consider is the inverse to the differential restricted to $CF^\bullet(L, \theta(L)) \xrightarrow{\sim} CF^\bullet(L, \theta(L))[1]$. Therefore the lowest order portion of b is given the count of the teardrops, appropriately shifted by the homotopy to live in $CF^\bullet(L, \theta(L))$.

Observe that treed strips contributing to the product on $CF^\bullet(K_{H_t}^{qu})$ have output in $CF^\bullet(L, \theta(L))$ only if they have exactly 1-strip like end, and that strip like end limits to an intersection point in $CF^\bullet(L, \theta(L))$. This observation shows allows us that the c_{ij} are closed.

Proposition A.3.14. c_{ij} is a closed element of $CF((L, b), (\theta(L), \Theta_* b))$.

Proof. Let $d : CF^\bullet((L, b), (\theta(L), \Theta_* b)) \rightarrow CF^\bullet((L, b), (\theta(L), \Theta_* b))$ be the bounding cochain deformed differential.

$$d(c_{ij}) = \sum_{k_1, k_2 > 0} m^{k_1|1|k_2} (b^{\otimes k_1} \otimes c_{ij} \otimes (\Theta_*(b))^{\otimes k_2})$$

Here, $m^{k_1|1|k_2}$ is the bimodule product of the pearly algebras on the intersection algebra, given by a count of treed strips with k_1 Morse inputs on L , k_2 Morse inputs on $\theta(L)$, and 1 input in $CF(L, \theta(L))$.

$$= \pi_{out} \left(\sum_{k_1, k_2 > 0} m_{K_{H_t}^{qu}}^{k_1+k_2} (b^{\otimes k_1} \otimes c_{ij} \otimes (\Theta_*(b))^{\otimes k_2}) \right)$$

This is a count of treed strips with one input and one output on $CF^\bullet(L, \theta(L))$. By our choice of Morse function, the Morse-like inputs of these treed strips must project to the self-intersection point. The Morse-like inputs on the treed strip which are indexed before c_{ij} must come from the copy of $CF^\bullet(L) \subset CF^\bullet(K_{H_t}^{qu})$, while those inputs indexed after c_{ij} come from the copy of $CF^\bullet(\theta(L))$. The portion of the bounding cochain b which lives in those two components are $(i_{qu}^-)_* b|_L = b$ and $(i_{qu}^-)_* b|_{\theta(L)} = \Theta_* b$ respectively

$$= \pi_{out} \left(\sum_{k_1, k_2 > 0} m_{K_{H_t}^{qu}}^{k_1+k_2} (((i_{qu}^-)_* b)^{\otimes k_1} \otimes c_{ij} \otimes ((i_{qu}^-)_* b)^{\otimes k_2}) \right)$$

Recall that c_{ij} is defined to be the restriction of the bounding cochain b to $CF(L, \theta(L))$,

$$= \pi_{out} \left(\sum_{k_1, k_2 > 0} m_{K_{H_t}^{qu}}^{k_1+k_2} (((i_{qu}^-)_* b)^{\otimes k_1} \otimes (i_{qu}^-)_* b \otimes ((i_{qu}^-)_* b)^{\otimes k_2}) \right)$$

This is the Maurer-Cartan equation applied to the pushforward of a bounding cochain, which is again a bounding cochain

$$= \pi_{out} \left(\sum_{k \geq 0} m^k (((i_{qu}^-)_* b)^{\otimes k}) \right) = 0.$$

□

Proposition A.3.15. The map $m^2(c_{H_t}, -) : CF^\bullet(\theta(L), T) \rightarrow CF^\bullet(L, T)$ is homotopic to the cobordism continuation map.

Proof. The proof comes from understanding the configurations of disks which show up in fig. 54. The chain complex $CF^\bullet(K_{H_t}^{qu}, T \times \gamma)$ can be decomposed as a vector space as

$$CF^\bullet(L, T) \oplus CF^\bullet(\theta(L), T)[1] \oplus CF^\bullet(L, T)[1] \oplus CF^\bullet(\theta(L), T)[2]$$

The differential on the complex can be decomposed into several different maps between these subcomplexes.

$$\begin{array}{ccc} CF^\bullet(L, T) & \xrightarrow{m_{ca}=\text{id}} & CF^\bullet(L, T)[1] \\ \downarrow h_1 & \searrow h_2 & \downarrow m_{ab}=\Theta_H \\ CF^\bullet(\theta(L), T)[1] & \xrightarrow{m_{db}=\text{id}} & CF^\bullet(\theta(L), T)[2] \end{array}$$

The interesting maps here are h_1 , m_{ab} and h_2 . When computing the Lagrangian intersection Floer theory between two Lagrangians which may be immersed, the differential not only counts treed strips, but also treed polygons with ends limiting to the bounding cochain. The map h_1 arises from the product of the bounding cochain on $K_{H_t}^{qu}$ contributing to the differential on $CF^\bullet(K_{H_t}^{qu}, T \times \gamma)$ (corresponding to the red triangle in fig. 54e). The element in the bounding cochain which contributes to this deformed differential is the quasi-unit element we just constructed, and so

$$h_1(-) = m^2(-, c_{H_t}) : CF^\bullet(L, T) \rightarrow CF^\bullet(\theta(L), T).$$

The map m_{ab} exactly matches our continuation map associated to the cobordism $K_{\theta_{ij}}$. The remaining map h_2 also corresponds to product with the quasi-unit, however the product is not restricted to the fiber and therefore interpolates between the maps m_{ab} and h_1 , providing a homotopy between the compositions

$$\text{id} \circ \Theta_{H_t}(-) \sim m^2(c_{H_t}, \text{id}(-))$$

which proves that the quasi-unit is a quasi-isomorphism of complexes. \square

A.3.3 The directed Fukaya category and Localization

Having defined a quasi-unit for a Hamiltonian isotopy, we will pick a sequence of admissible Hamiltonian isotopies which give us enough transversality to define Lagrangian intersection Floer theory, and define a directed Fukaya pre-category with these isotopies. We will then localize the Fukaya pre-category at the quasi-isomorphisms associated to those Hamiltonian isotopies to obtain the Fukaya category. The objects of this Fukaya category will be Lagrangian branes equipped with bounding cochains. We start with a countable collection of Lagrangians, and then construct new Lagrangians by taking Hamiltonian isotopies and pushing forward bounding cochains along these isotopies.

Definition A.3.16. *Let $\text{Ob}_0 = \{(L_\alpha, b_\alpha)\}$ be a countable collection of unobstructed Lagrangian branes. A infinitesimal wrapping datum for Ob_0 is a*

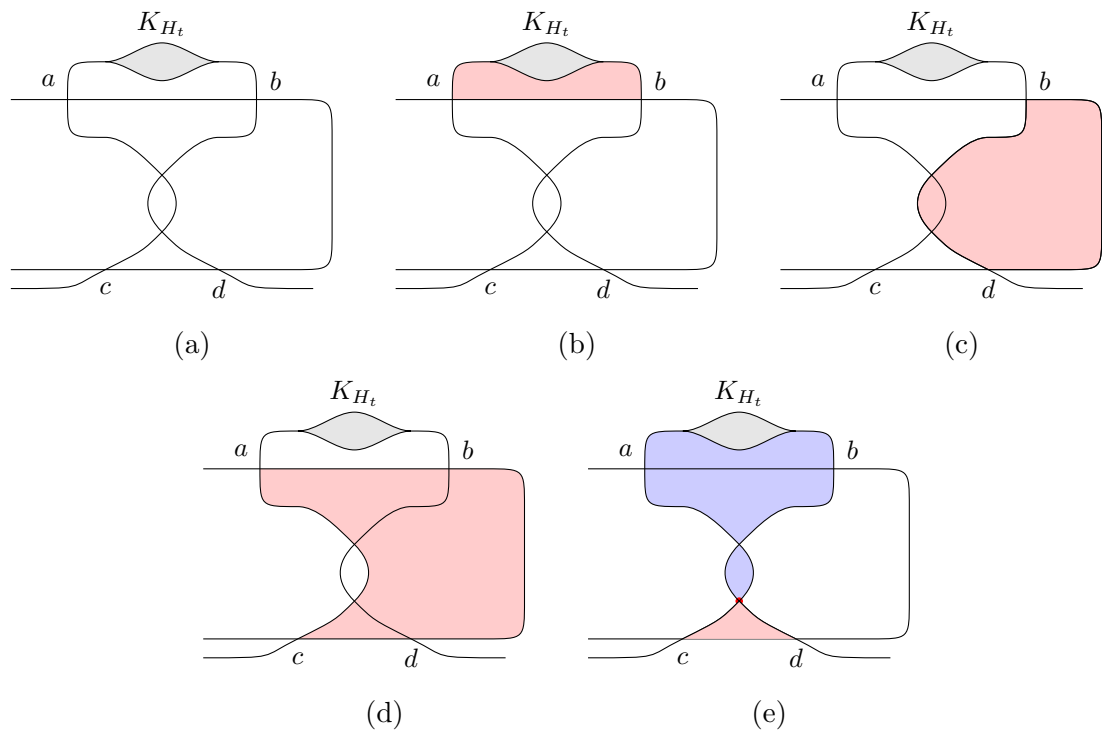


Figure 54: Comparing a count of disks shows that multiplication by the quasi-unit is the same as continuation from trace of Hamiltonian isotopy.

- A choice of an increasing sequence of angles $0 = \xi_1 < \xi_2 < \dots < \pi$.
- A choice for integers $0 \leq i < j$ a time dependent Hamiltonian H_t^{ij} with compact support in $(0, 1)$ giving us a Hamiltonian isotopy θ_{ij} .

We call θ_{ij} a monomial admissible Hamiltonian wrapping isotopy. We require that this data satisfy the following properties:

- θ_{00} is the identity
- The sequence of Hamiltonians send the zero section to a Lagrangian with fixed arguments given by the sequence of angles so that $\arg(z^\alpha(\theta_i(\sigma_0))|_{U_\alpha} = \xi_i$
- For each $i < j$ and $L, L' \in \text{Ob}_0$ we have that $\theta_i(L)$ intersects $\theta_j(L')$ transversely.
- The wrapping is infinitesimal so that $\arg(z^\alpha(\theta_i(\sigma_0))|_{U_\alpha} < \pi$ for all i .
- For all $0 < i < j$, we have that $\theta_{jk} \circ \theta_{ij} = \theta_{ik}$.

Let $\Theta_{ij} : CF^\bullet(\theta_i(L)) \rightarrow CF^\bullet(\theta_j(L))$ be the continuation map associated to our choices of Hamiltonian isotopies θ_{ij} and cobordisms $K_{\theta_{ij}}$. Given a wrapping datum, define

$$\text{Ob}_k := \{\theta_{0k}(L_\alpha), (\Theta_{0k})_* b_\alpha\}$$

Given a wrapping datum for Ob_0 , we define a preliminary directed Fukaya category with objects

$$\text{Ob}(\text{Fuk}^\rightarrow(X)) := \bigcup_{k \in \mathbb{N}} \text{Ob}_k(X).$$

The homomorphisms of this category are defined by

$$\text{hom}^\rightarrow((L_0, b_0), (L_1, b_1)) := \begin{cases} CF^\bullet_{b_0, b_1}(L_0, L_1) & \text{if } L_0 \in \text{Ob}_i, L_1 \in \text{Ob}_j \text{ and } i < j. \\ \Lambda \cdot \text{id} & \text{if } L_0 = L_1 \\ 0 & \text{otherwise.} \end{cases}$$

The differentials on complexes of the category $\text{Fuk}^\rightarrow(X)$ are defined by the count of treed-strips corrected by bounding cochains, and the higher product maps are also counted with corrections coming from these bounding cochains.

$$m^k : \text{hom}(L_0, L_1) \otimes \text{hom}(L_1, L_2) \otimes \dots \otimes \text{hom}(L_{k-1}, L_k) \rightarrow \text{hom}(L_0, L_k)$$

$$\langle m^k(z_1 \otimes \dots \otimes z_k), z_0 \rangle = \begin{cases} \sum_{\beta, \underline{x}} T^{w_b(u)} \# \mathcal{M}_\beta(z_0, \underline{z}, \underline{x}^t) \} & \text{When } l_i \in \text{Ob}_{j_i}, j_0 < \dots < j_k. \\ 0 & \text{Otherwise} \end{cases}$$

This gives $\text{Fuk}^\rightarrow(X)$ the structure of a non-curved A_∞ category. This category is directed by the index of Ob_k . To obtain the Fukaya category from this, we localize at the quasi-units so that all of the $(\theta_i(L_\alpha), (\Theta_i)_* b_\alpha)$ become isomorphic objects.

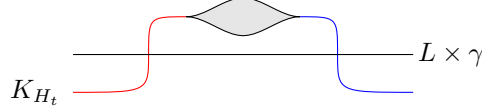


Figure 55: A cobordism configuration yielding a PSS type isomorphism from the pearly model on $CF^\bullet(L)$ to the Lagrangian intersection Floer theory on $CF^\bullet(L, \theta(L))$. Note that the intersection on the left hand side is a clean intersection, and not transverse.

Remark A.3.17. *A more geometric approach to define this category is to set up*

$$\hom((L_0, \theta_0), (L_0, \theta_0)) = CF^\bullet(L_0, H_0)$$

as the pearly-model. However, as we do not know how to construct continuation maps from this to the Lagrangian intersection Floer homology (via a PSS-like theorem) we do not take this approach. One possible way to show that quasi-units constructed induce a quasi-isomorphism between $CF^\bullet(L)$ and $CF^\bullet(L, \theta(L))$ would be to consider a cobordism K with two self-intersections in the parameter space of the cobordism. To find a model of $CF^\bullet(L)$ inside of $CF^\bullet(K)$, we could make K intersect itself cleanly along $L \subset K$. The differential on $CF^\bullet(K)$ would then count cascaded treed strips contained in L – see fig. 55. We expect that such a count will show that the quasi-unit gives a PSS type isomorphism between $CF^\bullet(L)$ and $CF^\bullet(L, \theta(L))$.

For a Lagrangian brane $(L, b) \in \text{Ob}_0$, and $i < j \in \mathbb{N}$, we have now associated a quasi-unit element $c_{ij} \in \hom(\theta_i(L), \theta_j(L))$. Summarizing the previous discussion:

Proposition A.3.18. *For given Lagrangian L and $i < j$, the quasi-units c_{ij} satisfy the following properties.*

- The elements $c_{ij} \in CF^\bullet(\theta_i(L), \theta_j(L))$ are closed.
- The composition of quasi-units is again a quasi-unit on homology

$$m^2(c_{ij}, c_{jk}) \sim c_{jk}.$$

- The map

$$m^2(c_{ij}, -) : CF^\bullet(\theta_j(L), L') \rightarrow CF^\bullet(\theta_i(L), L')$$

is homotopic to the cobordism continuation map Θ_{ij} .

- The map

$$m^2(c_{ij}, -) : CF^\bullet(\theta_i(L), L') \rightarrow CF^\bullet(\theta_j(L), L')$$

is a quasi-isomorphism.

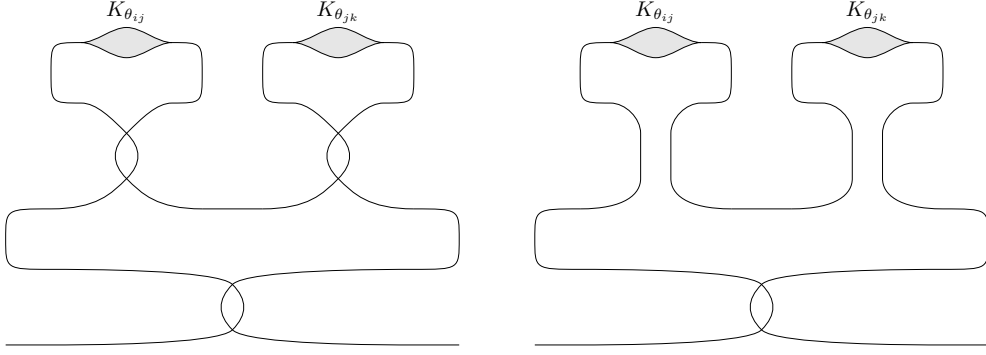


Figure 56: Multiplicative Property of Quasi-units.

Proof. The first three items are propositions A.3.9, A.3.14 and A.3.15. The first property is the equivalent of [Han18, Proposition 3.15] for Lagrangians unobstructed by bounding cochains. The proof of the composition rule comes from the Hamiltonian continuation between the Lagrangians drawn in fig. 56. One then defines the bounding cochain defining the continuation c_{jk} by taking the pushforward of the bounding cochains defining the continuation for c_{ij} and c_{jk} . \square

From this construction, we get a collection of quasi-units in the directed Fukaya category $\text{Fuk}^\rightarrow(X)$.

Definition A.3.19. *Let X be a symplectic manifold and let $\text{Ob}_0 = \{L_\alpha\}$ be a countable collection of mutually transverse unobstructed Lagrangian branes. Suppose additionally we have a wrapping datum allowing us to define the directed pre-category $\text{Fuk}^\rightarrow(X)$. The monomial admissible unobstructed Fukaya category is the localization of $\text{Fuk}^\rightarrow(X)$ at the set of quasi-units c_{ij} .*

Here, the localization is the image of $\text{Fuk}^\rightarrow(X)$ inside of $\text{mod } - (\text{Fuk}^\rightarrow(X))/\text{cone}(Q)$, where Q is the set of quasi-units and the quotient category is constructed following [LO+06].

A.4 Lagrangian Cobordisms with Obstructions

In this section, we outline an extension of the results of [BC14] to the obstructed setting using the tools of appendix A.

Theorem A.4.1. *Given $W : X \rightarrow \mathbb{C}$ a Laurent polynomial, and Δ a monomial admissibility condition for X , there is a monomial admissibility condition $(W + z_0, \Delta + \Delta_{k+1})$ on $X \times \mathbb{C}$ defining a Fukaya category of unobstructed Lagrangian cobordisms, $\text{Fuk}_{\Delta + \Delta_{k+1}}(X \times \mathbb{C})$. Furthermore, whenever $K : (L_i^+_{i=0}^{k-1} \rightsquigarrow L^-)$ is a Lagrangian cobordism, there are k objects Z_0, \dots, Z_{k-1} in the $\text{Fuk}_\Delta(X)$, with $Z_0 = L_0^+$ and $Z_k \simeq L^-$ which fit into k exact triangles*

$$L_i^+ \rightarrow Z_{i-1} \rightarrow Z_i \rightarrow L_i^+[1].$$

The category of Lagrangian cobordisms appearing in the proof of theorem 2.2.2 is constructed by considering counts of disks with moving boundary conditions.

As suggested by the statement of the theorem, we construct a different category of Lagrangian cobordisms using the techniques previously developed for Fukaya category of monomial admissible unobstructed Lagrangians. The author was made aware of the connection between admissibility conditions, Künneth formula, and the category of Lagrangian cobordisms from Hiro Tanaka. To do this, we generalize our definition of monomial admissibility.

Definition A.4.2. *A multiply stopped monomial admissibility condition is a monomial admissibility condition (W, Δ) for X , as well as a selection for each monomial z^α a sequence of increasing angles*

$$\underline{\zeta}^\alpha = \{0 = \zeta_1^\alpha < \zeta_2^\alpha < \cdots < \zeta_n^\alpha\} \in [0, 2\pi).$$

We say that a Lagrangian L is admissible with respect to a multiply stopped admissibility condition $(W, \Delta, \underline{\zeta}^\alpha)$ if the argument of $c_\alpha z^\alpha$ restricted to L matches one of the ζ_i^α outside of a compact subset.

The language of monomial admissibility conditions extends to symplectic toric varieties, where $W : X_\Sigma \rightarrow \mathbb{C}$ is a holomorphic function whose restriction to the open $(\mathbb{C}^*)^n$ chart is a Laurent polynomial, and the regions C_α are required to cover all but a compact subset of the moment polytope of X_Σ . The simplest example of this (and the only example which we will use) is the example of $z : \mathbb{C} \rightarrow \mathbb{C}$. When equipped with a single stop, this category has no non-zero objects. When we equip this with multiple stops, we obtain a more interesting category. Let $(\mathbb{C}, z_0, \Delta_k)$ be a k -stopped monomial admissibility condition on the complex plane. We note that $\text{Fuk}_{\Delta_k}(\mathbb{C}, z_0)$ is the category of Lagrangian cobordisms on X when X is a point.

Definition A.4.3. *Let (X_1, W_1, Δ_1) and (X_2, W_2, Δ_2) be two symplectic toric varieties equipped with monomial admissibility conditions. Let $\text{val}_1 : X_1 \rightarrow Q_1$, $\text{val}_2 : X_2 \rightarrow Q_2$ be the standard moment maps. First shrink the subsets C_k^α for Δ_k if necessary so that the argument of z^α is controlled over all of C_i^α . The sum monomial admissibility condition on $X_1 \times X_2$ is the admissibility condition $(W_1 + W_2, \Delta_1 + \Delta_2)$, where*

$$\begin{aligned} \Delta_1 + \Delta_2 := & \{(C_1^\alpha \times Q_2) \subset Q_1 \times Q_2 \mid C_1^\alpha \in \Delta_1\} \\ & \sqcup \{(Q_1 \times C_2^\alpha) \subset Q_1 \times Q_2 \mid C_2^\alpha \in \Delta_2\}. \end{aligned}$$

This sum monomial admissibility condition extends in a natural way to multiply stopped monomial admissibility conditions.

Definition A.4.4. *Let (W, Δ) be a monomial admissibility condition on $X = (\mathbb{C}^*)^n$. We define the space of Lagrangian k -cobordisms to be the space $X \times \mathbb{C}$ with sum monomial condition $(W + z_0, \Delta + \Delta_k)$.*

A Lagrangian k -cobordism is a Lagrangian submanifold $K \subset X \times \mathbb{C}$ which is monomial admissible for the monomial admissibility condition $(W + z_0, \Delta + \Delta_k)$. This definition for a Lagrangian cobordism does not explicitly define the “ends” of the cobordism as in definition 2.2.5. However, the monomial admissibility condition forces the Lagrangian to have well-defined ends.

Claim A.4.5. *Let K be a Lagrangian k -cobordism. There exist Lagrangian submanifolds $\{L_i\}_{i=1}^k$ in X so that in the complement of a compact $C \subset \mathbb{C}$, we have*

$$K \setminus \pi_{\mathbb{C}}^-(C) = \bigcup_{1 \leq i \leq k} (\zeta_i \cdot \mathbb{R}_+) \times L_i.$$

We call the Lagrangians L_i the ends of the Lagrangian cobordism.

A key portion of the data of a Lagrangian submanifold in $\text{Fuk}_{\Delta + \Delta_k}^{\rightarrow}(X \times \mathbb{C}, W + z_0)$ is the data of a brane structure, which allows us to construct bounding cochains on the Lagrangian submanifolds. A Lagrangian cobordism with a brane structure should have ends which are also equipped with a brane data. To do this, we will now fix a radius R_{big} , and require that the set $C \subset X \times \mathbb{C}$ on which the Lagrangian cobordism are non-cylindrical to have valuation $|z_0(C)| < R_{big}$. We now equip our Lagrangian submanifolds with a brane structure which is bottlenecked at the radius of R_{big} in the following way.

Definition A.4.6. *Let $K \subset X \times \mathbb{C}$ be a Lagrangian k -cobordism. Suppose that this cobordism has ends $\{L_i\}_{1 \leq i \leq k}$. A Morse function $h : K \rightarrow \mathbb{R}$ is k -cobordism admissible if it is $\Delta + \Delta_k$ monomial admissible, and there exists (Δ -monomial admissible) Morse functions $h_i : L_i \rightarrow \mathbb{R}$ for the ends so that at each end*

$$h|_{|z_0| > R_{big} - \epsilon} = h_i + (|z_0| - R_{big})^2 + c_i.$$

When $K \subset X \times \mathbb{C}$ is equipped with a k -cobordism admissible Morse function, we expect that there exist maps $\pi_i : CF^{\bullet}(K, h) \rightarrow CF^{\bullet}(L_i, h_i)$ (see the discussion immediately following assumption A.3.2.) A k -cobordism admissible brane structure on a Lagrangian cobordism $K \subset X \times \mathbb{C}$ is a choice of k -cobordism admissible Morse function, and a bounding cochain b_K for the pearly algebra $CF^{\bullet}(K, h)$. Given a k -cobordism admissible brane structure, the ends of the Lagrangian cobordism inherit Lagrangian brane structures by pushforward of the $(\pi_i)_* b_k$. We may now define the Fukaya category of Lagrangian cobordisms using the same machinery used to define the Fukaya category of monomial admissible Lagrangians. The modifications to the monomial admissible Fukaya category are the following:

- One must generalize the notion of infinitesimal wrapping data for a monomial admissibility condition to include the possibility of multiple stops.
- One must build some compatibility between the infinitesimal wrapping data for $W + z_0$ and infinitesimal wrapping data for W .

For the first condition, we require that the angles of the infinitesimal wrapping data are chosen so that $\zeta_i + \xi_k \in [\zeta^i, \zeta^{i+1})$ for all k ; this ensures that no leg which lies in one stopped region crosses into the next stopped region upon applying the infinitesimal wrapping Hamiltonian. For the second condition, we require that outside of a compact region that the infinitesimal wrapping Hamiltonians $H_t^i : X \times \mathbb{C} \rightarrow \mathbb{R}$ split as

$$H_t^i = H_{X,t}^i(z_1, \dots, z_n) + H_{\mathbb{C},t}^i(z_0)$$

where $H_{X,t}^i$ and $H_{\mathbb{C},t}^i$ come from infinitesimal wrapping data chosen for (X, W, Δ) and $(\mathbb{C}, z_0, \Delta_k)$.

Definition A.4.7. *Let W, Δ determine a monomial admissibility condition on X . We define the Fukaya pre-category of k -ended cobordisms as the monomial admissible unobstructed Fukaya category $\text{Fuk}_{\Delta+\Delta_k}^{\rightarrow}(X \times \mathbb{C}, W + z_0)$.*

Consider a curve $\gamma_{ij} : \mathbb{R} \rightarrow \mathbb{C}$ which limits to the stops ζ_i, ζ_j . From this curve, one can build an A_{∞} inclusion functor

$$\begin{aligned} \mathcal{I}_{ij}^{\rightarrow} : \text{Fuk}_{\Delta}^{\rightarrow}(X) &\rightarrow \text{Fuk}_{\Delta+\Delta_k}^{\rightarrow}(X \times \mathbb{C}) \\ L &\mapsto L \times \gamma_{ij}. \end{aligned}$$

The Hamiltonian perturbation data for the Lagrangians $L \times \gamma_{ij}$ is chosen to have the “squiggly” perturbation as in [BC14, Section 4.2].

Let Q_X be the set of quasi-units for $\text{Fuk}_{\Delta}^{\rightarrow}(X)$, and let $Q_{X \times \mathbb{C}}$ be the set of quasi-units for $\text{Fuk}_{\Delta+\Delta_k}^{\rightarrow}(X \times \mathbb{C})$. By choosing infinitesimal wrapping data for $\text{Fuk}_{\Delta+\Delta_k}^{\rightarrow}(X \times \mathbb{C})$ to be consistent with the infinitesimal wrapping data $\text{Fuk}_{\Delta}^{\rightarrow}(X)$, the quasi-units for $\text{Fuk}_{\Delta}^{\rightarrow}(X)$ are mapped to quasi-units for $\text{Fuk}_{\Delta+\Delta_k}^{\rightarrow}(X \times \mathbb{C})$,

$$\mathcal{I}_{ij}(\text{cone}(Q_X)) \subset \text{cone}(Q_{X \times \mathbb{C}}).$$

Claim A.4.8. ([LO+06, Section 3]) Suppose that $\mathcal{F} : \mathcal{C}_1 \rightarrow \mathcal{C}_2$ is an A_{∞} functor, with $\mathcal{B}_i \subset \mathcal{C}_i$ full A_{∞} subcategories. Suppose that $\mathcal{F}(\mathcal{B}_1) \subset \mathcal{B}_2$. Then there is an A_{∞} functor

$$\mathcal{F}_{/B} : \mathcal{C}_1/\mathcal{B}_1 \rightarrow \mathcal{C}_2/\mathcal{B}_2.$$

This means that after localizing at quasi-units we will still obtain a functor of A_{∞} categories,

$$\mathcal{I}_{ij} : \text{Fuk}_{\Delta}(X) \rightarrow \text{Fuk}_{\Delta+\Delta_k}(X \times \mathbb{C}).$$

The rest of the proof follows from the same geometric constructions used in [BC14].

References

[Abo09] Mohammed Abouzaid. “Morse homology, tropical geometry, and homological mirror symmetry for toric varieties”. *Selecta Mathematica* 15.2 (2009), pp. 189–270.

[Abo14] Mohammed Abouzaid. “Family Floer cohomology and mirror symmetry”. *arXiv:1404.2659* (2014).

[AENV+14] Mina Aganagic, Tobias Ekholm, Lenhard Ng, Cumrun Vafa, et al. “Topological strings, D-model, and knot contact homology”. *Advances in Theoretical and Mathematical Physics* 18.4 (2014), pp. 827–956.

[AGL16] Michela Artebani, Alice Garbagnati, and Antonio Laface. “Cox rings of extremal rational elliptic surfaces”. *Transactions of the American Mathematical Society* 368.3 (2016), pp. 1735–1757.

[AKO06] Denis Auroux, Ludmil Katzarkov, and Dmitri Orlov. “Mirror symmetry for del Pezzo surfaces: vanishing cycles and coherent sheaves”. *Inventiones mathematicae* 166.3 (2006), pp. 537–582.

[Arn80] Vladimir Igorevich Arnol’d. “Lagrange and Legendre cobordisms. I”. *Functional Analysis and Its Applications* 14.3 (1980), pp. 167–177.

[AS18] Mohammed Abouzaid and Ivan Smith. “Khovanov homology from Floer cohomology”. *Journal of the American Mathematical Society* (2018).

[Aur07] Denis Auroux. “Mirror symmetry and T-duality in the complement of an anticanonical divisor”. *Journal of Gökova Geometry Topology* 1 (2007), pp. 51–91.

[Aur08] Denis Auroux. “Special Lagrangian fibrations, wall-crossing, and mirror symmetry”. *Surveys in Differential Geometry* 13.1 (2008), pp. 1–48.

[Aur14] Denis Auroux. “A beginners introduction to Fukaya categories”. *Contact and Symplectic Topology*. Springer, 2014, pp. 85–136.

[BC13] Paul Biran and Octav Cornea. “Lagrangian cobordism. I”. *Journal of the American Mathematical Society* 26.2 (2013), pp. 295–340.

[BC14] Paul Biran and Octav Cornea. “Lagrangian cobordism and Fukaya categories”. *Geometric and functional analysis* 24.6 (2014), pp. 1731–1830.

[BC15] Paul Biran and Octav Cornea. “Lagrangian cobordism in Lefschetz fibrations”. *arXiv preprint arXiv:1504.00922* (2015).

[BO95] Alexei Bondal and Dmitri Orlov. “Semiorthogonal decomposition for algebraic varieties”. *arXiv preprint alg-geom/9506012* (1995).

[CL06] Octav Cornea and François Lalonde. “Cluster homology: an overview of the construction and results”. *Electronic Research Announcements of the American Mathematical Society* 12.1 (2006), pp. 1–12.

[CLS11] David A Cox, John B Little, and Henry K Schenck. *Toric varieties*. American Mathematical Soc., 2011.

[COGP91] Philip Candelas, Xenia C. De La Ossa, Paul S. Green, and Linda Parkes. “A pair of Calabi-Yau manifolds as an exactly soluble superconformal theory”. *Nuclear Physics B* 359.1 (1991), pp. 21–74. ISSN: 0550-3213.

[CW15] François Charest and Chris T Woodward. “Floer theory and flips”. *arXiv:1508.01573* (2015).

[FHKV+08] Bo Feng, Yang-Hui He, Kristian D Kennaway, Cumrun Vafa, et al. “Dimer models from mirror symmetry and quivering amoebae”. *Advances in Theoretical and Mathematical Physics* 12.3 (2008), pp. 489–545.

[FOOO07] K Fukaya, YG Oh, K Ono, and H Ohta. “Lagrangian intersection Floer theory-anomaly and obstruction-Chapter 10”. *Preprint available on K. Fukaya’s homepage* (2007).

[For16] Jens Forsgård. “On dimer models and coamoebas”. *arXiv:1602.01826* (2016).

[Fuk02] Kenji Fukaya. “Floer homology for families-a progress report”. *CONTEMPORARY MATHEMATICS* 309 (2002), pp. 33–68.

[Fuk10] Kenji Fukaya. *Lagrangian intersection Floer theory: anomaly and obstruction, Part I*. Vol. 41. American Mathematical Soc., 2010.

[Fuk93] Kenji Fukaya. “Morse homotopy, A_∞ Category and Floer homologies”. *Proceeding of Garc Workshop on Geometry and Topology*. Seoul National Univ. 1993.

[Fuk96] Kenji Fukaya. “Morse homotopy and its quantization”. *Geometric topology (Athens, GA, 1993)* 2 (1996), pp. 409–440.

[Gro11] Mark Gross. *Tropical geometry and mirror symmetry*. 114. American Mathematical Soc., 2011.

[GS03] Mark Gross and Bernd Siebert. “Affine manifolds, log structures, and mirror symmetry”. *Turkish Journal of Mathematics* 27.1 (2003), pp. 33–60.

[GS13] Mark Gross and Bernd Siebert. “Logarithmic Gromov-Witten invariants”. *Journal of the American Mathematical Society* 26.2 (2013), pp. 451–510.

[Gul08] Daniel R Gulotta. “Properly ordered dimers, R-charges, and an efficient inverse algorithm”. *Journal of High Energy Physics* 2008.10 (2008), p. 014.

[Han18] Andrew Hanlon. “Monodromy of Fukaya-Seidel categories mirror to toric varieties”. *arXiv preprint arXiv:1809.06001* (2018).

[Hau15a] Luis Haug. “Lagrangian antisurgery”. *arXiv:1511.05052* (2015).

[Hau15b] Luis Haug. “The Lagrangian cobordism group of T^2 ”. *Selecta Mathematica* 21.3 (2015), pp. 1021–1069.

[HK] Paul Hacking and Ailsa Keating. “HMS for log-Calabi-Yau surfaces”. *In preparation* ().

[HV00] Kentaro Hori and Cumrun Vafa. “Mirror symmetry”. *arXiv preprint hep-th/0002222* (2000).

[Jor77] Camille Jordan. “Mémoire sur les équations différentielles linéaires à intégrale algèbriques.” *Journal für die reine und angewandte Mathematik* 84 (1877), pp. 89–215.

[Kon94] Maxim Kontsevich. “Homological Algebra of Mirror Symmetry”. *Proceedings of the International Congress of Mathematicians*. 1994.

[KOS06] Richard Kenyon, Andrei Okounkov, and Scott Sheffield. “Dimers and amoebae”. *Annals of mathematics* (2006), pp. 1019–1056.

[KS01] Maxim Kontsevich and Yan Soibelman. *Homological mirror symmetry and torus fibrations*. World Scientific, 2001.

[LO+06] Volodymyr Lyubashenko, Sergiy Ovisienko, et al. “A construction of quotient A_∞ -categories”. *Homology, Homotopy and Applications* 8.2 (2006), pp. 157–203.

[LW14] Jiayong Li and Katrin Wehrheim. “ A_∞ Structures from Morse Trees with Pseudoholomorphic Disks”. *Preliminary Draft* (2014).

[Mat18] Diego Matessi. “Lagrangian pairs of pants”. *arXiv:1802.02993* (2018).

[Mik05] Grigory Mikhalkin. “Enumerative tropical algebraic geometry in \mathbb{R}^2 ”. *Journal of the American Mathematical Society* 18.2 (2005), pp. 313–377.

[Mik18] Grigory Mikhalkin. “Examples of tropical-to-Lagrangian correspondence”. *arXiv:1802.06473* (2018).

[Mir89] Rick Miranda. *The basic theory of elliptic surfaces*. ETS, 1989.

[MW15] Cheuk Yu Mak and Weiwei Wu. “Dehn twists exact sequences through Lagrangian cobordism”. *arXiv preprint arXiv:1509.08028* (2015).

[Pol] Leonid Polterovich. *Notes from Polyfold Lab*. June 2017.

[Pol91] Leonid Polterovich. “The surgery of Lagrange submanifolds”. *Geometric & Functional Analysis GAFA* 1.2 (1991), pp. 198–210.

[PT17] James Pascaleff and Dmitry Tonkonog. “The wall-crossing formula and Lagrangian mutations”. *arXiv:1711.03209* (2017).

[Sei17] Paul Seidel. “Fukaya A_∞ -structures associated to Lefschetz fibrations. IV”. *arXiv:1709.06018* (2017).

[SS18] Nick Sheridan and Ivan Smith. “Lagrangian cobordism and tropical curves”. *arXiv preprint arXiv:1805.07924* (2018).

[STWZ15] Vivek Shende, David Treumann, Harold Williams, and Eric Zaslow. “Cluster varieties from Legendrian knots”. *arXiv:1512.08942* (2015).

- [Sub10] Aleksandar Subotic. “A monoidal structure for the Fukaya category”. PhD thesis. Harvard University, 2010.
- [Sym02] Margaret Symington. “Four dimensions from two in symplectic topology”. *arXiv preprint math/0210033* (2002).
- [SYZ96] Andrew Strominger, Shing-Tung Yau, and Eric Zaslow. “Mirror symmetry is T-duality”. *Nuclear Physics B* 479.1-2 (1996), pp. 243–259.
- [Ton18] Dmitry Tonkonog. “String topology with gravitational descendants, and periods of Landau-Ginzburg potentials”. *arXiv:1801.06921* (2018).
- [TWZ18] David Treumann, Harold Williams, and Eric Zaslow. “Kasteleyn operators from mirror symmetry”. *arXiv preprint arXiv:1810.05985* (2018).
- [UY13] Kazushi Ueda and Masahito Yamazaki. “Homological mirror symmetry for toric orbifolds of toric del Pezzo surfaces”. *Journal für die reine und angewandte Mathematik (Crelles Journal)* 2013.680 (2013), pp. 1–22.
- [Via14] Renato Vianna. “Infinitely many exotic monotone Lagrangian tori in $\mathbb{C}\mathbb{P}^2$ ”. *arXiv:1409.2850* (2014).
- [Via17] Renato Vianna. “Infinitely many monotone Lagrangian tori in del Pezzo surfaces”. *Selecta Mathematica* 23.3 (2017), pp. 1955–1996.